



**Paloma Levy Lopes**

**Desenvolvimento de curativos anti-inflamatórios à base de amido utilizando moléculas derivadas de subprodutos do tomate**

**Development of anti-inflammatory starch-based dressings using tomato byproducts-derived molecules**



**Paloma Levy Lopes**

**Desenvolvimento de curativos anti-inflamatórios à base de amido utilizando moléculas derivadas de subprodutos do tomate**

**Development of anti-inflammatory starch-based dressings using tomato byproducts-derived molecules**

Dissertação apresentada à Universidade de Aveiro para cumprimento dos requisitos necessários à obtenção do grau de Mestre em Biotecnologia, realizada sob a orientação científica da Doutora Idalina José Monteiro Gonçalves, Investigadora Júnior no Laboratório Associado CICECO – Instituto de Materiais de Aveiro, do Departamento de Engenharia de Materiais e Cerâmica da Universidade de Aveiro, e da Doutora Sílvia Lancha Petronilho, Investigadora de Pós-doutoramento do Departamento Química da Universidade de Trás-os-Montes e Alto Douro em colaboração, como Estagiária de Pós-Doutoramento, com o Departamento de Química da Universidade de Aveiro.

Dedico este trabalho aos meus pais.

## **o júri**

presidente

Prof. Doutor Manuel António Coimbra Rodrigues da Silva  
Professor associado com agregação da Universidade de Aveiro

Orientadora

Prof.<sup>a</sup> Doutora Idalina José Monteiro Gonçalves  
Investigadora Júnior da Universidade de Aveiro

Arguente

Prof.<sup>a</sup> Doutora Susana Cecília de Brito Gomes Guerreiro  
Investigadora Júnior do Instituto e Inovação em Saúde i3S – Universidade do Porto

## **agradecimentos**

Às minhas orientadoras, Doutora Idalina Gonçalves e Doutora Sílvia Petronilho, pela eterna paciência e compreensão, pelos conselhos e ensinamentos que tanto ajudam na minha formação profissional. À Professora Catarina Almeida e Doutora Joana Tulha, por me terem recebido de forma tão carinhosa e me terem acompanhado durante o meu período no iBiMED. À Professora Adelaide Almeida e à Doutora Maria Bartolomeu, pelo generoso apoio e acompanhamento durante a minha estadia no Departamento de Biologia da Universidade de Aveiro. Ao Professor José António Lopes da Silva e ao Doutor Rodolfo Ferreira pela receção, apoio e ajuda durante o meu trabalho. A todos os colegas de laboratório e investigadores, nos diversos grupos em que estive inserida, pela ajuda e apoio.

Aos meus pais, pelo amor e carinho, pelo apoio incondicional, paciência e voz de razão frente às adversidades que encontrei. À minha irmã, cunhado e sobrinha, pelos momentos de lazer e descontração. Tal qual aos meus amigos, pelo riso, compreensão e irreverente e amada gozação.

## palavras-chave

Subprodutos da Indústria Agroalimentar; Repiso do Tomate; Polissacarídeos; Compostos fenólicos; Tratamento de feridas; Dispositivos médicos ativos; Economia Circular.

## resumo

Muitos dos curativos para feridas atualmente utilizados não são os ideais para um processo de cura total, rápido e eficaz devido à sua reduzida biocompatibilidade, oriunda da sua natureza sintética e da ausência de propriedades funcionais. Como alternativa têm sido desenvolvidos novos curativos de origem biológica com atividade antimicrobiana e/ou anti-inflamatória. No entanto, os polímeros de origem natural até à data utilizados provêm de alimentos, atuando como competidores para a alimentação humana. As biomoléculas derivadas dos subprodutos da indústria agroalimentar podem ajudar a superar esta competição.

Neste trabalho foi estudada a viabilidade da utilização de moléculas derivadas dos subprodutos de tomate para o desenvolvimento de pensos à base de amido com propriedades anti-inflamatórias. Para o efeito foi estudada a influência da concentração (1%, 5% e 10% m/m em relação à massa seca de amido) de extratos solúveis em água quente derivados do repiso de tomate, ricos em polissacarídeos (TE) e/ou compostos fenólicos (PE), nas propriedades cromáticas, mecânicas, físico-químicas e ativas (anti-inflamatórias e antimicrobianas) dos filmes à base de amido obtidos pelo método de evaporação do solvente. Num conceito de economia circular, o amido foi recuperado de lamas provenientes do processamento industrial de batata.

Os extratos TE e PE apresentaram, respetivamente, 14,7% e 18,5% de proteína, 43,7% e 28,6% de polissacarídeos, 2,8% e 15,1% de compostos fenólicos e promissora atividade antioxidante ( $IC_{50}$  de 2,5 mg/mL e 0,8 mg/mL, respetivamente). Quando incorporados em formulações à base de amido, os extratos TE e PE permitiram desenvolver filmes transparentes com coloração amarelada e menor rigidez e resistência à tração do que os filmes controlo. TE originou filmes hidrofóbicos e flexíveis, enquanto PE diminuiu a hidrofobicidade e extensibilidade dos filmes. Quanto às propriedades ativas, ambos os filmes com TE e PE demonstraram atividade anti-inflamatória quando na presença de um agente pró-inflamatório, observando-se, ao fim de 24 h, uma diminuição da inflamação de cerca de 48% e 100% para os filmes à base de amido com 10% de TE e PE, respetivamente. Com o intuito de desenvolver pensos à base de amido, neste trabalho também se otimizou a eletrofiação de soluções à base de amido. Após o ajuste do solvente, da concentração de amido e do tempo necessário para a sua dissolução foram obtidas fibras à base amido, porém em baixa quantidade para posterior aplicação no desenvolvimento de pensos.

As biomoléculas existentes no repiso de tomate e o amido recuperado das lamas de lavagem de batata mostraram-se promissores para o desenvolvimento de curativos anti-inflamatórios de origem biológica, o que permitirá promover dispositivos médicos para cura de feridas mais biocompatíveis e funcionais dos que os materiais derivados de polímeros sintéticos inertes.

## keywords

Agrifood Industry Byproducts; Tomato Pomace; Polysaccharides; Phenolic compounds; Wound healing; Active medical devices; Circular Economy.

## abstract

Most wound dressings currently used are not ideal for a total, fast, and effective healing process due to their reduced biocompatibility derived from their synthetic nature and lack of bioactive properties. Alternatively, new bio-based dressings with antimicrobial and/or anti-inflammatory activity have been developed. However, the natural polymers currently used come from food, acting as competitors for human nutrition. Agrifood byproducts-derived biomolecules can help overcome this competition.

In this work, the feasibility of using tomato byproducts-derived molecules for the development of starch-based dressings with anti-inflammatory properties was studied. For this purpose, the influence of tomato pomace-derived hot-water soluble extract concentration (1%, 5%, and 10% w/w in relation to starch dry weight), rich in polysaccharides (TE) and/or phenolic compounds (PE), on the chromatic, mechanical, physicochemical, and active properties (antimicrobial and anti-inflammatory) of starch-based films obtained by solvent casting was studied. In a circular economy concept, starch was recovered from industrial potato processing slurries.

TE and PE extracts showed, respectively, 14.7% and 18.5% of protein, 43.7% and 28.6% of polysaccharides, 2.8% and 15.1% of phenolic compounds, and promising antioxidant activity ( $IC_{50}$  values of 2.5 mg/mL and 0.8 mg/mL, respectively). When incorporated into starch-based formulations, TE and PE allowed to develop transparent films with a yellowish coloration and less rigid and traction resistant films than the control films. TE originated hydrophobic and flexible films, while PE decreased the films' hydrophobicity and stretchability. Regarding the active properties, after 24h, both films with TE and PE revealed anti-inflammatory activity in the presence of a pro-inflammatory agent, where, for starch-based films with 10% TE and 10% PE, the inflammation decreased by *ca.* 48% and 100%, respectively. To develop starch-based dressings, in this work the electrospinning of starch-based solutions was also optimized. After adjusting the solvent, starch concentration, and dissolution time, starch-based fibers were obtained, although in small amount for application in the development of dressings.

The tomato pomace-derived molecules and starch recovered from potato washing slurries have shown to be promising raw materials for the development of biobased anti-inflammatory dressings, which will allow to promote more biocompatible and functional wound healing devices than the materials derived from inert synthetic polymers.

## Index

<b>1. Introduction</b> .....	<b>1</b>
1.1 Skin wounds: General considerations.....	1
1.2 Constrains to Skin Wound healing.....	5
1.3 Current Skin Wound Treatments.....	6
1.4 Wound Dressings.....	7
1.5 Wound dressings from natural polymers.....	11
1.6 Food for materials: economic constraints and byproducts as a solution.....	20
1.6.1 Potato.....	21
1.6.2 Tomato.....	22
<b>2. Objectives</b> .....	<b>33</b>
<b>3. Experimental section</b> .....	<b>34</b>
3.1 Materials.....	34
3.2 Recovery of starch from potato industry washing slurries.....	34
3.3 Tomato Pomace (TP) preparation.....	35
3.4 Acidified hot-water extraction of TP.....	35
3.5 Recovery of hot-water extracts' phenolic compounds using a C <sub>18</sub> column.....	36
3.6 Chemical characterization and evaluation of antioxidant and cytotoxicity properties of TP-derived extracts.....	37
3.7 Production of starch/TE- and starch/PE-based films.....	40
3.8 Characterization of starch/TE- and starch/PE-based films.....	41
3.8.1 Chromatic properties.....	41
3.8.2 Thickness and Mechanical performance.....	41
3.8.3 Wettability.....	42
3.8.4 Water solubility and moisture content.....	43
3.8.5 Anti-inflammatory activity.....	43
3.8.6 Antimicrobial properties.....	44
3.8.7 Cytotoxicity.....	45
3.9 Electrospinning of starch-based solutions.....	45
3.10 Statistical analyses.....	46
<b>4. Results and Discussion</b> .....	<b>46</b>
4.1 Tomato pomace characteristics.....	46
4.2. Extraction yield and chemical characteristics of TP-derived extracts.....	48
4.3 Characteristics of starch/TE- and starch/PE-based films.....	56
4.3.1 Chromatic properties.....	56
4.3.2 Mechanical properties.....	58
4.3.3 Wettability.....	60
4.3.4 Moisture content and Water solubility.....	62
4.3.5 Anti-inflammatory activity.....	63
4.3.6 Antimicrobial activity.....	64



<b>5. Conclusion</b> .....	<b>69</b>
<b>6. Future work</b> .....	<b>70</b>
<b>References</b> .....	<b>71</b>

## Abbreviations list

- CFU – Colony Forming Units
- CVD – Cardiovascular Disease
- DW – Dry Weight
- ECM – Extracellular Matrix
- EPS – Extracellular Polysaccharide Matrix
- EUROSTAT – European Statistical Office
- FAOSTAT – Food and Agriculture Organization Corporate Statistical Database
- FTA – Fresh Tannic Acid
- FW – Fresh Weight
- HA – Hyaluronic Acid
- INE – Instituto Nacional de Estadística
- IP – Insoluble Polysaccharides
- LPS – Lipopolysaccharide
- PBS – Phosphate-Buffered Saline
- PCL – Polycaprolactone
- PE – Polyphenol-enriched Extract
- PEG – Polyethyleneglycol
- PEO – Poly(ethylene oxide)
- PGA – Polyglycolic Acid
- PLA – Polylactic Acid
- PTA – Thermally Processed Tannic Acid
- PU – Polyurethane
- PVA – Poly(vinyl alcohol) Acid
- RPMI – Roswell Park Memorial Institute
- SP – Soluble Polysaccharides
- TE – Hot-water soluble (total) Extract
- THP-1 – Tohoku Hospital Pediatrics-1
- TP – Tomato Pomace
- TPC – Total Phenolic Content
- TS – Tensile Strength
- TSA – Tryptic Soy Agar
- TSB – Tryptic Soy Broth
- YM – Young's Modulus

## List of Figures

<b>Figure 1.</b> Schematic representation of human adult skin. Adapted from Ambekar et al <sup>9</sup> .....	2
<b>Figure 2.</b> Wound healing phases. Adapted from Andreu <i>et al.</i> <sup>8</sup> .....	3
<b>Figure 3.</b> Schematic representation of the wound healing process phases. Adapted from Tottoli <i>et al.</i> <sup>6</sup> .....	4
<b>Figure 4.</b> Scanning Electron Microscopic (SEM) image of a <i>Staphylococcus aureus</i> biofilm. Source: CDC Public Health Image Library/ Rodney M. Donlan, Ph.D.; Janice Carr, 2005. ....	6
<b>Figure 5.</b> Examples of currently marketed semi-permeable film dressings. ....	8
<b>Figure 6.</b> Examples of currently marketed foam dressings <b>a)</b> with adhesive borders and <b>b)</b> without adhesive borders. ....	8
<b>Figure 7.</b> Examples of currently marketed hydrocolloid dressings <b>a)</b> with adhesive borders and <b>b)</b> without adhesive borders. ....	9
<b>Figure 8.</b> Examples of currently marketed alginate dressings. ....	9
<b>Figure 9.</b> Examples of currently marketed hydrogel dressings: <b>a)</b> amorphous gel, <b>b)</b> impregnated gauze and <b>c)</b> sheet.....	10
<b>Figure 10.</b> Scheme of an ideal wound dressing membrane. Adapted from Kamoun <i>et al.</i> <sup>34</sup> .....	11
<b>Figure 11.</b> Examples of currently marketed <b>a)</b> collagen film and <b>b)</b> collagen sponge.....	12
<b>Figure 12.</b> Chemical structure of chitosan. ....	13
<b>Figure 13.</b> Chemical structure of hyaluronic acid. ....	14
<b>Figure 14.</b> Chemical structure of cellulose. ....	14
<b>Figure 15.</b> Chemical structure of <b>a)</b> amylose and <b>b)</b> amylopectin.....	15
<b>Figure 16.</b> Scanning electron microscope image of a starch granule. Adapted from Pilling <i>et al.</i> <sup>47</sup> 16	16
<b>Figure 17.</b> Schematic representation of starch gelatinization and retrogradation processes. Adapted from Liu <i>et al.</i> <sup>45</sup> . ....	17
<b>Figure 18.</b> SEM images of control hydrogel membrane (left) and hydrogel membrane with 0.5 g turmeric added (right). Adapted from Hassan <i>et al.</i> <sup>33</sup> .....	19
<b>Figure 19.</b> World potato production and area harvested per year. Adapted from FAOSTAT.....	21
<b>Figure 20</b> World tomato production and area harvested per year. Adapted from FAOSTAT.....	23
<b>Figure 21.</b> Scheme of the transformation of tomato and the byproducts generated.....	24
<b>Figure 22.</b> Tomato pomaces obtained by different processing techniques: Hot break ( <b>a)</b> and <b>b)</b> ) and <b>c)</b> cold break. Adapted from Shao <i>et al.</i> <sup>81</sup> . ....	25
<b>Figure 23.</b> Chemical structure of <b>a)</b> pectin and <b>b)</b> pectic polysaccharide <sup>100</sup> .....	27
<b>Figure 24</b> Chemical structure of <b>a)</b> lycopene, <b>b)</b> $\beta$ -carotene and <b>c)</b> vitamin A.....	29
<b>Figure 25.</b> Chemical structure of <b>a)</b> L-ascorbic acid (vitamin C) and <b>b)</b> $\alpha$ -tocopherol (vitamin E). .	30
<b>Figure 26.</b> Chemical structure of <b>a)</b> caffeic acid, <b>b)</b> chlorogenic acid, <b>c)</b> naringerin, <b>d)</b> quercetin, e) rutin, and f) kaempferol. ....	32
<b>Figure 27.</b> Schematic representation of lycopene's bioactivity. Adapted from Agarwal <i>et al.</i> <sup>102</sup> .....	33
<b>Figure 28.</b> Potato washing slurries <b>a)</b> and recovered starch. <b>b)</b> .....	35
<b>Figure 29.</b> Tomato pomace. <b>a)</b> Frozen and <b>b)</b> lyophilized sample.....	35
<b>Figure 30.</b> Sequential hot acidified hot-water extraction (100 °C, 10 min), followed by vacuum filtration, concentration via evaporation, and freeze-drying.....	36
<b>Figure 31.</b> Solid phase extraction with methanol and acidified water, followed by concentration via evaporation, and freeze-drying.....	38
<b>Figure 32.</b> Folin-Ciocalteu method for TPC estimation plate assay, with white-dark blue gradient indicating increasing concentration of polyphenols.....	38
<b>Figure 33.</b> DPPH assay plate with yellow-purple gradient indicating the increasing quenching of the DPPH radical, whose natural color is purple.....	39
<b>Figure 34.</b> THP-1 cell culture plate <b>a)</b> and flow cytometer used <b>b)</b> .....	40
<b>Figure 35.</b> Procedure for the development of starch-, starch/TE- and starch/PE-based	

films .....	40
<b>Figure 36.</b> Chroma meter CR-400 colorimeter and its calibration plate.....	41
<b>Figure 37.</b> Texture analyzer used (left) and a zoom to its closed claws with a film strip (right)....	41
<b>Figure 38.</b> Tensiometer used to determine the films wettability properties. ....	43
<b>Figure 39.</b> Film samples immersed in sodium azide aqueous solution.....	43
<b>Figure 40.</b> ELISA assay <b>a)</b> before reaction termination and <b>b)</b> after reaction termination. ....	45
<b>Figure 41.</b> TSA plates and respective dilutions set-up .....	45
<b>Figure 42.</b> Electrospinning set-up used including <b>a)</b> syringe pump, and <b>b)</b> metal rotary collector with electrode wire. ....	45
<b>Figure 43.</b> Distribution of unmilled tomato pomace particle size (% weight).....	47
<b>Figure 44.</b> Distribution of milled tomato pomace particle size (% weight).....	48
<b>Figure 45.</b> Extracts obtained. <b>a)</b> TE and <b>b)</b> PE.. ....	49
<b>Figure 46.</b> Sugars composition of TE and PE in <b>a)</b> concentration and <b>b)</b> %mol.....	50
<b>Figure 47.</b> HPLC chromatogram (295 nm) of PE (5 mg/mL) and quantification of the peaks found via HPLC expressed in mg of caffeic acid equivalents/100 g of dry weight sample.....	52
<b>Figure 48.</b> Cytotoxicity of TE and PE after 24 and 48h of THP-1 cell culture, in the presence and absence of pro-inflammatory LPS.....	53
<b>Figure 49.</b> Anti-inflammatory activity of TE and PE. N.d denotes not detected, for [TNF- $\alpha$ ] below that of the smallest standard (31.25 pg/mL).....	54
<b>Figure 50.</b> MIC assay plate, denoting the strong yellow color due to the extracts' natural color, that hindered the bacterial O.D determination at 600 nm, where yellow absorbs the most as well. ....	55
<b>Figure 51.</b> Antimicrobial activity against <i>Staphylococcus aureus</i> of TP-derived extracts. ....	56
<b>Figure 52.</b> Visual appearance of Sstarch-, starch/TE-, and starch/PE-based films.....	57
<b>Figure 53.</b> Lightness (L*) and blue-yellow (b*) coordinate of starch-, starch/TE-, and starch/PE-based films. ....	57
<b>Figure 54.</b> Thickness <b>a)</b> and traction performance properties of starch-, starch/TE-, and starch/PE-based films starch- and starch/TP extracts-based films: tensile strength <b>b)</b> , Young's modulus <b>c)</b> , and elongation at break <b>d)</b> . ....	59
<b>Figure 55.</b> Water contact angle of starch-, starch/TE-, and starch/PE-based films "Top" and "Bottom" are related to the film faces exposed to air and in direct contact with the plate during the solvent casting process, respectively.....	61
<b>Figure 56.</b> Moisture content <b>a)</b> and solubility <b>b)</b> of starch-, starch/TE-, and starch/PE-based films. ....	62
<b>Figure 57.</b> Leaching of colored compounds from the residual water resulted from the solubility assays carried out for starch-, starch/TE-, and starch/PE-based films.....	66
<b>Figure 58.</b> Anti-inflammatory activity of starch- and starch/TP extracts-based films. "n.d" denotes not detected for [TNF- $\alpha$ ] below that of the smallest standard (31.25 pg/mL).....	63
<b>Figure 59.</b> Antibioassays carried out using starch- and starch/TE-based films.. ....	65
<b>Figure 60.</b> Colony forming units (CFU) obtained for against <i>Staphylococcus aureus</i> bacteria for starch-, starch/5% TE- and starch/5% PE-based films. ....	65
<b>Figure 61.</b> Solubility of starch-, starch/1.0-10% TE- and starch/1.0-5.0% PE-based films in RPMI cell culture medium. ....	66
<b>Figure 62.</b> Electrospinning of 25% starch-based solutions prepared in 75:25 FA/H <sub>2</sub> O.....	68

## 1. Introduction

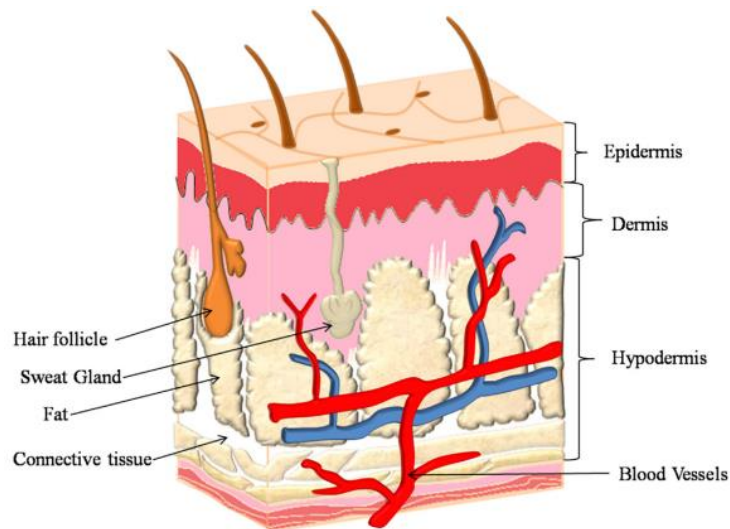
Wound dressings have an important role in wound healing. However, none of the current commercial options combine all requirements necessary for a quick and peerless cutaneous wound healing that should be optimized to be efficient at all healing stages and wound type and characteristics. Novel strategies for the development of wound dressings include the use of natural origin polymers to produce scaffolds with structural and biochemical similarity to the natural extracellular matrix (ECM). One good example of those biopolymers is starch, that has been exploited to develop dressings in the form of films, hydrogels, and hydrocolloids due to its abundant and inexpensive nature, biocompatibility, biodegradability, and potential for sustainable production. Moreover, to speed up the endogenous healing process, the development of active materials, with anti-inflammatory and/or antimicrobial activity, has attracted huge attention due to the possibility to create a next generation of bioactive wound dressings. In the search of sustainable alternatives to pursue this new trend, agrifood industry byproducts, often discarded and still rich in valuable biomolecules, could be exploited to develop this kind of materials.

Potato and tomato are the top two most in-demand vegetables worldwide, with productions of about 370 and 180 million tons, in 2019, respectively, whose industrial processing generates huge amounts of byproducts<sup>1,2</sup>. Considerable amounts of starch have been recovered from the potato washing slurries of potato chips industry<sup>3</sup>. Following the same trend, tomato processing also generates non-value byproducts, such as the tomato pomace (a mixture of tomato seeds, peels, and pulp). Tomato pomace is rich in active molecules like carotenoids and phenolic compounds with potential to be used in the development of active materials<sup>2</sup>. Therefore, in this study, it was hypothesized that starch and tomato pomace-derived polysaccharides- and/or phenolic-rich extracts can be combined and used in the development of active wound dressings.

### 1.1 Skin wounds: General considerations

The skin is the largest organ in the human body and plays a crucial role in many functions, such as protecting against external assailants, thermoregulation, fluid homeostasis, sensory detection, and vitamin D synthesis<sup>4-7</sup>. Skin comprises three different layers: i) the keratinized and high cellularized epidermis; ii) the acellular dermis of collagen-rich extracellular matrix with fibroblasts, follicles, glands, nerves, and capillary vessels embedded; and iii) the hypodermis which mainly consists of blood vessels and adipose tissue (**Fig. 1**). Skin forms an effective barrier between the external environment and our

organism, providing physical and biochemical protection against water loss, pathogens, and other harmful assailants<sup>5,8</sup>.



**Figure 1.** Schematic representation of human adult skin. Adapted from Ambekar *et al.*<sup>9</sup>

Skin wounds are disruptions in the normal anatomical structure of the tissue which lead to an abnormal behavior<sup>8</sup>. Damage or loss of the integrity of skin caused by a cutaneous wound may impair the skin functions at various extents ranging from significant disability to even death<sup>5</sup>. Most skin wounds can heal naturally, as normally, only the epidermis and dermis are affected, however, if the wound reaches deeper levels, such as the hypodermis, fascia, muscle, tendon, bone, and viscera, it can be classified as an ulcer, producing more severe outcomes<sup>8</sup>. Thus, wounds can be classified as superficial wounds (only epidermis is affected), partial thickness wound (affected dermis), and full-thickness wounds, when the hypodermis and other deeper tissues are also affected<sup>9,10</sup>.

Wounds can also be classified as acute and chronic wounds. Acute skin wounds often arise from trauma (e.g., burns, lacerations, abrasions) and surgical procedures and repair themselves in an organized and well-timed process (8-12 weeks)<sup>4,8,11</sup>. Meanwhile, chronic wounds are often caused by metabolic disturbances due to systemic diseases such as diabetes (diabetic ulcers), vascular insufficiency (vascular ulcers) or obesity<sup>12,13</sup>, and are unable to repair optimal anatomical and functional integrity in the same timeframe, normally being stuck in a state of persistent inflammation<sup>4,13</sup>. For instance, pressure ulcers are relatively common chronic wounds in patients with long-term reduced mobility and end up leading to progressive injury into deeper tissues such as muscle, tendon, and bone, as well as to infection, septicemia, and even death<sup>8</sup>. Venous ulcers are another type of chronic wound produced by venous hypertension or by failure in venous valves. Foot ulcers are common complications in diabetic patients, and often results in amputation in 85% of

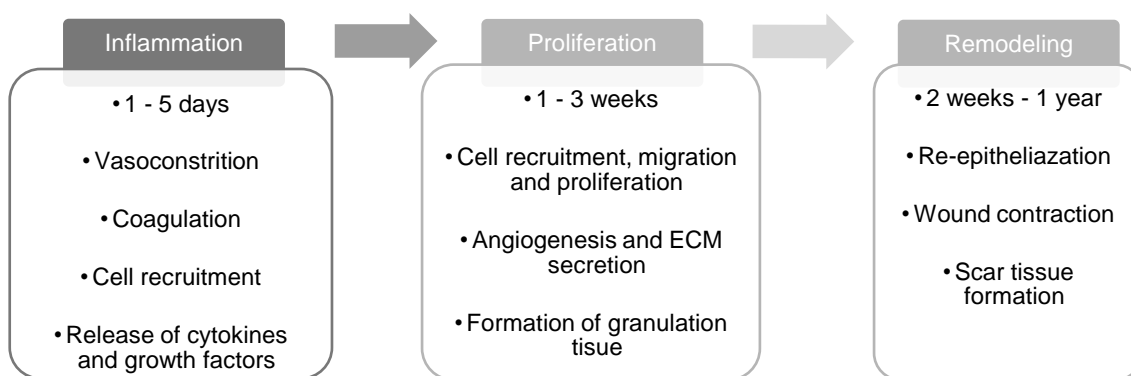
cases<sup>4,8</sup>. **Table 1** summarizes the differences between acute and chronic wounds.

**Table 1.** Key differences in acute and chronic wounds.

Acute Wounds	Chronic Wounds
<b>Repair themselves in an organized and timely manner</b>	Fails to return to anatomical and functional integrity in a timely manner
<b>Normally caused by trauma and surgical procedures</b>	Normally borne from pre-existing conditions
<b>Affects at most the dermis</b>	May affect deeper tissues and even bone

The Eucomed Advanced Wound Care Sector Group reported in 2008 that there are 4 million annual wound incidences in Europe<sup>8</sup>. Studies have also estimated a 13.7% median prevalence rate of pressure wounds in Europe, with results ranging between 4.6-27.2% depending on the country<sup>14</sup>. Another study conducted in 2018 showed a 17.5% wound prevalence rate in Alentejo continuing care unities in Portugal, of which 82% were chronic wounds. In turn, 80% of the chronic wounds registered were pressure ulcers<sup>15</sup>. Furthermore, it has been calculated that in Europe, in hospitals performing 10,000 operations per year, 3–4% of the surgeries lead to an infected wound with an annual cost of about € 2 million<sup>8</sup>.

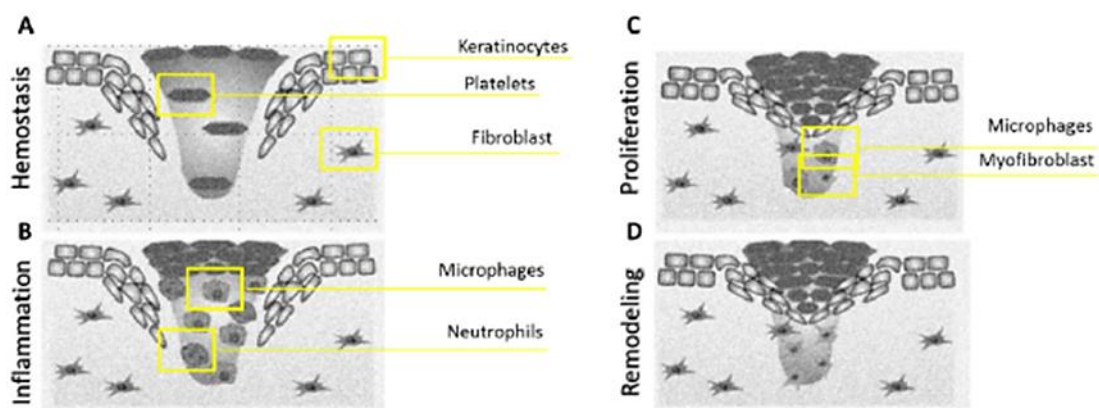
The wound healing process begins almost immediately after a wound occurs, to ensure the total restoration of the skin structure and function that has been disrupted. This highly complex and dynamic process consists of three differentiated but overlapping phases: inflammation, proliferation, and remodeling (**Fig. 2**)<sup>4,6,8,9</sup>.



**Figure 2.** Wound healing phases. Adapted from Andreu *et al.*<sup>8</sup>

The **inflammation** phase occurs immediately upon injury and last for 1 to 5 days. It commences by vasoconstriction and coagulation, followed by acute local inflammatory

response<sup>6,8</sup>. Thrombocytes rush to the wound site and release clotting factors to form temporary fibrin plugs to stop blood loss after a blood vessel is injured<sup>6,7,9</sup>. They also release growth factors and pro-inflammatory cytokines to aid in later wound healing phases, especially to promote the recruitment of cells involved in inflammation response, also inducing vasodilation in the process<sup>6,9,16</sup>. This process is also defined by some authors as the **hemostasis** phase (**Fig. 3**)<sup>4,7,9</sup>. Inflammation occurs as neutrophils, monocytes, macrophages and lymphocytes rush to the wound attracted by the chemo signals released previously and begin cleansing the wound of pathogens, foreign bodies and damaged tissue via phagocytosis, release of reactive oxygen species (ROS), antimicrobial peptides, eicosanoids, proteolytic enzymes and inflammatory cytokines and growth factors of their own, contributing as well to inflammation and help in later cell proliferation and migration<sup>7-9,16</sup>. After this, the **proliferation** phase occurs and normally lasts for 1 week. In this phase, exposure to hydrogen peroxide, pathogens and the cytokines and factors released in the inflammation stage activates keratinocytes, fibroblasts, microphages and macrophages, and endothelial cells, pushing them to migrate and proliferate, stimulating angiogenesis (formation of new blood vessels from preexisting ones), and wound closure by forming a new temporary connective tissue called granulation tissue. This tissue is poorly differentiated and highly vascularized as a result of the induced angiogenesis and the ECM produced by fibroblasts<sup>4,8,9,16,17</sup>. At the end of the wound healing process occurs the **remodeling** phase, that can last from 2 weeks to over 1 year. It is characterized by the ceasing of the processes initiated in the previous phases, maturation of the ECM and the blood vessels created previously by angiogenesis and formation of scar-tissue depending on the depth of the wound (**Fig. 3**)<sup>6,8-10</sup>.



**Figure 3.** Schematic representation of the wound healing process phases. Adapted from Tottoli *et al.*<sup>6</sup>.



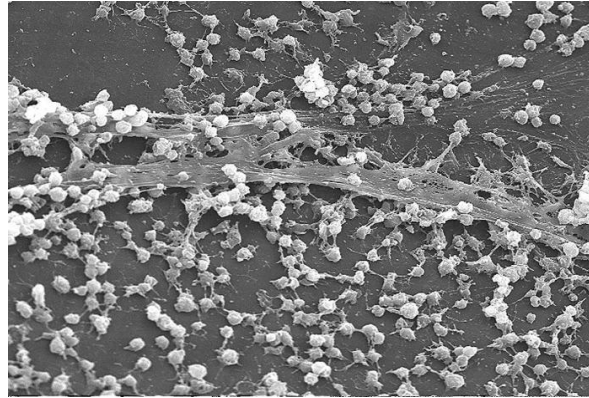
## 1.2 Constrains to Skin Wound healing

Different factors related to general health and well-being like age, metabolic disorders, nutritional deficiencies, drugs and environmental factors, as well as local factors like pain, hypothermia and hypoxia may hinder wound healing<sup>11,18,19</sup>. In addition, chronic wounds' frequent correlation to well-defined pathologies is also due to proven effects that such conditions have on the healing process at different stages<sup>8,19</sup>. Different clinical studies have shown that insufficient production, defective release, and/or increased degradation of growth factors, like vascular endothelial growth factor (VEGF), associated with diseases such as diabetes<sup>20,21</sup> and venous inefficiency<sup>22</sup>, leads to insufficient angiogenesis, compromising nutrient supply and promoting hypoxia of the wound, thus delay healing in chronic cases, for example<sup>8,10,17</sup>.

Control of inflammation is also an essential factor in a successful wound healing process, as it dictates the progression of the process itself. Excessive, inappropriate or uncontrolled inflammation, as is in the case of chronic wounds, promotes tissue injury and prolongs the wound healing process, preventing its progression past the inflammatory phase, with bacterial infection being one of the main factors in inducing chronic inflammation<sup>7,8,13</sup>. On the other hand, insufficient inflammation as a result or caused by poor immune cell recruitment also delays healing and promotes infection if the wound site is not cleaned properly. Thus, inflammation and immune cell responses must be proportional according to the situation at hand, increasing to respond appropriately to infection, yet clearing effectively to allow wound resolution<sup>16</sup>.

Intact skin flora normally possesses  $10^5$  microcolonies with no negative effects. However, wounds provide favorable environment for bacteria due to higher degrees of moisture and easier nutrient access<sup>23</sup>. Thus, bacteria previously part of the endogenous skin microflora can colonize and infect wounds and cause the deterioration of granulation tissue, growth factors and extracellular matrix components, thus interfering with the wound healing process and prolonging the inflammatory stage<sup>6,7,23</sup>. This can happen mainly due to virulence factors that mediate bacterium adhesion, nutrient acquisition, leucocyte attack and bloodstream invasion, and endotoxin production, that trigger an elevated production of proinflammatory cytokines<sup>7,23</sup>. As such, successful wound healing has been shown to be dependent on decreasing and maintaining a bacterial level below  $10^5$  per gram of tissue<sup>23</sup>. Bacteria can also form biofilms, becoming highly resistant against antibiotics (50-1000 times more resistant than normal bacteria). These biofilms consist of surface-attached consortium of bacteria enclosed in a self-secreted extracellular polysaccharide matrix (EPS) (**Fig. 4**)<sup>6,8,23</sup>. Biofilms are often difficult to be eradicated by phagocytic cells as

they have difficulty in penetrating biofilms' EPS and due to excreted products from the bacteria within the film, as these consortium often have their own phenotype and metabolic rates<sup>23</sup>.



**Figure 4.** Scanning Electron Microscopic (SEM) image of a *Staphylococcus aureus* biofilm.

Source: CDC Public Health Image Library/ Rodney M. Donlan, Ph.D.; Janice Carr, 2005.

Similarly, exudate is a normal feature of healing wounds, being essential in the stimulation of cell migration at the edge of the wound, angiogenesis, and connective tissue synthesis<sup>24</sup>. It is also a marker of the chronic state of an injury and/or a sign of wound treatment effectiveness as there is increasing evidence that corrosive exudate components cause destructive effects, such as continuous ECM degradation, for example<sup>6</sup>. As such, an insufficient or excessive exudate production can delay healing, distress patients, and consume considerable healthcare resources<sup>8</sup>.

### 1.3 Current Skin Wound Treatments

The coverage of wounds in the form of dressings or skin substitutes are the most common devices used to aid skin repair and regeneration. Natural skin substitutes, such as xenografts (donor of different species), allografts (donor of same species), and autografts (donor is the own patient) are commonly used for wound healing. Even so, limitations, such as limited donor sites, risk of infection, slow healing, and poor integration, have led to the use of engineered wound dressings as the preferred method<sup>4,5,12</sup>. Various upcoming methods, such as vacuum-assisted wound closure, engineered skin substitutes, low-power light therapy, ultrasound and electricity, stem cell therapy, growth factors, and cytokine therapy, have also emerged in recent years, with some being used to replace the traditional

methods<sup>4,12,18</sup>. On the other hand, some methods like stem cell therapy and growth factors still suffer from lack of assessment by large-scale studies and thus are not widely used<sup>13</sup>. Others methods, like engineered skin substitutes, have drawbacks like wound contraction, scar formation, poor integration with host, fragility, and production costs that limit its widespread use<sup>4,5</sup>.

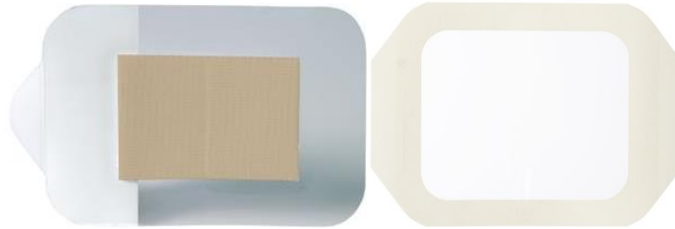
The use of antimicrobial compounds has become normal for the prevention and management of infection in wounds. Particularly, antiseptics have been preferred due to the ongoing risk of resistance to topical and systemic antibiotics. The range of topical antiseptics agents currently used includes alcohols, acetic acid, chlorhexidine, hydrogen peroxide, potassium permanganate, and products containing iodine and silver, among others. Dressings in particular that incorporate antiseptics can successfully be used in topical management to reduce the bacterial load<sup>4,6,8</sup>.

#### 1.4 Wound Dressings

At first, it was believed that a dry environment was needed for a successful wound healing, and passive textile-based dressings, as gauze and lint, were the first wound dressing used to absorb exudate and cover and protect the wound from infection<sup>25</sup>. However, this type of cover excessively drained the wound and caused skin maceration upon removal as it stuck to the wound, thus delaying healing<sup>11,25,26</sup>. In addition, the non-occlusive nature of the woven fibers in combination with the need for frequent changes represented an inability to prevent bacterial infections<sup>8,26,27</sup>. Since then, it was shown that instead a moist environment favored wound healing during late 20<sup>th</sup> century<sup>28</sup>, and interactive dressings were developed with the intention to modify and manipulate one or more aspects of the wound environment such as moisture, being permeable to water vapor and oxygen, and impermeable to bacteria. Currently available dressings focus on combinations of these distinct properties with the most common and popular products taking the form of semipermeable films, foams, hydrocolloids, alginates, and hydrogels and, that make them suitable for the treatment of a particular type of wound<sup>7,8,12,27,29</sup>.

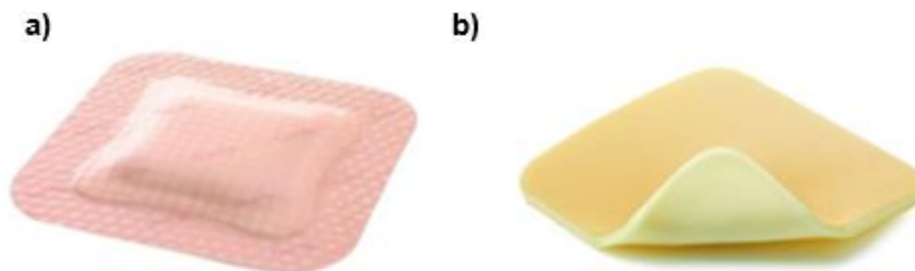
**Semipermeable films dressings** are thin, elastic, flexible polyurethane dressings coated with an acrylic adhesive impermeable to bacteria (**Fig. 5**). They are gas permeable but waterproof and conform easily to the patient's body. They can be used as a primary or secondary dressing, and as films are transparent, the wound can be easily monitored. However, they are suitable only for delicate and minimally exudative superficial wounds because of its non-absorbent nature, allowing exudate accumulation, which can cause skin maceration via waterlogging, as well as its adhesive that loses function when in contact with

moisture. The adhesive backing on films may also potentially damage the new epidermis so patients with fragile skin, like the elderly, should be cautioned in such case <sup>7,30,31</sup>.



**Figure 5.** Examples of currently marketed semi-permeable film dressings.

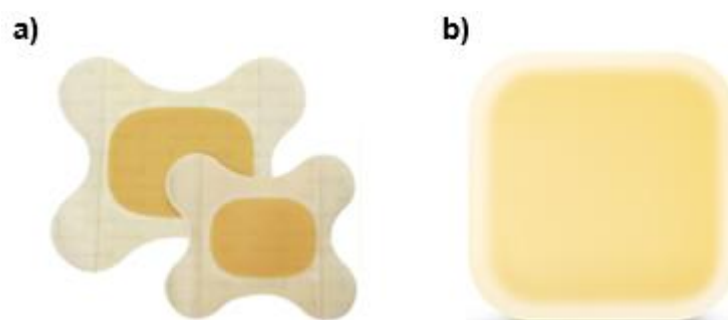
**Foam dressings** are semipermeable bilaminate hydrophilic/hydrophobic polyurethane or silicone-based dressings suitable for moderate to high volumes of wound exudate. They allow the passage of exudate through the non-adherent, hydrophilic, wound-contacting surface into the insulating hydrophobic foam<sup>26</sup>, providing thermal insulation to the wound, a moist wound environment, and atraumatic dressing removal. They can conform well to body surfaces and are comfortable, but normally need a secondary dressing to maintain its stability unless it comes equipped with adhesive borders (**Fig. 6**). They are not fit for minimal exudate wounds as they are too drying, and they may also produce a malodorous odor during use. Bioactive foam dressings which release agents such as antimicrobials, moisturizers or anti-inflammatory analgesics into the wound are also available<sup>24–26,30,31</sup>.



**Figure 6.** Examples of currently marketed foam dressings **a)** with adhesive borders and **b)** without adhesive borders.

**Hydrocolloid dressings (Fig. 7)** consist of absorptive ingredients like carboxymethylcellulose, pectin or gelatin. They are an occlusive dressing, consisting of two layers, inner colloidal layer and outer water-impermeable layer, thus not allowing water, oxygen, or bacteria into the wound<sup>11</sup>, and only being able to absorb minimal to moderate amounts of exudate. They are conformable to the patient's body and adhere well to high-

friction areas, such as the heels, and can be worn for several days before changing, thus decreasing supply costs and pain associated with dressing changes. Hydrocolloids are suited for more superficial wounds, pressure ulcers, burns, and graft donor sites due to its occlusive nature. Disadvantages include the risk of contact dermatitis, low mechanical stability, opaqueness and an unpleasant odor from a yellow gel formed under the dressing. Patients should be counseled to expect this as it may be confused with infection <sup>7,30,31</sup>.



**Figure 7.** Examples of currently marketed hydrocolloid dressings **a)** with adhesive borders and **b)** without adhesive borders.

**Alginate dressings** are available in non-woven fibrous sheets and ropes (**Fig. 8**). The alginate forms a gel when it was in contact with wound fluid, absorbing up to 20 times of their weight in wound fluid, which makes them effective for wounds with moderate to heavy exudate. They can remain in place for several days, thus requiring less frequent dressing changes. However, as alginates are highly absorbent, they should not be used with dry wounds or wounds with minimal drainage as its removal can then be painful. Additionally, alginates require a secondary dressing to secure the alginate since its high porosity and non-adhesive properties leads to low attachment to the skin, which increases the cost per dressing change. Another disadvantage of alginates is their tendency to allow wound fluid to collect between the dressing and surrounding intact skin; leading to undesirable maceration<sup>25,30,31</sup>.



**Figure 8.** Examples of currently marketed alginate dressings.

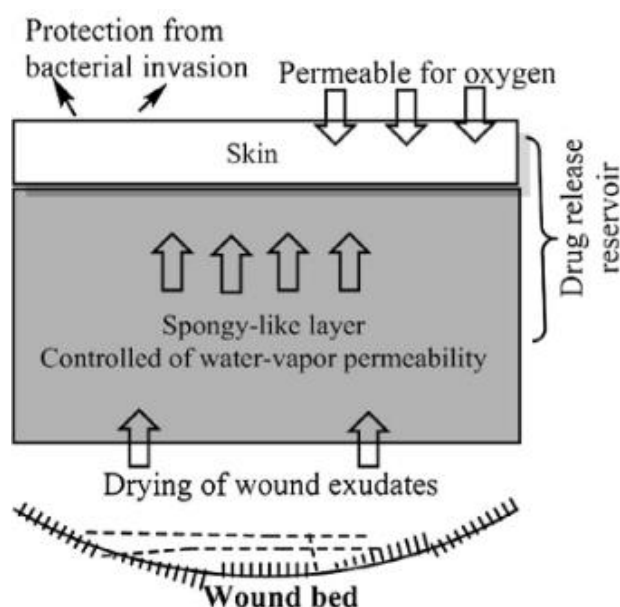
**Hydrogel dressings** are three-dimensional water- or glycerin-based products available in three forms: amorphous gel, impregnated-gauze, and sheet hydrogel (**Fig. 9**). They have high moisture content (70 - 90%)<sup>11</sup> that gifts the dressing with cushioning and cooling properties that make the dressings' removal easy and painless, and as they are transparent, wound monitoring can be done without removing the dressing<sup>32,33</sup>. Hydrogels can be used on a wide variety of wounds that need a moist environment as pressure ulcers, dry chronic wounds, surgical wounds, and burns, however, they display weak mechanical properties, thus demanding a secondary dressing<sup>7,30</sup>. Furthermore, the high content in water makes exudate absorption limited, and thus can lead to skin maceration. Hydrogel dressings that act as a release platform have also been developed containing hyaluronic acid, antimicrobials and antibiotics<sup>7,30,32,33</sup>.



**Figure 9.** Examples of currently marketed hydrogel dressings: **a)** amorphous gel, **b)** impregnated gauze, and **c)** sheet.

Currently, to try help in the healing of persistent wounds and in the development of an ideal dressing, bioactive dressings capable of delivering active substances with a direct role in the wound healing process or being made of such material, as antimicrobials and antibiotics, collagen or enzyme debriding agents, have risen in interest<sup>8,29</sup>. Thus, the development of bioactive dressings capable of active interaction with the wound has the potential to become the next generation of wound dressings. Still, despite all the efforts in recent times, no wound dressing developed until now has all the requirements for an ideal wound dressing, and, as such, research in this field is still necessary. The ideal wound dressing (**Fig. 10**) should adequately absorb wound exudate, be impermeable to bacteria, maintain a moist environment, have sufficient mechanical stability, good gas exchange, nontoxic/nonallergenic properties, thermal insulation, allow minimal frequency of dressing

change, ease of application and removal, long shelf-life, and be comfortable and conformable, cost effective, and promote wound healing through its base material and/or be able to release wound healing mediators and/or antibacterial compounds, according to the wound requirements<sup>4,8,12,27</sup>.



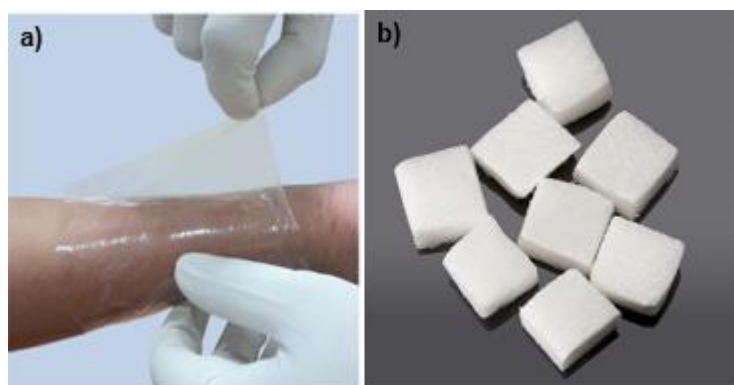
**Figure 10.** Scheme of an ideal wound dressing membrane. Adapted from Kamoun *et al.*<sup>34</sup>

## 1.5 Wound dressings from natural polymers

Different synthetic polymers, as polylactic acid (PLA), polyglycolic acid (PGA), polycaprolactone (PCL), polyurethane (PU), polyvinyl alcohol (PVA), polyethyleneoxide (PEO), and polyethyleneglycol (PEG), among others, have been used to produce scaffolds for use in wound management and tissue engineering<sup>8</sup>. Synthetic polymers' strength over natural polymers scaffolds is their easy stability and reproducibility, making their industrial production easier to be scaled-up compared to the natural polymers, while their main limitation lies on their lack of biocompatibility<sup>6</sup>. Thus, wound dressings made from natural origin polymers can serve as a good alternative to synthetic ones due to their biocompatibility, biodegradability, nontoxicity, non-inflammatory biological characteristics, ease of availability and abundance, and similarities to the ECM<sup>8,29,35</sup>. These polymers can be classified into four categories based on their structure, as polysaccharides (cellulose, alginate, dextran, chitosan, and pullulan), polypeptides and proteins (collagen, gelatin, fibrinogen, elastin), polynucleotides (DNA, RNA), and polyesters (polyhydroxyalkanoates, PLA), although polysaccharides and proteins are the most

common natural polymers used under the field of tissue engineering<sup>29,35</sup>.

**Collagen** is the major protein component of the ECM<sup>5,8</sup>, and as such, dressings based on this polymer have excellent biocompatibility. Multiple scaffolds based on this material as nanofibers, hydrogels and sponges have been developed to be used as wound dressings (**Fig. 11**)<sup>5,6,36</sup>. Collagen sponges, for example, have high porosity and high exudate absorption useful for high exudate wounds like burns, but limitations like high cost of production and difficulty in storage prevent it from widespread use<sup>36</sup>. Furthermore, they have poor mechanical stability as they are rapidly degraded<sup>5,6</sup>. **Gelatin**, a protein derived from collagen, has also been used in the production of films and sponges wound dressings with lower immunogenicity and greater cell adhesion than collagen, but also shows low mechanical strength<sup>5,6</sup>. **Fibrin** glues in the form of suspension, gel, membrane, or sheets have also been used due to characteristics as reduced inflammation, immune response, toxicity, and enhanced cell adhesion, and for the release of growth factors, cytokines or other bioactive molecules like delivering keratinocytes to burn wounds<sup>5,6,8</sup>. Crosslinking techniques and combinations with artificial materials or inorganic fillers have shown to be able to solve protein-based polymers' main drawbacks as wound dressing, low mechanical stiffness, and allow the production of scaffolds with enhanced mechanical properties, although their biocompatibility can be affected<sup>5,8,29</sup>.

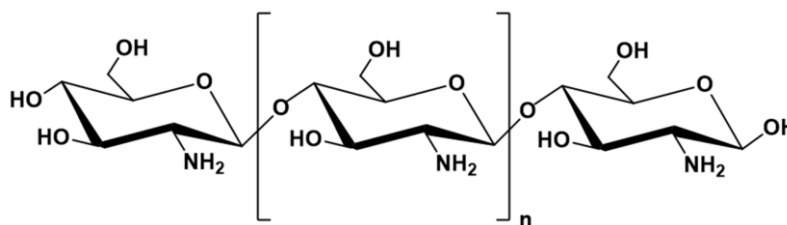


**Figure 11.** Examples of currently marketed **a)** collagen film and **b)** collagen sponge.

Looking to the polysaccharide-based polymers, chitin, chitosan, alginate, and hyaluronic acid have been the most broadly explored for use in nanostructured dressings development<sup>6,8</sup>. **Chitin** is an abundant natural polymer obtained from crustacean exoskeletons (crabs, shrimps) or generated via a fungal fermentation process. It is a homopolysaccharide made of N-acetyl-D-glucosamine residues linked through  $\beta$ -(1, 4)-glycosidic bonds<sup>37,38</sup>. **Chitosan** (produced by deacetylation of chitin) (**Fig. 12**) and chitin are

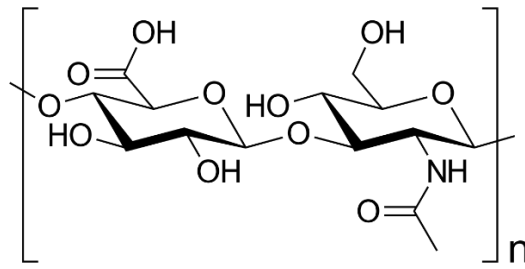


non-toxic, biodegradable, and biocompatible in nature and have been used in open wounds in various forms such as gels, powders, films, and fibers due to their high durability, good cell binding capacity, good liquid absorption and anti-bacterial and anti-fungal activity<sup>4,6,38</sup>. In addition, chitosan has been shown to promote collagen and hyaluronic acid synthesis, fibroblast proliferation, cytokine production and angiogenesis<sup>5,6,37,38</sup>. The major drawbacks of this kind of dressing are its high cost and water permeability, and low tensile strength and flexibility, which limits its storage and application<sup>4,38,39</sup>. **Alginate** is also a natural polysaccharide, extracted from algae, that has been shown to be widely in highly exuding wounds and burns due to its good absorption, hemostatic, and anti-microbial properties<sup>6,29,35</sup>. The use of chitosan in combination with alginate, for wound dressing, is also well documented<sup>4,8</sup>.



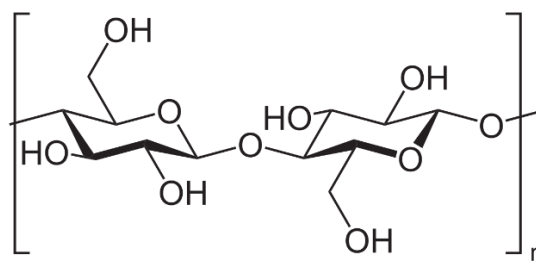
**Figure 12.** Chemical structure of chitosan.

**Hyaluronic acid (HA)** is a main component of the extracellular matrix (ECM) and is involved in the inflammatory response, angiogenesis, and tissue regeneration process during wound healing<sup>40</sup>. It is a highly hydrophilic glycosaminoglycan (**Fig. 13**)<sup>37</sup>, and thus facilitates nutrient diffusion, helps to rid the wound of metabolic waste products and controls hydration during the wound healing process<sup>4</sup>. In addition, HA is involved in the fibrin clot formation and in keratinocyte migration and proliferation<sup>4,40</sup>. However, its performance as a wound dressing and its role in the wound healing process in general are dependent on factors like the pH and temperature of the site and the molecular weight of the HA used, going as far as delaying the process in certain conditions<sup>40</sup>. HA-based commercial dressings are already available in the form of films, gels, sponges and membranes, among others, but possess high production costs, weak cell adhesion/proliferation capability and mechanical stability, fast degradation and high solubility<sup>4,40</sup>. Blending techniques have tried to solve some of these problems<sup>40</sup>.



**Figure 13.** Chemical structure of hyaluronic acid.

**Cellulose** is the most abundant naturally occurring polysaccharide in nature, being produced by bacteria or plants. It is a homopolysaccharide formed out of  $\beta$ -D-glucopyranose residues linked through  $\beta(1,4)$  glycosidic bonds (**Fig. 14**). Although microbial and plant cellulose are chemically identical, microbial cellulose is much more of a “pure” material when compared to plant cellulose, which is associated with hemicelluloses, lignin, and pectin. Microbial cellulose has excellent hydrophilicity, water-uptake capacity, permeability, and tensile strength, making it a much more attractive wound dressing material compared to plant cellulose. Additionally, it can help wound healing through regulation of angiogenesis and formation of connective tissue<sup>37</sup>. Cellulose wound dressings can also be used as healing scaffold/matrix for partial- and full-thickness chronic wounds, as it stimulates the granulation and epithelialization process. The modification of cellulose has also shown feasibility in the incorporation by co-immobilization of different active molecules such as enzymes, antioxidants, hormones, vitamins and antimicrobial drugs, since it lacks functionalization such as antimicrobial activity<sup>29</sup>.

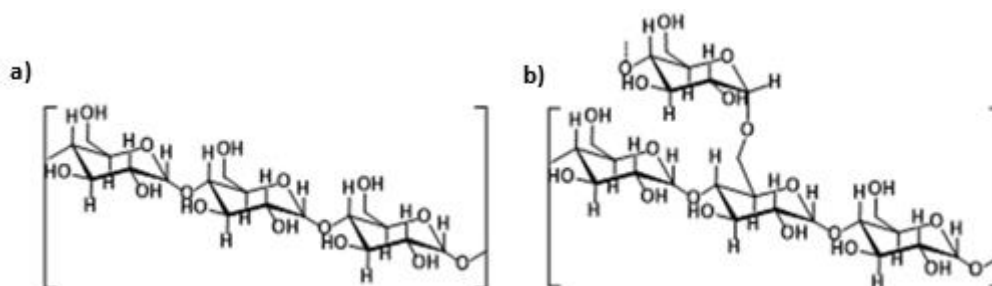


**Figure 14.** Chemical structure of cellulose.

**Starch** has also been explored as a material for the production of films, hydrogels, hydrocolloids, ointments and nanofibrous scaffolds with potential to be used as wound dressings<sup>41</sup>. Most of these efforts have been centered around the use of chemically modified starch or blends with synthetic polymers due to starch’s high hydrophilicity, and as starch shows no antimicrobial activity in its native state, it needs to be functionalized with

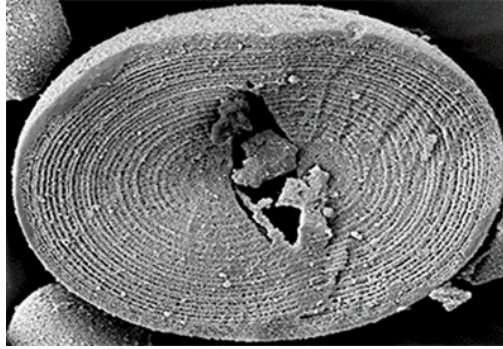
antimicrobial agents to prevent wound-related infections<sup>37</sup>. Since starch was the biopolymer selected in this thesis, its structure and applications as a wound dressing will be discussed in more detail.

Starch is a molecule composed by two types of polysaccharides, amylose and amylopectin, both made of chains of D-glucopyranose residues. In amylose, these residues are mainly linear joined by ( $\alpha$ 1,4) glycosidic bonds (degree of polymerization about 6000) (**Fig. 15a**), while in amylopectin the D-glucopyranose chains are highly branched with ( $\alpha$ 1,6) bonds (degree of polymerization about 2 million) (**Fig. 15b**)<sup>35,42–45</sup>.



**Figure 15.** Chemical structure of **a)** amylose and **b)** amylopectin.

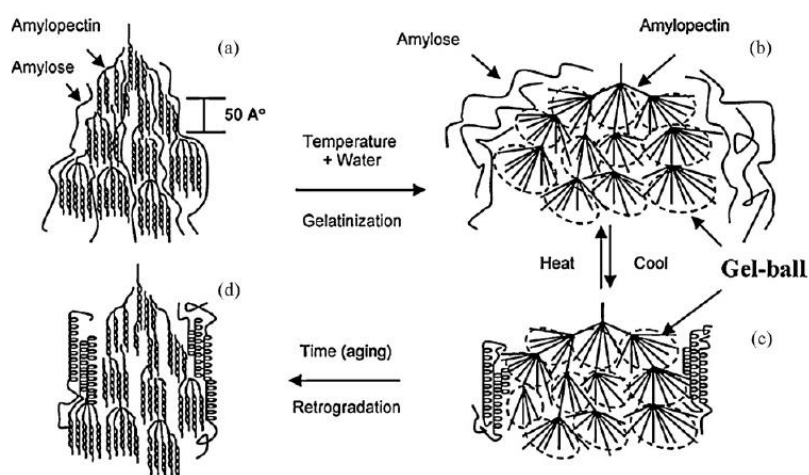
Starch is an abundant compound present in green plants, occurring naturally in the form of granules in the stem, tuberous tissues, and seeds of plants, and also in algae and certain bacteria, serving as the main energy reserve in plants<sup>35,43–49</sup>. The potato, for example, is known to be one of the most abundant and common sources of starch, alongside other tuber, roots and cereals<sup>43</sup>. Starch granules are made up of an amorphous nucleus of disorganized amylose and amylopectin molecules, surrounded by alternating concentric rings of amorphous material (amylose and amylopectin side chains) and semicrystalline (predominantly amylopectin) (**Fig. 16**), where the molecules are organized into double helix conformations<sup>43–49</sup>. The amylose/amylopectin ration varies based on the botanical origin, genetic background and growing conditions, but average values are of about 20–25% amylose and 75–80% amylopectin by weight<sup>35</sup>.



**Figure 16.** Scanning electron microscope image of a starch granule. Adapted from Pilling *et al.*<sup>47</sup>

Other non-carbohydrate compounds in starch granules contribute at most only a few per cent by weight, but includes lipids, proteins, ashes, and phosphates<sup>35,42,49</sup>. Lipids, when present, tend to form a helical complex with amylose, causing a reduced water binding capacity, clarity, swelling and stability of starch molecule<sup>35,42,49</sup>. Meanwhile, protein plays a critical role in formation of clear and transparent solution<sup>35</sup>. Phosphate in the form of monophosphate causes increased viscosity, clarity, improved stability of solution and also leads to slow retrogradation rate in tubers and roots<sup>35,42,49</sup>. In addition to phosphorus, trace amounts of other elements such as potassium and magnesium are also relatively abundant<sup>43</sup>.

Starch is widely used as thickener, gelling agent, glue, and water retainer in food industries and paper companies<sup>44</sup>. This versatility arises from its gelatinization capacity, when in the presence of plasticizers and under the influence of temperature. Indeed, when a dispersion of starch is heated above its gelatinization temperature, the water penetrates the starch granules and causes their swelling and bursting by the disruption of hydrogen bridges established between molecules' hydroxyl groups. As a result, the initial crystalline order is lost, leading to the formation of an amorphous gel, constituting the gelatinization process (**Fig. 17**). With the cooling of this gel, the hydrogen bonds previously lost are re-established in a stronger manner than initially observed, causing consequent solvent syneresis<sup>35,44–46,48</sup>. This process constitutes the retrogradation of starch which, in conjunction with solvent evaporation, allows to obtain a homogeneous film with structural, mechanical, and physicochemical characteristics very different from the initial dispersion<sup>35,46</sup>.



**Figure 17.** Schematic representation of starch gelatinization and retrogradation processes. Adapted from Liu *et al.*<sup>45</sup>

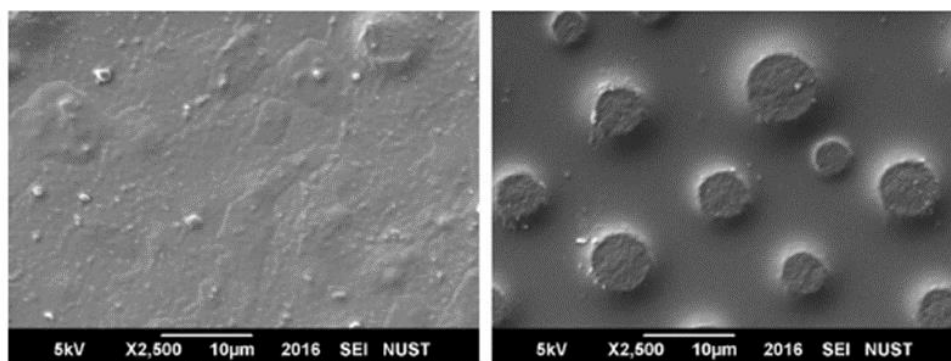
Starch-based films are described as isotropic, odourless, tasteless, colourless, and non-toxic. Nevertheless, starch can originate resistant and rigid films, thus with diminished extensibility<sup>44,45,50</sup>, which limits their application range. These structural characteristics are mainly the result of the extensive retrogradation that potato starch suffers when gelatinized due to a high amylose content (about 30% amylose, on average)<sup>43</sup>, compared to starch from other plant sources, as the linear conformation of amylose is representative of a greater facility of re-establishing the hydrogen bonds between molecules, when compared to amylopectin<sup>44,49,51</sup>. The addition of plasticizer agents emerges as a solution to this fragility, improving its flexibility. These agents should be compatible with the starch polymers responsible for the films' matrix and should be able to decrease the intermolecular forces and increase the polymeric chains mobility. Thus, the use of plasticizers increases the intermolecular space and consequently minimize the retrogradation extension, which in turn decreases the films rigidity. An example of a common compound used as a plasticizer agent in the production of starch-based films is glycerol: it increases the extensibility of films, but reduces their elasticity, also reducing tensile strength<sup>45,50,52</sup>. Moreover, starch-based films, due to the various hydroxyl groups in the starch's glucose residues, are hydrophilic and very sensitive to moisture conditions. To overcome these drawbacks and thus improve mechanical and psychochemical performance, the incorporation of hydrophobic compounds has been studied, including the incorporation of phenolic compounds. Piñeros-Hernandes *et al.*<sup>53</sup> incorporated antioxidant rosemary extract into cassava starch-based films (5%(w/V)) and observed that the surface hydrophobicity of the active films was affected as they achieved 40% higher contact angle values (about 51°) than the control

ones (about 37°), and water vapor permeability and mechanical properties of the active films were also positively affected. Gonçalves *et al.*<sup>54</sup> studied the incorporation of oil and waxes recovered from potato chip byproducts into starch-based films, and found that both increased starch films' hydrophobicity, though oil's triacylglycerides caused a higher water contact angle variability than the waxes, who were richer in phenolic compounds.

Furthermore, the absence of active properties decreases the interest of using starch-based films in high value applications like clinical applications. To this end, several biomolecules have been incorporated into starch-based formulations in order to improve not only their mechanical and physicochemical properties but also to assign antioxidant<sup>39,53,55</sup>, UV-protective<sup>53,56</sup>, and antimicrobial properties<sup>55,57</sup>, among others. Herein, the incorporation of anti-inflammatory and/or anti-microbial compounds like essential oils, proteins, and vitamins have been explored. Bonilla *et al.*<sup>39</sup> synthesized glycerol-plasticized wheat starch and chitosan blend films (4:1) with added antioxidants, namely basil essential oil, thyme essential oil, citric acid, and  $\alpha$ -tocopherol, to test improvements in the functionalization of the films via antioxidant activity. The antioxidants were added at a starch:antioxidant mass ratio of 1:0.1. The greatest antioxidant capacity of the films was reported for films containing  $\alpha$ -tocopherol. In addition, some of the antioxidants incorporated also modified the films' mechanical and physicochemical properties: oxygen barrier properties were significantly improved in all cases, while water vapour barrier properties were slightly improved with citric acid and  $\alpha$ -tocopherol addition. The improvement of these properties is beneficial against microbial growth. Citric acid also promoted an increase in the elastic modulus, but a decrease in film stretchability. Piñeros-Hernandes *et al.*<sup>53</sup> obtained antioxidant cassava starch-based films via incorporation of rosemary extract. The polyphenols content of the active films ranged between 4.4 and 13.6 mg GA/g, with the films showing an increase in their antioxidant activity in a polyphenols dose-dependent manner. Pyla *et al.*<sup>57</sup> incorporated fresh and thermally processed tannic acid (FTA and PTA, respectively) into starch-based films to test its functionalization in relation to antimicrobial activity. Inhibition of *Escherichia coli* O157:H7 and *Listeria monocytogenes* was assessed by two methods. Disc-diffusion assay revealed that the PTA/starch film showed larger inhibition zones than the FTA/starch film at the same tannic acid concentrations (0.45 mg to 4.5 mg per disc). Viable cell count assays also showed that the PTA/starch film had stronger antimicrobial activity on the pathogens tested than the FTA/starch film: *L. monocytogenes* multiplied up to 9.22 log CFU/ml and *E. coli* had a 5-log reduction at 48 h of incubation with the FTA/starch film, while the PTA/starch film caused a 2.72 log decrease in *L. monocytogenes* cells and a 7-log reduction in *E. coli* cells over the same time period.

Moreno *et al.*<sup>55</sup> developed glycerol-plasticized potato starch-based films containing 0.1% (w/w) lactoferrin, 0.2% (w/w) lysozyme, or a 1:1 ratio of both by casting to test the incorporation of antimicrobial activity into the films as both proteins contain antimicrobial properties. The films were characterized as to their mechanical, psychochemical and antioxidant and antimicrobial properties. The incorporation of lactoferrin, especially, increased the film's brittleness, although it also enhanced the water vapor and oxygen barrier properties, and a synergistic antimicrobial action against *E. coli* and coliforms was observed when both proteins were simultaneously applied.

In terms of specific wound dressing application, the developed work is focused in the preparation of starch-based scaffolds and hydrogels containing natural compounds with bioactive properties. Pal *et al.*<sup>32</sup> developed corn starch/PVA blend-based hydrogels by crosslinking with glutaraldehyde of 10%(w/V) of PVA with 5% (w/V) heat-treated corn-starch suspension. The membrane obtained showed higher mechanical strength than human skin and was cytocompatible, having heightened the proliferation of mouse fibroblasts at a rate of 1.49 in comparison to the no hydrogel control. In addition, it also showed a good diffusion coefficient suitable for the delivery of vitamins/healing factors, thus possessing potential to be used as a wound dressing and even aiding in tissue repair and in drug delivery. Hassan *et al.*<sup>33</sup> also developed similar starch/PVA hydrogels with added turmeric (**Fig. 18**) to confer the gels with antimicrobial properties. Anti-bacterial activity against gram-negative *E. coli* and gram-positive *S. aureus* bacterium was observed with increase of turmeric content until the 0.5 g mark, for a maximum inhibition zone of 9.9 mm and 11.3 mm, respectively, after which no further increase in anti-bacterial activity was observed. Similarly, the membrane also registered higher tensile strength than human skin. It also showed lower water vapor transmission (WVT) rate and higher moisture retention values when compared to the control, which is beneficial to wound healing.



**Figure 18.** SEM images of control hydrogel membrane (left) and hydrogel membrane with turmeric (right). Adapted from Hassan *et al.*<sup>33</sup>

Ramnath *et al.*<sup>58</sup> studied the efficacy of composite biomaterials made of soya protein (2%) and sago starch (10%) (1:6) crosslinked with glutaraldehyde (1  $\mu$ L) as temporary wound-dressing materials using the rat as an animal model. Full-thickness 4 cm<sup>2</sup> excision wounds were made on the back of male rats, followed by the application on the wounds of the dressings developed and cotton gauze impregnated with gentamicin for control. These were changed periodically at an interval of 4 days. The wounds treated with the films healed completely on 20<sup>th</sup> day after wound creation, while the control only showed complete healing on the 25<sup>th</sup> day. The composite adequately absorbed excess exudates and maintained a moist environment at the wound site and also showed a significant increase in total collagen and in the rate of wound contraction. Other works tested the antimicrobial ability of starch-based composite materials with incorporated compounds such as antibiotics<sup>59</sup>, zinc oxide<sup>60</sup>, citric acid<sup>61</sup>, and silver nanoparticles<sup>62</sup>.

## **1.6 Food for materials: economic constraints and byproducts as a solution**

One of the biggest difficulties in transposing the starch-based formulations, till now developed, into mass-produced products is the starch's origin. Currently, starch-based materials are produced using starch directly extracted from foodstuffs, whose primary application should be feeding. The competition between the materials development and the food industry is not economically or ethically sustainable, and thus, new low-cost and sustainable alternatives must be explored. Herein, the use of non-value renewable resources such as the agrifood byproducts should be addressed. Total food waste produced during the whole food producing and distribution chain (from farmers to consumers) were accounted as 88 billion tons, in 2012, within the EU-28, resulting in about 20% of all food produced being wasted<sup>63</sup>, while on a global level, approximately one third of all food produced is wasted throughout the food value chain annually, amounting to about 1.3 billion tons per year according to FAO<sup>64</sup>.

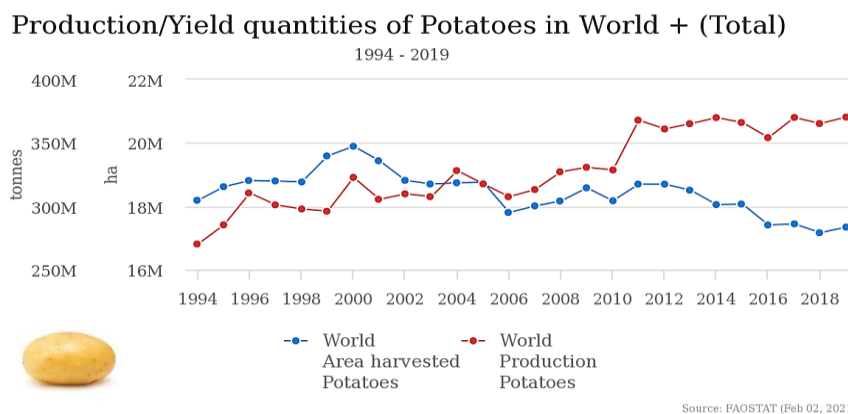
Agrifood byproducts generated during industrial processing of crops are often disposed of or delegated to be used as animal feed, plant fertilizer, composting, and biogas material, despite often being valuable sources of bioactive compounds. Thus, instead of simply being discarded or being relegated to non-high value applications, agrifood industry byproducts should be integrated into new industrial processing chains. Many agrifood byproducts have underexplored potential to be used as resources for the obtention of bioactive compounds, such as antioxidant carotenoids, phenolic compounds, essential oils, or valuable proteins and polysaccharides, like starch,  $\beta$ -glucans, and lignin. In turn, these can be used as functional ingredients or additives in the food industry due to their health



properties, or to increase products' properties, like color, smell, texture or flavor, or nutritional value. Similarly, these compounds can be used for development of new materials, as polysaccharides and proteins can serve as sturdy and reliable base materials, that can then be functionalized with bioactive compounds with antioxidant or antimicrobial and be applied as active packaging, edible coating, or as a wound dressing, an alternative that remains underexplored<sup>65</sup>.

### 1.6.1 Potato

Potato is the edible root of the plant *Solanum tuberosum* and is the most in-demand vegetable in the world (**Fig. 19**), having reached a production of 370 million tons in 2019<sup>1</sup>.



**Figure 19.** World potato production and area harvested per year. Adapted from FAOSTAT.

Besides its fresh consumption, potatoes can be processed into various products as frozen preparations, chips, soups, purée, flour, gnocchi, pancakes, and all other kinds of potato-based snacks. In almost of these products' fabrication, potatoes must go through processes as washing and peeling, which results in the disposal of considerable amounts of byproducts mainly in the form of potato peels and wastewaters. Several ways have been studied to try and recycle both of these byproducts into high added-value products, with means of valorization of the potato peel being studied in the form of extraction of phenolic compounds from the peels, liquefaction via chemical or enzymatic means for substrate usage for ethanol production for biofuel or biopolyols applications, as well as extraction of volatile compounds for use as food aroma additives, among others<sup>65</sup>. Meanwhile, potato washing slurries have been shown to be rich source of starch, various nutrients, enzymes, and microbial oils<sup>66</sup>. Washing, peeling, blanching, slicing, or frying operations generates wastewaters with high starch content, and studies have proven that up to 60% of such starch can be recovered<sup>3</sup>. However, potato washing slurries have been underexplored, with

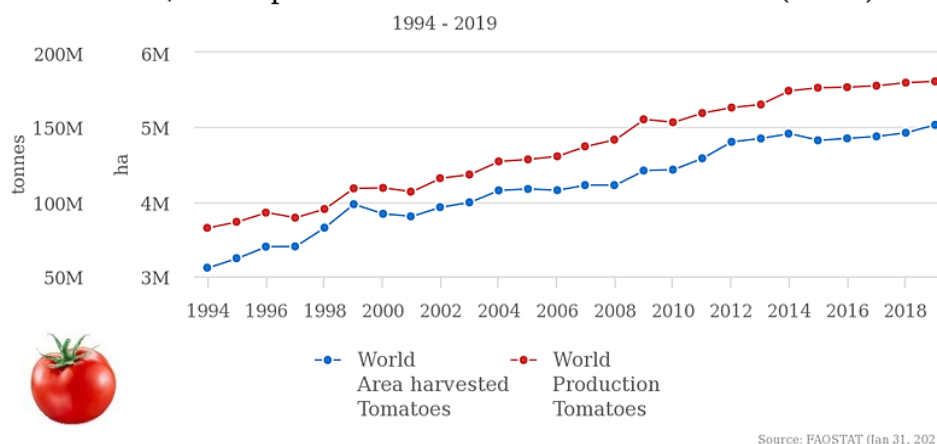
applications limited as media to produce fermentation products or for the recovery of starch, which then is applied in the general areas that a commercial starch is applied. But starch recovered from this byproduct can give rise to other applications, including the production of thermoplastics films, which have the potential be applied into various areas, the most popular being biodegradable packaging, while other areas include its' application as wound dressing. By using starch recovered from the potato industry byproducts for the development of such products, direct competition with the food industry because of the use of commercial starch can be avoided and, instead, a sustainable production of new products can be achieved, all the while contributing for a circular economy. This proper valorisation of valuable compounds can also be extended to develop and functionalize starch-based materials.

The natural original of bioactive compounds are also often utilized in the food industry, as is the case of essential oils, vitamins, and spices, and so, would also generate competition with this industry. In addition, a higher content of these molecules can sometimes be found in agrifood byproducts discarded rather than in the parts used in industrial processing, so can byproducts valorisation take an even higher economic importance.

### 1.6.2 Tomato

Tomato (*Solanum lycopersicum* L. syn. *Lycopersicon esculentum* Mill., Fam. Solanaceae) is the world's second most in-demand vegetable crop after potatoes<sup>67,68</sup>: According to FAO, in 2019, tomato world production reached about 180 million tons, in comparison to potatoes' 370 million tons<sup>1</sup> (**Fig. 20**). In Europe, both Italy and Spain contributed about 30% of tomato production in the EU-28 in 2019<sup>67,69</sup>, with Portugal being third (9%), in a total EU-28 production of 16.6 million tons<sup>69</sup>. This was also the year where tomato production in Portugal reached its all-time high, with 1.4 million tons<sup>67,70</sup>, with a production of 1.2 million tons foreseen for 2020<sup>71</sup>.

## Production/Yield quantities of Tomatoes in World + (Total)



**Figure 20.** World tomato production and area harvested per year. Adapted from FAOSTAT.

From the chemical point of view, tomato is an important source of proteins and essential amino acids as lysine, carbohydrates and sugars as fructose and glucose, lipids, like polyunsaturated fatty acids as octadecadienoic acid, and bioactive compounds, as carotenoids like  $\beta$ -carotene and lycopene, vitamins, like vitamins C and E, phenolic compounds, like rutin and quercetin, and minerals, like calcium and potassium<sup>68,72–74</sup>. Depending on the fruit's ripening stage and cultivar, over 500 to 800 of different bioactive compounds have been detected<sup>75</sup>. **Table 2** has the tomato's nutritional composition.

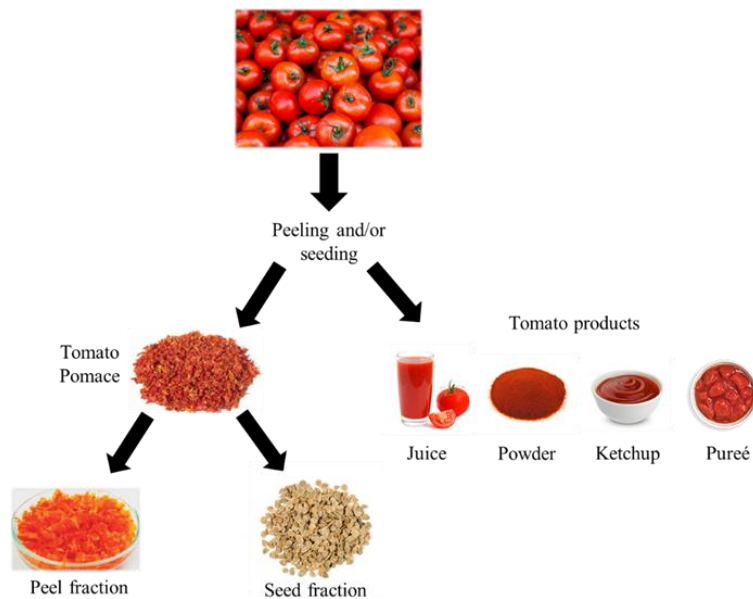
**Table 2.** Nutritional composition of tomato. Adapted from the USDA reference database<sup>76</sup>.

Tomato composition (%)	
Protein	0.88
Fat	0.20
Carbohydrates	3.89
Ash	0.50
Water	94.52

According to the USDA database for food nutrition, tomato is composed of, mainly, water, making up 94.5% of tomato. Next, carbohydrates make up the second biggest portion of tomato, being about 3.89%, including 1.20% of non-starch polysaccharides and 2.63% of sugars, of which fructose and glucose make up about 1.37 and 1.25%. Protein makes up about 0.88% of tomato and includes 18 of the 20 standard amino acids. Fat in tomato makes up only about 0.20%, and includes polyunsaturated fatty acids (0.08%), specifically

octadecadienoic acid, monounsaturated fatty acids (0.03%), specifically octadecenoic acid, and saturated fatty acids (0.03%), specifically hexadecenoic and octadecanoic acids. Minerals in tomato include  $\text{Ca}^{2+}$ ,  $\text{Cu}^{2+}$ ,  $\text{F}^{-}$ ,  $\text{Fe}^{2+}$ ,  $\text{Mg}^{2+}$ ,  $\text{Mn}^{2+}$ ,  $\text{P}^{3-}$ ,  $\text{K}^{+}$ ,  $\text{Na}^{+}$ , and  $\text{Zn}^{2+}$ , with ash making up about 0.50% of tomato. Bioactive compounds include lycopene,  $\alpha$ - and  $\beta$ -carotene, lutein and zeaxanthin, vitamin A, thiamin, riboflavin, niacin, pantothenic acid, vitamin B6, folate, vitamin C, vitamin K and vitamin E, including  $\alpha$ -,  $\beta$ - and  $\gamma$ -tocopherol, as well as  $\alpha$ -tocotrienol<sup>76</sup>. The content of these bioactive compounds and their bioactivity is affected by environmental and genetic factors and agricultural practices, as well as processing conditions, among others, although some studies have also pointed out that some of them, like carotenoids, tocopherols, polyphenols, some terpenes and sterols seem to resist common processing techniques like heat treatments<sup>72,73</sup>. Still, the consumption of these compounds in tomato and tomato-based foodstuffs have commonly been associated to decreases in the risk of chronic degenerative diseases induced by oxidative stress and inflammation. Several studies have demonstrated anticarcinogenic, cardioprotective, and hepatoprotective of these bioactive compounds, either isolated or in combined extracts, mainly due to its antioxidant and anti-inflammatory properties<sup>68,77-79</sup>.

Tomato is one of the most versatile foods in term of forms of consumption in human diet, able of being processed in products such as paste, soup, juice, sauce, ketchup, purée, powder, or concentrate apart from its raw consumption<sup>2,68,80</sup>. From its yearly  $1.8 \times 10^6$  tons production, a quarter undergoes processing<sup>73</sup> and, as such, large amounts of byproducts are created in the form of tomato pomace (TP) (**Fig. 21**).



**Figure 21.** Scheme of the transformation of tomato and the byproducts generated.

The composition and yield of TP can widely vary depending on the processing techniques applied beforehand<sup>2,72,81</sup>. When the integral shape of the original fruit remains in the final product, such as in canned tomatoes, TP is only composed of peels without seeds. However, in the case of homogenized products, such as juice and paste, TP is a mixture of discharged peels and seeds plus a small amount of pulp<sup>2</sup> (**Fig. 22**).



**Figure 22.** Tomato pomaces obtained by different processing techniques: Hot break (**a** and **b**) and cold break (**c**). Adapted from Shao *et al.*<sup>81</sup>.

On average, TP accounts for approximately 1.5–5% (w/w) of the raw material<sup>80,82,83</sup>, and accounts for 5-30% (w/w) of the total waste of tomato processing<sup>72,84</sup>. As such, the total yield of TP can be estimated to be, roughly,  $2.7\text{--}9.0 \times 10^6$  tons per year. Currently, disposal and poor utilization of this by product leads to environmental burden and waste of valuable compounds of nutritional and pharmacological interest, as only lycopene extraction has generated some commercial interest, even though more than 100 secondary metabolites have been annotated in aqueous-methanol extracts of peel from ripe tomato fruits<sup>75</sup>, including valuable bioactive compounds, like flavonoids, phenolic acids, and vitamins with antioxidant activity, and others like polysaccharides, oil, and protein<sup>2,72,81,82,84–87</sup>. Thus, a proper valorization of this byproduct and its transformation into products of high added value can feed into the principle of circular economy.

The proximate compositions of whole TP as well as its components (peels and seeds) are reported below in **Table 3**.

**Table 3.** Proximate composition of tomato pomace and its peel and seed fractions. Adapted from Lu *et al.*<sup>2</sup>

Chemical composition (dry weight)						
Material	(mg/ 100 g)	(g/ 100 g)				Reference
	Lycopene	Polysaccharides	Protein	Ash	Fat	
Peel	-	78.6	10.5	5.9	4.0	84
	-	87.6–88.5	6.0–6.2	2.0–2.3	-	85

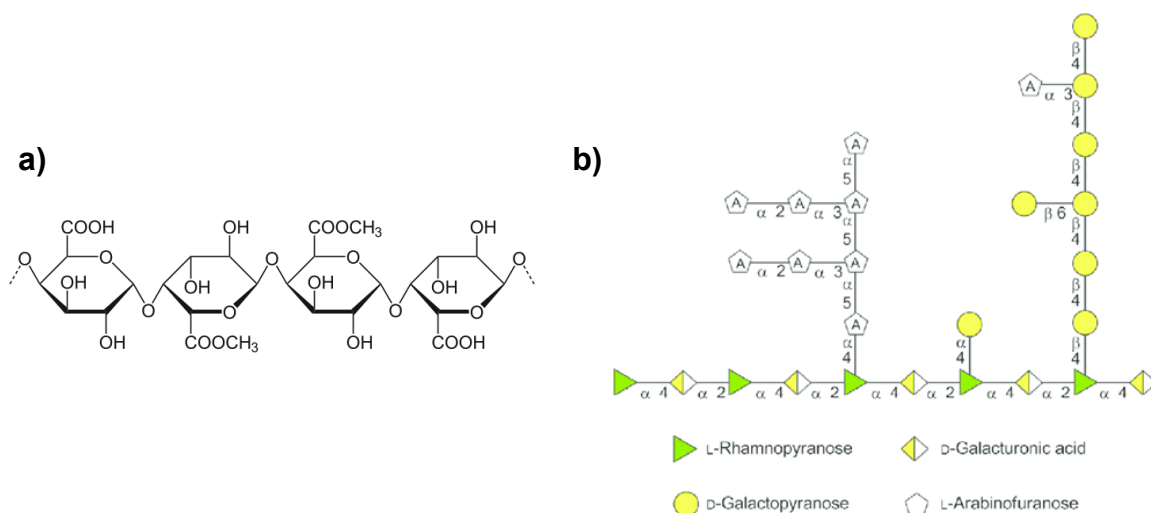
	-	74.5–76.7	11.0–11.1	4.9–6.5	4.9–5.5	88
	-	62.8–69.9	1.0–1.9	1.0–3.3	1.6–2.0	89
	-	-	23.3	3.9–4.2	3.5–6.2	90
	13.59	-	-	-	-	91
	7.36	-	-	-	-	92
	288	-	10.1	25.7	3.2	83
Seed	-	16.0	32.0	5.0	22.0	86
	-	-	27.2	3.4	17.8	93
	-	-	39.7	4.7–5.3	22.2–22.7	90
	-	-	23.60	3.64	24.5	94
	-	-	35.0–40.9	-	19.8–23.4	95
Pomace	-	59.0	19.3	3.9	5.9	82
	-	39.1	24.7	5.3	9.9	96
	9.8–17.2	58.5–68.0	15.1–22.7	2.9–4.4	8.4–16.2	81
	-	46.0	16.0	4.0	2.0	86
	-	48.6–54.0	16.8–23.2	-	11.2–16.7	80

It is generally known that tomato peel is rich in dietary fiber and lycopene, while the seed is rich in fat and protein<sup>80,81,84,97</sup>. Tomato peel dietary fiber values can reach a maximum of 88.53%, with lycopene reaching a maximum of ca. 0.3% (w/w)<sup>83</sup>. The phenols content in tomato peels is in the range of 0.158%<sup>2</sup>, being made of phenolic acids such as caffeic, procatechic, vanillic, catechin, gallic<sup>84</sup>, ferulic, sinapic, chlorogenic, *p*-coumaric, and trans-cinnamic acids, and flavonoids, such as quercetin-3-O- $\beta$  glucoside, rutin, isorhamnetin, kaempferol, naringenin, quercetin, apigenin, and myricetin<sup>2</sup>.

Tomato seeds' oil content was reported to be in the range of 0.0178 to 0.0245%, 80% of which are unsaturated fatty acids, mainly linoleic (0.376 – 0.727%) and oleic (0.0155 – 0.0297%) acids, as well as palmitic, stearic, and arachidic acids. Tomato seed oil also contains phytochemicals such as vitamin E, lycopene, policosanol, phytosterol,  $\beta$ -carotene, and phenolics. In addition to oil, tomato seeds also contain high amounts of protein (maximum of 40.9%), with high concentrations of amino acids, such as glutamic acid (max. 24.37%), aspartic acid (max. 10.32%), and lysine (max. 5.9%)<sup>2,80,97</sup>.

In relation to pomace, polysaccharides are the major compound of tomato pomace, ranging from 39.11% to 68.04%, with the predominant contribution being from the tomato peel, as its content in the seeds has only been measured by Fuentes *et al.*<sup>2,98</sup> to be about 16.00%<sup>86</sup>, while tomato peel presents values ranging from 62.79 up to 88.53%. The ratio of soluble:insoluble polysaccharides is about 1:5, mainly due to reduced pectin (**Fig. 23a**) content in comparison to insoluble polysaccharides like cellulose (**Fig. 14**), thus also being responsible for the pomace's low solubility. Pectin is a common component of fruits' cell walls and is composed of (1,4) D-galacturonosyl (GalUA) units. Pectic polysaccharides can

also contain (1,2) D-rhamnopyranosyl residues in the backbone, as well as side chains containing arabinosyl and galactosyl residues (**Fig. 23b**), for example<sup>99</sup>. Del Valle *et al.*<sup>82</sup>, for example, reported a 59.0% content of insoluble polysaccharides, while pectin (soluble polysaccharide) showed only to be about 7.55% of tomato pomace. Protein content ranges between 15.4% and 23.7% for total protein, 5.4% and 20.5% total fat, and 4.4% and 6.8% mineral content. While the information of total content of sugars in tomato pomace is scarce, Del Valle *et al.*<sup>82</sup> found it represented about 25.73% of tomato pomace with glucose, fructose and sucrose making up the top soluble sugars content from this material.



**Figure 23.** Chemical structure of **a)** pectin and **b)** pectic polysaccharide<sup>100</sup>.

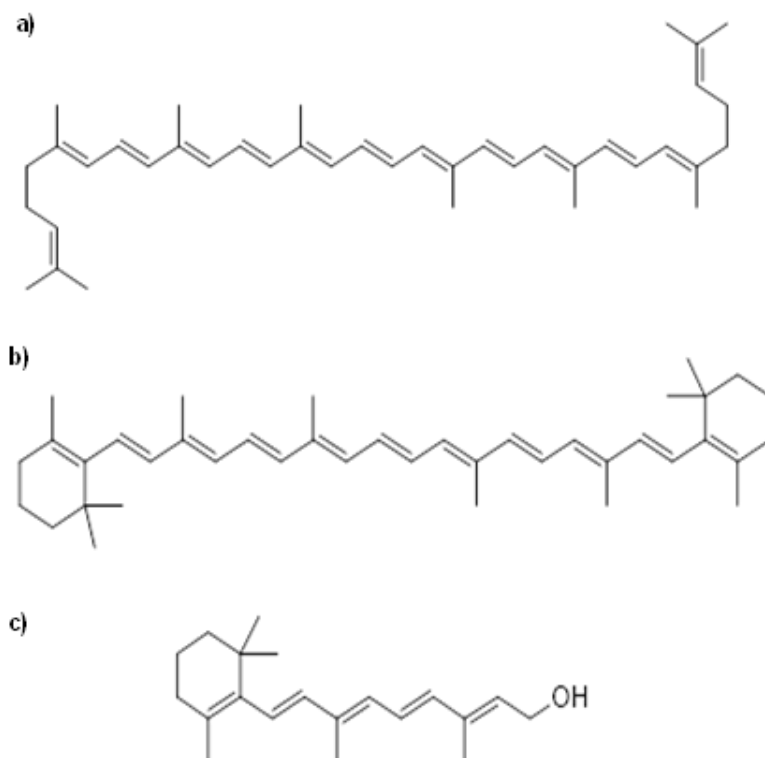
As is the case of all physical-chemical analysis, variability in the content of a certain class of compounds determined by various authors for either tomato peel, seed or pomace must be considered. These can be attributed to a number of different factors, as differences in the chemical composition of a crop or variety, maturity of the fruit, growth conditions, processing parameters, analytical methods employed as well as the raw material composition and processing conditions applied<sup>2,82</sup>. Extraction methods, for example, invariably affect the quantitative and qualitative yield of bioactive compounds as proteins, fibers, and phenolic compounds, as they employ different physical-chemical principles via ultrasounds, microwaves, ultrafiltration, electrical and high pressure-based technologies. Liquid extraction procedures yield varies according to the solvent used, as well as the temperature/pressure and time of processing, for example. High temperatures normally result in higher losses in heat-sensitive bioactive compounds yield in comparison to the use of pressure or ultrasound waves, as these allow lower processing temperatures, for example<sup>67,73,75</sup>.

The major bioactive compounds found in tomato are carotenoids. Carotenoids are a family of lipid-soluble antioxidants that share a tetraterpenoid structure (8 isoprene units) and a series of centrally located conjugated double bonds<sup>101</sup>. In nature, carotenoids act as pigments in plants and some algae and fungi, conferring the yellow, orange, and red colors to the producing organism like fruits and vegetables. Carotenoids normally possess outstanding antioxidant properties that can be beneficial to human health by enhancing the immune system and reducing the risk of the onset of degenerative diseases such as cancer, cardiovascular diseases, cataract and macular degeneration, but as they are only synthesized by plants and microorganisms, carotenoids must be consumed via dietary habits<sup>72,77,101</sup>.

Lycopene is the most abundant carotenoid in ripe tomato, representing about 80 to 90% of all carotenoids present, almost exclusively in the peel<sup>68,102</sup>. Lycopene has been attracting attention in the food, cosmetics, and pharmaceutical industries due to its high antioxidant potential, found to be the one with highest antioxidant activity amongst all carotenoids<sup>102</sup>. Lycopene is a highly unsaturated symmetrical acrylic isomer of  $\beta$ -carotene (**Fig. 24**), with 11 linearly conjugated and 2 unconjugated double bonds, the first of which is responsible for the deep red colour that lycopene possesses. In addition, it also confers lycopene with its high antioxidant potential, twice that of  $\beta$ -carotene (**Fig. 24**), despite the lack of the  $\beta$ -ionone ring structure responsible for provitamin A activity in  $\beta$ -carotene, for example<sup>68,101,103,104</sup>. The main disadvantage of lycopene is related to its low bioavailability, which depends not only on the different lycopene biochemical isoforms, but also on the dose and context of ingestion and on the genetics of each individual<sup>77</sup>. Lycopene naturally exists predominantly in all-trans configuration<sup>68,101–103</sup>, but may undergo cis isomerization as a result of food processing (due to heat, enzyme, oxygen, light etc). Even so, processed tomato products show better bioavailability than raw tomatoes, pointing towards better absorption of cis-isoform lycopene<sup>68,78,103,105</sup>. Tomato normally contain up to 0.01% (w/w) of lycopene, but a maximum of ca. 0.3% of lycopene content has been registered in tomato peels before<sup>83</sup>. This content varies depending on genetic, agricultural, and environmental factors and ripening stages, with lycopene content increasing as the fruit ripens<sup>68</sup>. In ripe red tomato fruits, the ratio of lycopene to  $\beta$ -carotene content varies widely between 1.5 and 40.  $\beta$ -carotene is a provitamin A carotenoid, i.e., it can be converted by the human body into two molecules of vitamin A (**Fig. 24**). In addition to lycopene and  $\beta$ -carotene, phytoene, phytofluene,  $\alpha$ -carotene,  $\zeta$ -carotene,  $\gamma$ -carotene, neurosporene, violaxanthin, neoxanthin, zeaxanthin,  $\alpha$ -cryptoxanthin,  $\beta$ -cryptoxanthin, cyclolycopene,  $\beta$ -carotene 5,6-epoxide and lutein are other carotenoids reported in tomato and tomato-based



products<sup>68,73,106,107</sup>. However, among these, only  $\alpha$ -carotene,  $\beta$ -carotene and  $\beta$ -cryptoxanthin have pro-vitamin A activity as they are the only ones subjectable to be converted to retinal by mammals<sup>107</sup>.

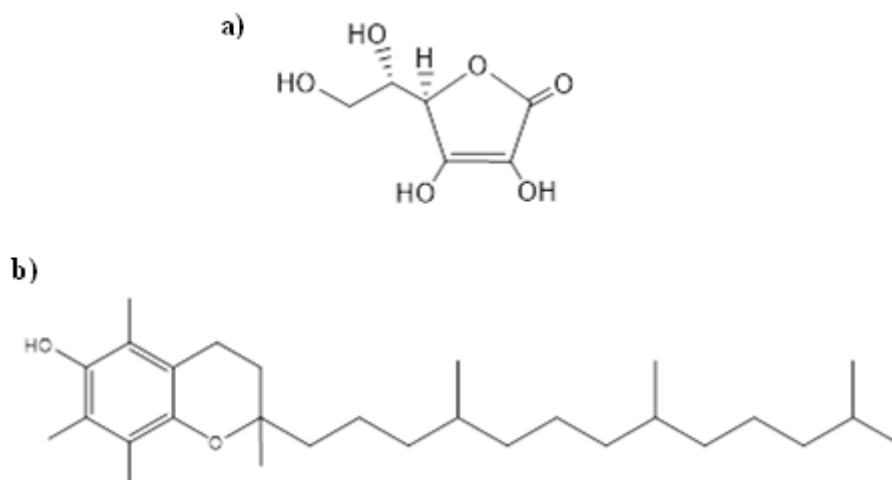


**Figure 24.** Chemical structure of **a)** lycopene, **b)**  $\beta$ -carotene, and **c)** vitamin A.

Vitamin C (L-ascorbic acid) and E (tocopherols and trienols, four of each) are the most abundant vitamins present in tomato. Vitamin C (**Fig. 25a**) is a powerful *in vivo* antioxidant and, as such, can act out various functions in the human body, including being an electron donor and participating in various molecules synthesis and metabolisms, including lipid, steroid and peptide metabolism, collagen synthesis, control of blood pressure and iron and copper balance, hemostasis, immune, endocrine, and endothelial function and fatty acid transport. Vitamin C has been found in high concentrations in immune cells and is consumed quickly during infections and hypothesis include that vitamin C modulates the activities of phagocytes, the production of cytokines and lymphocytes, and the number of cell adhesion molecules in monocytes. Unlike other antioxidants, vitamin C can act enzymatically and non-enzymatically to quench both oxygen radicals and other reactive oxygen species (ROS) by oxidizing to non-toxic molecules like dehydroascorbic acids (DHA). Vitamin C can also regenerate vitamin E when the later has been oxidized by

radicals. Vitamin C also has prooxidant effects in relation to transition metals such as copper and iron, generating ROS in turn, but no significance of these reactions has been reported *in vivo* so far. Different levels of ascorbic acid have been reported in tomatoes (0.008 - 0.021%), since it is affected by different factors such as genetic and environmental variations, like light exposure, as well as processing techniques such as thermal treatments, who are known to cause the loss of vitamin C content in foods<sup>68,108-110</sup>.

Vitamin E (**Fig. 25b**) is a lipophilic group of 8 molecules that share vitamin C's antioxidant and electron donating power, being described as a anti ROS cell membrane protector. Epidemiological studies have also shown that high intakes of vitamin E were linked to a reduced risk of cardiovascular diseases, and that vitamin E can act synergistically with lycopene in inhibiting leukemia and prostate carcinoma cell proliferation<sup>110</sup>. The amounts of tocopherols in tomatoes also vary in a range from 0.17 to 1.44 x 10<sup>3</sup> % (w/w). The tomato fruit also presents folates (12-18 µg/100 g of fresh weight), a complex group of water-soluble compounds known as vitamin B9. As humans are incapable of producing any of these vitamins, we are dependent on dietary sources like the tomato fruit for the intake of these compounds<sup>68,109</sup>.

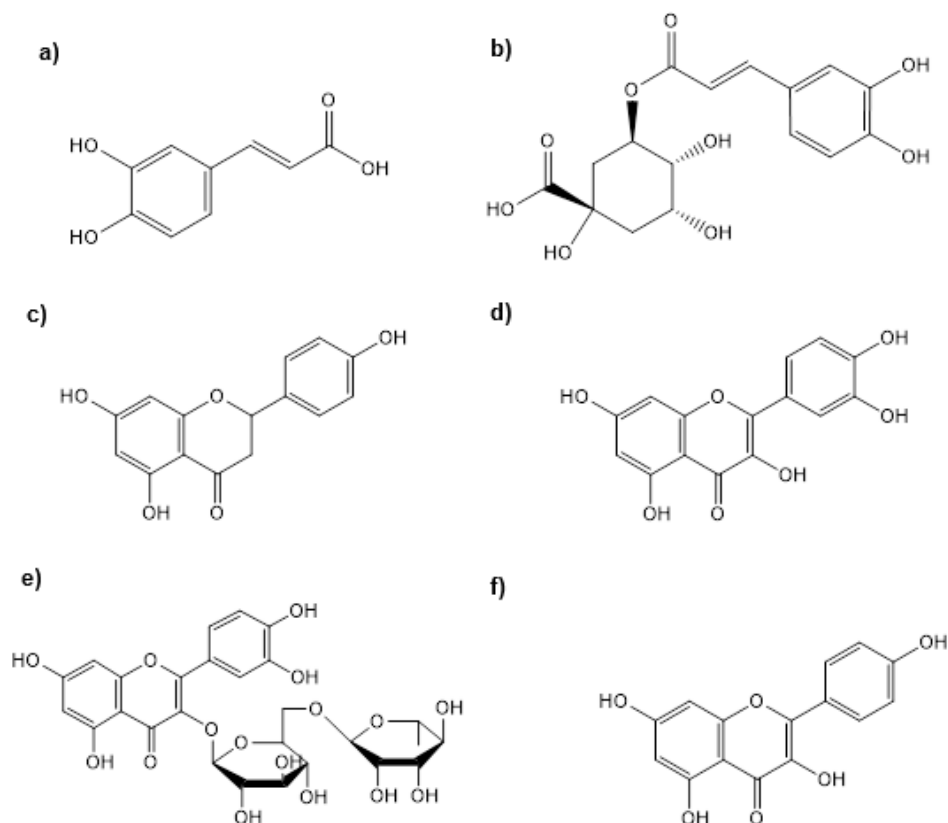


**Figure 25.** Chemical structure of **a**) L-ascorbic acid (vitamin C) and **b**) α-tocopherol (vitamin E).

Phenolic compounds are one of the main groups of secondary metabolites and phytochemicals found in plants. They can be divided in different groups, as flavonoids (anthocyanins, flavanols, flavones, or isoflavones), phenolic acids, tannins, stilbenes and lignans. In plants, including tomato, they tend to accumulate and be restricted to the skin<sup>110</sup>, where they play a potential role as antioxidants in UV-protection or as defense chemicals against assailants, as well as being essential for plant growth and reproduction<sup>86</sup>. In recent years, phenolic compounds have attracted increasing attention due to their actions

on the prevention of a large variety of diseases which have been associated to their antioxidant and radical-scavenging activities<sup>72,74,86,111</sup>. As such, polyphenols have varying effects' including anti-inflammatory, anti-diabetic, anti-obesity, anti-microbial, anti-thrombotic, anti-atherogenic, anti-proliferation, anti-allergic properties, cardioprotective, and vasodilatory effects<sup>87,111</sup>. Flavonoids, for example, are known for their prevention of some types of cancer, cellular antioxidant activity, and hemolysis inhibition<sup>74</sup>.

Hydroxycinnamic acid derivatives, like caffeic acid and its ester chlorogenic acid, are the main tomato phenolic acids (**Fig. 26**), with other acids like ferulic, p-coumaric, rosmarinic and others existing in lesser quantities, though qualitative and quantitative presence may vary according to cultivar and growth conditions<sup>68,73,112</sup>. Phenolic compounds have *in vitro* antioxidant activity and can possibly inhibit the formation of mutagenic and carcinogenic compounds. These antioxidant effects are due to their aromatic or phenolic rings. The molecule becomes a radical themselves after donating a hydrogen atom to the free radicals, however, they can become stabilized by the resonance delocalization of the electron within the aromatic ring and formation of quinone structures. Curiously, the antioxidant mechanism of chlorogenic acid is analogous to lycopene ones. Tomato contains flavanones such as naringenin and its' glycosylated derivatives, and flavanols such as quercetin, rutin, and kaempferol and its' glycosylated derivatives (**Fig. 26**). They are commonly found in the skin and in small amount in the other parts of the fruit<sup>68,106,109</sup>.

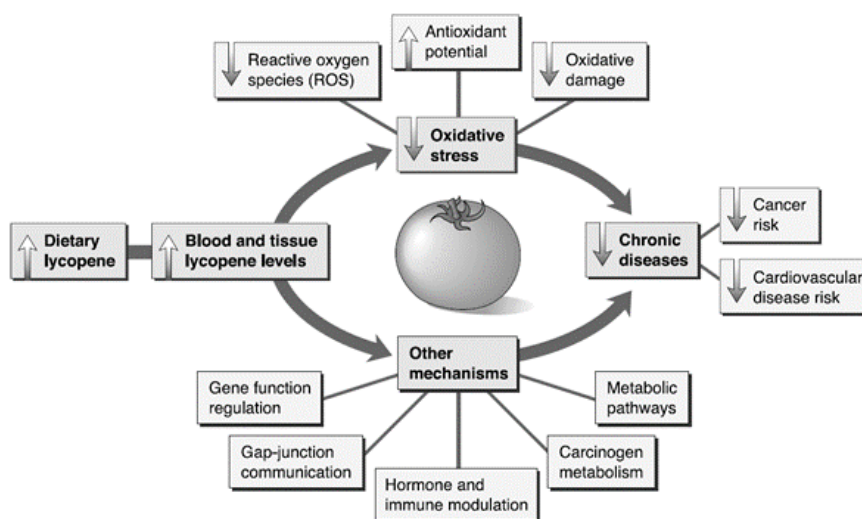


**Figure 26.** Chemical structure of **a)** caffeic acid, **b)** chlorogenic acid, **c)** naringenin, **d)** quercetin, **e)** rutin, and **f)** kaempferol.

Tomato's bioactive compounds and its bioactivity is centered around the quenching of reactive oxygen species (ROS). ROS are common byproducts of normal cellular metabolism. However, environmental stresses like drought, starvation, wounding, high salt, high light, exposure to pollutants, among others, can lead to the imbalance/accumulation of these compounds in the human body, giving rise to a phenomenon known as oxidative stress. This phenomenon can cause a myriad of negative effects like protein damage, lipid peroxidation, DNA damage and finally cell death, and thus, can play a role in the development of degenerative diseases as cancers, cardiovascular diseases, diabetes, as well as aging itself and in delaying wound healing by prolonging inflammation<sup>68,102,108</sup>. Bioactive compounds like antioxidants can play an important role inhibiting these molecules that contribute to diseases' onset, mostly through free-radical scavenging, but also through metal chelation, inhibition of cellular proliferation, and modulation of enzymatic activity and signal transduction pathways<sup>107</sup>.

Organisms themselves have a range of efficient mechanisms to detoxify these species by both enzymatic and non-enzymatic means. Amongst the non-enzymatic mechanisms, low-molecular-weight antioxidants such as glutathione (GSH), vitamin C

and E, as well as carotenoids and phenolics are able to non-enzymically interact directly with ROS<sup>108</sup>. As such, due to the high amount of such compounds in tomato, they can act as free radical scavengers of ROS. Furthermore, as mechanical and heat treatments help the release of bioactive compounds from the tomato matrix, thus increasing their bioavailability, by products like tomato pomace may offer greater potential as ROS scavengers<sup>68,102</sup>. Lycopene can, for example, protect biomolecules, such as proteins, lipids, and DNA, against oxidative damage and reactive oxygen species (ROS) by increasing the overall plasma antioxidant potential (**Fig. 27**). It can act as well in the regulation of various cellular processes such as gene functions and modulation of metabolic pathways, inter-cell (gap junction) communication, angiogenesis, and hormonal and immune response, all of which can positively affect the wound healing process. It has also been observed that lycopene can promote apoptosis and inhibit cell proliferation both *in vitro* and *in vivo*<sup>102–104</sup>. Evidence also suggests that polyphenols can behave as antioxidant by transition metal chelation, quench ROS by reducing them into less aggressive aroxyl radicals or by affecting enzymes that catalyze redox reactions responsible for superoxide anion production, including important enzymes involved in ATP generation, like mitochondrial succinoxidase and NADH-oxidase, for example<sup>112,113</sup>.



**Figure 27.** Representation of lycopene’s bioactivity. Adapted from Agarwal *et al.* (2000)<sup>103</sup>.

## 2. Objectives

This work aimed to study the feasibility of using tomato pomace (TP)-derived molecules for developing anti-inflammatory and antimicrobial starch-based materials. TP-derived hot-water soluble (TE) and/or phenolic-rich (PE) extracts were obtained and

characterized. The influence of TE and PE extracts on the chromatic, wettability, water solubility, thickness, mechanical (tensile traction, elasticity, and plasticity), and active (anti-inflammatory and antimicrobial activities) properties of starch-based films was studied. Moreover, targeting to exploit the feasibility of developing starch-based gauzes, the electrospinning of starch-based solutions was also optimized.

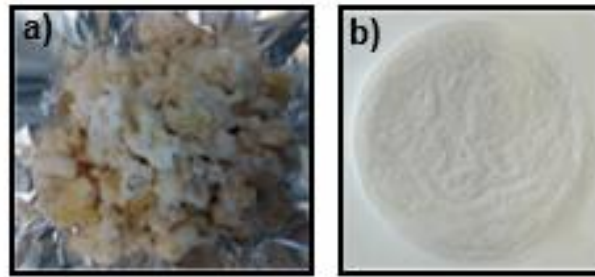
### 3. Experimental section

#### 3.1 Materials

Potato washing slurries were supplied by a Portuguese potato chips industry, A Saloinha, Lda. Tomato pomace (TP) mainly consisting of tomato peel and seeds were supplied by HIT Tomato, Italagro, S.A. All the purchased chemicals were of analytical grade and used without further purification: acetic acid (Carlo Erba), formic acid (Chem-Lab, 99%), gallic acid (Panreac, 99%), caffeic acid (Sigma Aldrich), glycerol (LabChem Inc, Portugal), sodium carbonate (Panreac, 99.5%), Folin-Ciocalteu reagent (Merck), 2,2-diphenyl-1-(2,4,6-trinitrophenyl)hydrazin-1-yl (DPPH) (Sigma Aldrich). Roswell Park Memorial Institute 1640 medium (RPMI, Invitrogen Life Technologies, Paisley, UK), 10% fetal bovine serum (FBS, Sigma Aldrich/Invitrogen Life Technologies, Paisley, UK), 1% Sodium Piruvate (Invitrogen Life Technologies, Paisley, UK), 1% penicillin/streptomycin (Invitrogen Life Technologies, Paisley, UK), Lipopolysaccharide (LPS, *Escherichia coli* (serotype O26:B6), Sigma–Aldrich, St Louis, MO, USA)). HPLC reagents: formic acid (Chem-Lab, 99%), acetonitrile (Carlo Erba Reagents, 99.9%).

#### 3.2 Recovery of starch from potato industry washing slurries

Starch (**Fig. 28b**) was recovered from pre-weighted and frozen potato industry washing slurries (**Fig. 28a**) through freeze-drying and sieving using a 150  $\mu\text{m}$  mesh stainless-steel sieve, following a described methodology<sup>54</sup>. The recovered starch was stored in a desiccator containing silica gel until further use.



**Figure 28.** Potato washing slurries **a)** and recovered starch **b)**.

### 3.3 Tomato Pomace (TP) preparation

Prior to TP preparation, its moisture content was determined by the weight difference registered between the lyophilized pomace and frozen pomace (**Fig. 29**) after freeze-drying for 13 days. Also, TP's granulometric separation was performed via 3 sequential cycles (1.4 mm.g<sup>-1</sup>/30min; 2 mm.g<sup>-1</sup>/15min, and 2.2 mm.g<sup>-1</sup>/5min) of sieving in sieves of 2 mm, 1 mm, and 0.710 mm (Retsch AS 200 Control Vibratory Sieve Shaker). A total of 4 packs of pre-weighted and freeze-dried tomato pomace were analyzed. Detailed information about the individual granulometric yields of each sample pack can be found in (**Table A1, annex**).

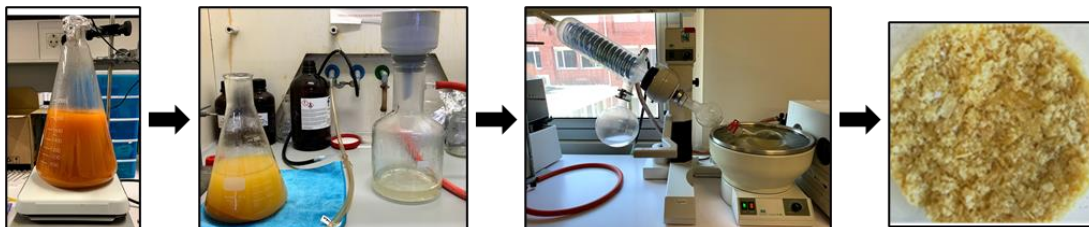


**Figure 29.** Tomato pomace. **a)** Frozen and **b)** lyophilized sample.

### 3.4 Acidified hot-water extraction of TP

TP-derived aqueous extracts were obtained via acidified hot-water extractions. Packs of freeze-dried TP were milled in 10 s cycles using a IKA A10 basic mill equipped with impact beater and further sieved using Retsch AS 200 Control Vibratory Sieve Shaker and sieves with 710  $\mu\text{m}$ , 300  $\mu\text{m}$ , and 150  $\mu\text{m}$  mesh to separate the tomato seeds from the tomato peels, with peduncles having been taken prior to the milling step (**Table A2, annex**). The 300  $\mu\text{m}$  and 150  $\mu\text{m}$  obtained peel fractions were then submitted to 3 sequential extractions in acidified boiling water (1% acetic acid (V/V), pH 2-3) at a solute (dry weight)

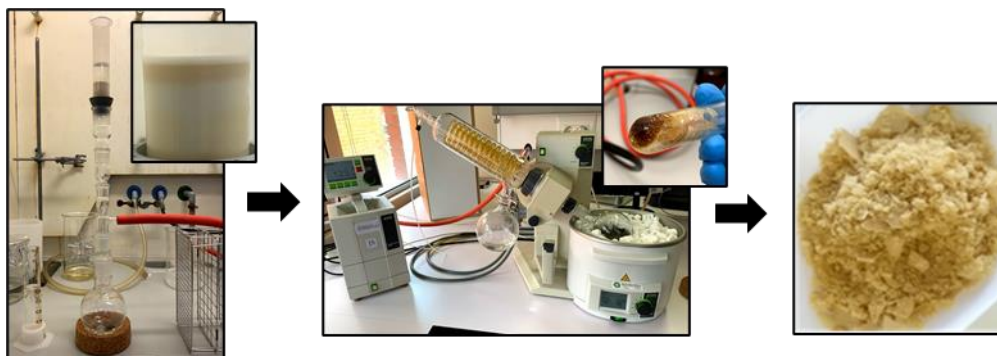
to a solvent ratio of 1:60 (g/mL) for 10 min, following the optimal conditions for polyphenol extraction determined by Fernandes *et al.* (2019)<sup>114</sup>. The extracts were then vacuum filtered using a 110 mm glass microfiber filter and concentrated under reduced pressure, and freeze-dried, resulting in a hot-water soluble total extract (TE) (**Fig. 30**).



**Figure 30.** Sequential acidified hot-water extraction, followed by vacuum filtration, concentration, and freeze-drying.

### 3.5 Recovery of hot-water extracts' phenolic compounds using a C<sub>18</sub> column

TP-derived phenolics-rich extracts were obtained via solid-phase extraction using Sep-Pak C18 cartridges (Discovery DSC-18 SPE Tube, 10 g bed wt., 60 mL, Supelco). Samples were prepared in acidified water (1% acetic acid (V/V), pH 2-3) and centrifugated (2000 G, 20 min, 4 °C) for precipitation of large particles. The column was preconditioned with 20 mL methanol followed by 20 mL distilled water, and 20 mL acidified water. Afterwards, 50 mL sample were loaded at a time onto the column and the aqueous fraction was eluted with 70 mL acidified water. The retained material was eluted using 70 mL acidified methanol (1% formic acid (V/V), pH 2-3) following the same procedure, and finally 50 mL of distilled water for column cleansing. The resultant phenolic-enriched extract (PE) was concentrated under reduced pressure to remove the methanol and then subsequently dissolved in water, frozen, and freeze-dried (**Fig. 31**)<sup>114</sup>.



**Figure 31.** Solid phase extraction with methanol and acidified water, followed by concentration via evaporation, and freeze-drying.



### 3.6 Chemical characterization and evaluation of antioxidant and cytotoxicity properties of TP-derived extracts

Protein content of TP-derived extracts was estimated by determining total nitrogen using a Truspec 630-200-200 elemental analyzer (St. Joseph, MI, USA) with a thermal conductivity detector (TDC) and employing a conversion factor of 5.84, as estimated for tomatoes by Fujihara S. *et. al.*<sup>115</sup>.

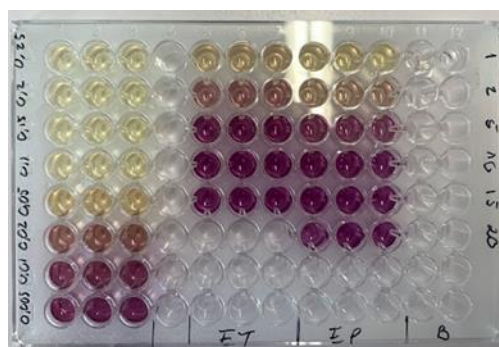
Neutral sugars composition was determined via gas chromatography (GC) (**Fig. A1, annex**), following an already described methodology<sup>114</sup>: acid pre-hydrolysis (200  $\mu$ L, 12 M H<sub>2</sub>SO<sub>4</sub> for 3 h at room temperature, orbital agitation), followed by hydrolysis (2.2 mL of water, 1 M H<sub>2</sub>SO<sub>4</sub> at 100 °C, 2.5 h), addition of 200  $\mu$ L of 2-desoxiglucose (1 mg/mL) per sample as intern standard, reduction with NaBH<sub>4</sub> (15% w/V in 3 M NH<sub>3</sub> during 1 h at 30 °C), 2 x 50  $\mu$ L of acetic acid in an ice bath and acetylation (3 mL of acetic anhydride in the presence of 450  $\mu$ L of 1-methylimidazole during 30 min at 30 °C). Samples were then diluted with 3 mL of water and 2.5 mL of dichloromethane, centrifuged (300 rpm, 30 s) and aspirated 2 times followed by the same procedure with only water more 2 times. Dichloromethane was evaporated in a *speedvac*, followed by the addition of 1 mL of anhydride acetone followed by evaporation 2 times. Samples were then resuspended in 50  $\mu$ L of anhydride acetone and read in a GC-Chromatograph (Clarus 500, Perkin Elmer, MA, USA, V<sub>injector</sub> of 2  $\mu$ L, T<sub>injector</sub> of 220 °C, T<sub>detector</sub> of 230 °C). Fructose was quantified by assuming that all mannose detected during the assay came from the epimerization of fructose during the reduction step, based on the Man:Fru epimerization ratio of 0.43, while glucose was quantified as the difference between all glucose and mannose detected. Samples were performed in duplicate and constituted the total and polyphenol-enriched extracts (2.0-3.0 mg per replica), and the aqueous fraction resultant from the polyphenol enrichment process (1.0-2.0 mg per replica).

Uronic acids were quantified via the 3-phenylphenol (MFF) colorimetric method: acid hydrolysis (0.5 mL of sample, 1 h in 1 M H<sub>2</sub>SO<sub>4</sub> at 100 °C), dilution with 3 mL of water followed by 4 mL with 200 mM of boric acid in concentrated sulfuric acid and agitation, hot water bath (100 °C, 10 min) and subsequent ice bath until cooled. Addition of 100  $\mu$ L of MFF into 2 of the 3 replicas and absorbance reading at 520 nm on 96-well microplate. Galacturonic acid (GalA) was used as standard at 10; 20; 40; 60; 80, and 100  $\mu$ g/mL (**Fig. A2, annex**)<sup>114</sup>.

Total phenolic content (TPC) was quantified using the Folin–Ciocalteu method, where the Folin–Ciocalteu reagent is reduced by the phenolic compounds present in the extract<sup>80</sup>,



of the sample is determined by its ability to donate electrons to neutralize the DPPH radical<sup>80</sup>, changing its natural purple color to yellow (**Fig. 33**): 250  $\mu$ L of a  $8.66 \times 10^5$  M DPPH ethanolic solution (absorbance in the 0.7-0.8 range) were joined by 50  $\mu$ L of varying concentrations of total or polyphenol-enriched extract aqueous samples in a 96-well microplate. A total of 3 independent replicates were performed for each sample.



**Figure 33.** DPPH assay plate with yellow-purple gradient indicating the increasing quenching of the DPPH radical, whose natural color is purple.

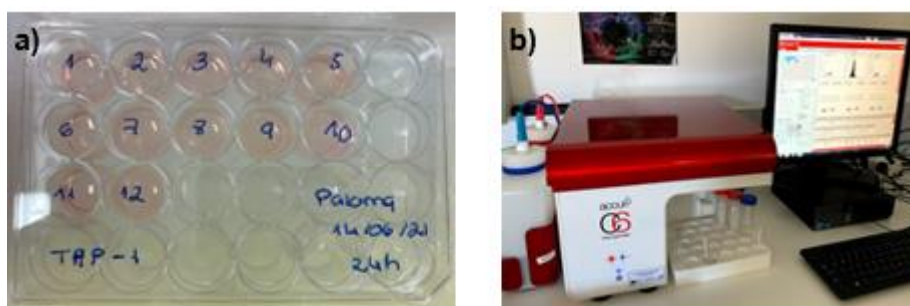
The plate was incubated in the dark for 30 min at room temperature and afterwards, absorbance was read at 517 nm using a microplate reader. Ethanol was used as blank, and all samples were performed in triplicate. Results were expressed as half maximum inhibitory concentration ( $IC_{50}$ ) (g/mL), which represents the amount of extract required to reduce the radical concentration to half of its initial concentration<sup>114</sup>, calculated from the graph of radical scavenging activity (RSA) (**Equation 1**) by extract concentration (**Fig. A5, annex**)<sup>116</sup>:

$$\%RSA = \frac{A_{DPPH} - A_{sample}}{A_{DPPH}} * 100 \quad (\text{Equation 1})$$

Cytotoxicity of TP-derived extracts was evaluated using THP-1 human monocyte cells. Cells were cultured in Roswell Park Memorial Institute 1640 medium supplemented with 10% fetal bovine serum and 1.0% Sodium Pyruvate in a humidified incubator containing 5.0%  $CO_2$  / 95% air at 37 °C. Cells were used at 2-20 passages and were sub-cultured every 2–3 days, maintaining cell density bellow  $1 \times 10^6$  cells/mL, by addition of new medium to a new culture flask alongside aliquots of the current cell passage at the desired cell density ratio ( $2-7 \times 10^6$  cells) according to the time interval until a new passage was made, and after cells were counted using a Double Neubauer Ruled Counting Chamber (Preciss Europe). Cell were counted via Trypan Blue on a 1:1 dilution.

For the cell viability assays, aliquots of 1 mL of THP-1 cells were cultivated in 24-wells

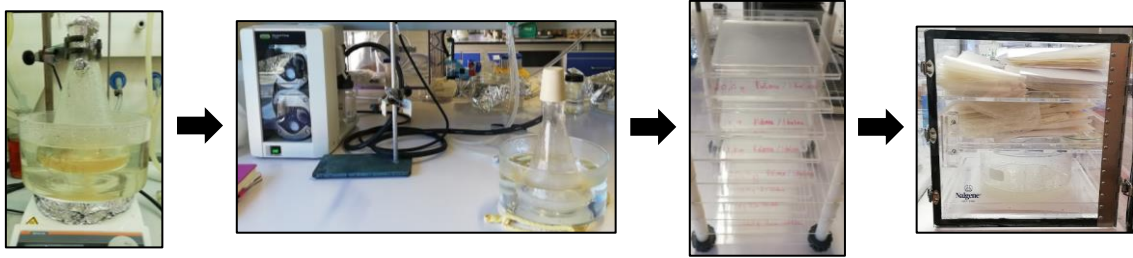
plate (**Fig. 34**) at a  $7.0 \times 10^5$  cells/mL density for 48 h in the presence and absence of pro-inflammatory agent LPS (2.0  $\mu\text{g/mL}$ ) and in the presence of total (50 and 120  $\mu\text{g/mL}$ ) and polyphenol-enriched (25, 50, and 120  $\mu\text{g/mL}$ ) extract, in DMSO-solubilized form. Cells were supplemented with 100 U/mL penicillin and 100  $\mu\text{g/mL}$  streptomycin before the assay to prevent bacterial growth in the cultures as both extracts. A pure THP-1 cell culture constituted the negative control, while a THP-1 + LPS culture constituted the positive control. Aliquots were taken at 24 h and 48 h after the assay's start and the cells and media fractions were separated via centrifugation (300 G, 4 °C, 5 min). After separation of phases and frozen storage of the media, cells were washed with 1x PBS and subsequently centrifugated. After solvent aspiration, cells were used for measurement of cell viability via flow cytometry (BD Accuri™ C6 Cytometer) – the cells were centrifugated again and after solvent aspiration, 100  $\mu\text{L}$  of IP solution (4.0  $\mu\text{L/mL}$ ) was added to the cell pellet. After resuspension and a waiting time of 15 min in the dark, samples were measured (**Fig. 34**). A minimum of 3 independent replicates were analyzed for all samples and results are expressed in percentage of cell death (**Table A3, annex**).



**Figure 34.** THP-1 cell culture plate **a)** and flow cytometer used **b)**.

### 3.7 Production of starch/TE- and starch/PE-based films

Starch (4% w/V) was dispersed into distilled water and mixed with glycerol (30% w/w related to the dry starch weight) and different TE and PE concentrations (1%, 5%, and 10% w/w related to the dry starch weight). After heating at 95 °C for 30 min with constant magnetic stirring (200 rpm), each gelatinized dispersion was degassed using a vacuum pump (Vacuum Pump V-300, Buchi), transferred ( $21.0 \pm 1.0$  g) to plexiglass molds (12 cm x 12 cm), and dried at 25 °C for 12 h<sup>54</sup>. The obtained films were pulled out from the plate and stored in a chamber with controlled relative humidity (RH) using a saturated magnesium nitrate solution (~50% RH) for at least 5 days prior characterization (**Fig. 35**). Films without extracts were also prepared and used as control.



**Figure 35.** Procedure for the development of starch-, starch/TE- and starch/PE-based films.

### 3.8 Characterization of starch/TE- and starch/PE-based films

#### 3.8.1 Chromatic properties

Chromatic properties of the films were determined, in triplicate, via the  $L^*$  (luminosity),  $a^*$  (green/red color), and  $b^*$  (blue/yellow color) parameters of the CIELAB color scale using a Chroma meter CR-400 colorimeter (Konica Minolta Sensing, Inc.) (**Fig. 36**) in indirect natural luminosity conditions<sup>54</sup>. Measurements were made in 5 different areas for each different sample and the average of the values for each parameter was calculated.  $\Delta E$  values were determined using the following **Equation 2**:

$$\Delta E = \sqrt{(\Delta L^*)^2 + (\Delta a^*)^2 + (\Delta b^*)^2} \quad \text{(Equation 2)}$$

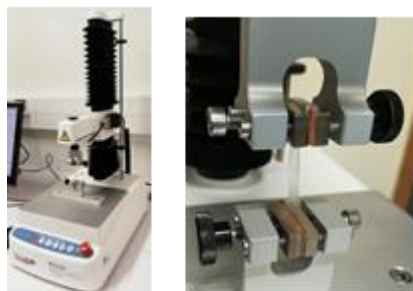
where  $\Delta L^*$ ,  $\Delta a^*$ , and  $\Delta b^*$  are the difference between the  $L^*$ ,  $a^*$ , and  $b^*$  values of the control and each film with extract (**Table A4, annex**)<sup>54,66,117</sup>.



**Figure 36.** Chroma meter CR-400 colorimeter and its calibration plate.

#### 3.8.2 Thickness and Mechanical performance

To determine the films mechanical properties, at least 10 strips (5 cm x 1 cm) were cut, and their thickness was measured using a micrometer (Mitutoyo Corporation) in 3-5 different parts of the sample. The mechanical properties analysis was performed through traction tests using a TA.XT.plusC texture analyzer (Stable Micro Systems) (**Fig. 36**) equipped with miniature traction claws (A/MTG).



**Figure 37.** Texture analyzer used (left) and a zoom to its closed claws with a film strip (right).

The test was performed at a speed of 0.5 mm/s and with a return distance of 30 mm. Mechanical parameters such as the Young's modulus, tensile strength, and elongation at break were determined based on the tension-deformation curves obtained (expressed in strength, N, by distance, mm) and were calculated using equations (3), (4), and (5) (Table A5, annex). At least 3 replicates of each film concentration were analyzed<sup>54</sup>.

$$\text{Tensile Strength (MPa)} = \frac{\text{force at rupture}}{\text{initial width} \cdot \text{initial thickness}} \quad \text{(Equation 3)}$$

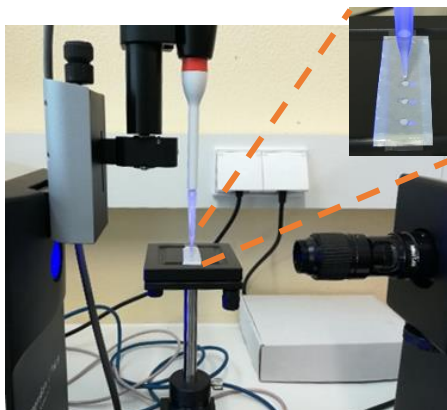
$$\text{Young's Modulus (MPa)} = \frac{\frac{\text{force at tangent's beginning point}}{\text{initial width} \cdot \text{initial thickness}}}{\frac{\text{Distance at tangent's beginning point}}{\text{initial length}}} \quad \text{(Equation 4)}$$

$$\text{Elongation at break (\%)} = \frac{\text{elongation at rupture}}{\text{initial length}} * 100 \quad \text{(Equation 5)}$$

### 3.8.3 Wettability

The films' wettability was determined by measuring the contact angle performed between a water drop and the film surfaces using a Attension Theta (Biolin Scientific), equipped with an image capture system (One Attension) instrument. Sessile drops of 3  $\mu\text{L}$  of ultrapure water were dispensed on 1 cm wide film strips using the instrument's incorporated micropipette (Fig. 38). A camera captured the image of the drop until droplet stabilization, with average contact angle being measured for each drop through the Equation of Young-Laplace<sup>117</sup>. These measurements were performed on the top surface exposed to air during drying (Top) and on the bottom surface in direct contact with the acrylic plate (Bottom) (Table A6, annex). A minimum of 3 strips of each developed film was analyzed and at least 12 water contact angle measurements were carried out per strip, with a minimum of 5 measurements being considered for mean contact angle consensus.





**Figure 38.** Tensiometer used to determine the films wettability properties.

### 3.8.4 Water solubility and moisture content

Pre-weighted samples of 4 cm<sup>2</sup> of each film concentration were immersed, in triplicate, in 30 mL of sodium azide aqueous solution (**Fig. 39**) and placed in an orbital agitator (80 rpm) for 7 days. Subsequently, the samples were taken out and dried at 105 °C with ventilation for 24 h and cooled down at room temperature in a desiccator until stabilization. Each sample was then weighed again. Solubility was expressed by dry weight loss percentage calculated via weight difference between the pristine film and the film used in the water solubility assay (**Table A6, annex**). The humidity of each film was also measured using a moisture analyzer (Kern DBS), in triplicate, and was taken into account for films' solubility determination (**Table A6, annex**)<sup>54</sup>.

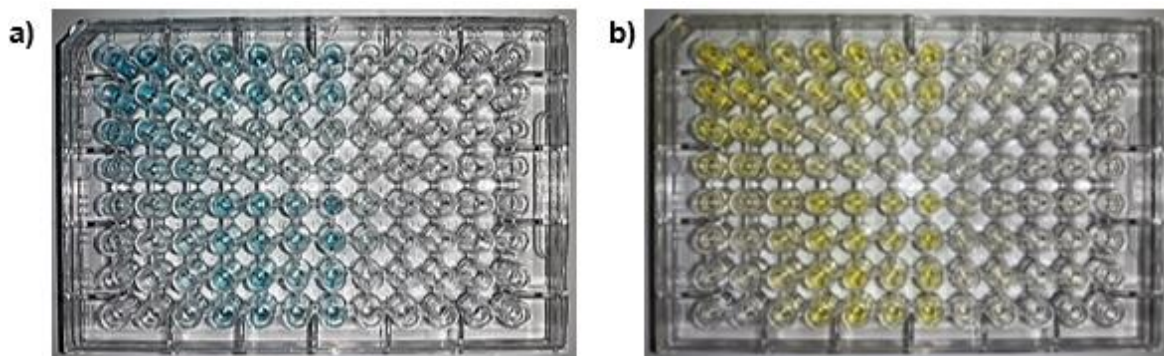


**Figure 39.** Film samples immersed in sodium azide aqueous solution.

### 3.8.5 Anti-inflammatory activity

TP-derived extracts' and films' anti-inflammatory activity was determined via a 3,3',5,5'-Tetramethylbenzidine (TMB) ELISA kit with human pro-inflammatory cytokine tumor necrosis factor  $\alpha$  (TNF- $\alpha$ ) as standard, following the procedure provided by Peptotech<sup>118</sup>. In summary, medium aliquots collected at the end of 24 h and 48 h of the

cytotoxicity assays served as the samples for the ELISA kit (**Fig. 40**). Solutions and reagents were prepared according to protocol and stored for further use in subsequent assays also in accordance with Peprtech's recommendation. TNF- $\alpha$  standard concentrations were used as follow: 0, 31.25, 62.5, 125, 250, 500, 1000, and 2000 pg/mL.



**Figure 40.** ELISA assay **a)** before and **b)** after reaction termination.

### 3.8.6 Antimicrobial properties

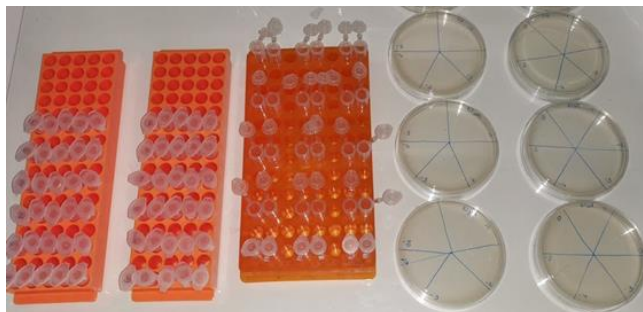
For the TP-derived extracts, minimum inhibitory concentration tests (MIC) were performed. *Staphylococcus aureus* was cultured in tryptic soy broth (TSB) growth medium for 24 h and then diluted in phosphate buffered saline (PBS, pH 7.4) to an adequate colony forming unit (CFU) level (optical density (O.D), 600 nm, 0.07-0.1 absorbance,  $\sim 10^7$ - $10^{10}$  CFU/mL). Subsequently, in triplicates, 100  $\mu$ L of bacterial suspension was added in conjunction with 100  $\mu$ L of varying concentrations of either TE or PE. Absorbance was measured for each microplate at 0 h and 24 h after incubation at 37  $^{\circ}$ C, in the dark, and, afterwards, 10  $\mu$ L in triplicate of each condition were plated in tryptic soy agar (TSA) plates.

Squares (4  $\text{cm}^2$ ) of starch/TE-based films were subjected to antibiogram tests via agar plating on confluent carpet of bacteria (*Staphylococcus aureus* and *Escherichia coli*), incubation for 24 h at 37  $^{\circ}$ C and observation of resultant bacterial growth inhibition halo formed around the film sample, for a minimum of 2 replicas for each film formulation.

Additionally, squares (1.96  $\text{cm}^2$ ) of control, starch/5% TE- and starch/5% PE-based films were incubated with 1.0 mL of *S. aureus* bacterial suspension in a 24 wells plate. The following controls were included in the assays: i) bacteria control - comprising just the bacteria suspension; ii) control films - comprising bacterial suspension and starch-based films without TE/PE. All the solutions were incubated with and without magnetic stirring for 24 h at 37  $^{\circ}$ C. For the quantification of colony-forming units per mL (CFU/mL), several dilutions (from  $10^{-1}$  to  $10^{-5}$  of the initial concentration) were done to each aliquot collected,



at both 0 and 24 h, via drop plating (10  $\mu\text{L}$ ) in TSA plates (**Fig. 41**). The plates were incubated at 37 °C during 24 h, and further the obtained colonies were counted.



**Figure 41.** TSA plates and respective dilutions set-up.

### 3.8.7 Cytotoxicity

Cytotoxicity of each developed film was evaluated using a similar procedure described for the determination of cytotoxicity of TP-derived extracts. In this case, 1,96  $\text{cm}^2$  of each starch-based films (control, 1%, 5%, and 10% TE and PE) were incubated with THP-1 cell. Films samples were separated from the 48h aliquots before analysis on the flow cytometer and frozen. A minimum of 1 replica was analyzed for all samples.

### 3. 9 Electrospinning of starch-based solutions

Electrospinning set-up was based on a horizontal syringe pump (PHD 2000, Harvard Apparatus, MA, USA) and a high-voltage power supply (CZE 1000R, Spellman) connected to an aluminum foil-covered rotary grounded metal collector and to the metal tip of a syringe through electrode wires (**Fig. 42**).



**Figure 42.** Electrospinning set-up used, including **a)** syringe pump and **b)** metal rotary collector with electrode wire.

Spinning dope was made by dissolution of starch (5-40%) in mixture of organic

solvents (DMSO and formic acid) with water, in a maximum ration of 15% water. For dissolution in DMSO, the starch suspensions were heated for a minimum of 30 min and a maximum of 2 h, while for dissolution in formic acid-based solutions, the starch suspensions were prepared at room temperature. Both solvents needed extended resting times that varied according to the starch concentration tested, varying from 1 day upwards to more than 1 week for gradual starch dissolution. Solutions were de-aerated via vacuum pump when substantial air bubbles were observed during the process. Electrospinning parameters then varied according to the solute concentration and solvent selected, with flow rates varying between 0.001 mL/min for fluid formic acid solution up to 50 mL/min for viscous DMSO formulations, and needle-to-collector distance varying between 8 to 25 cm. All mats obtained were dried *overnight* at 40 °C.

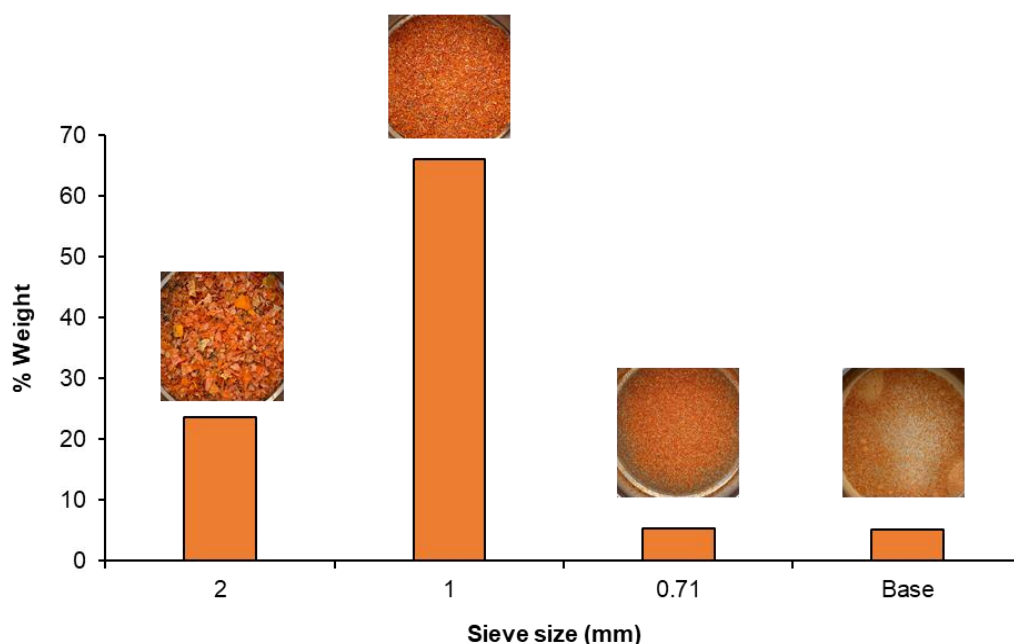
### **3. 10 Statistical analyses**

Microsoft Excel 2018 software and GraphPad Prism® 8 (GraphPad Software, CA, USA) were used to carry out *t*-tests of equal variances and 0.05 *p*-values to analyze the statistical significance of data obtained in all the developed starch-, starch/TE- and starch/PE-based films characterization tests. Significance between the different samples was represented in the form of lowercase letters. Values of  $p < 0.05$  of the mean comparison between the groups of values was considered as statistically significant in each experiment.

## **4. Results and Discussion**

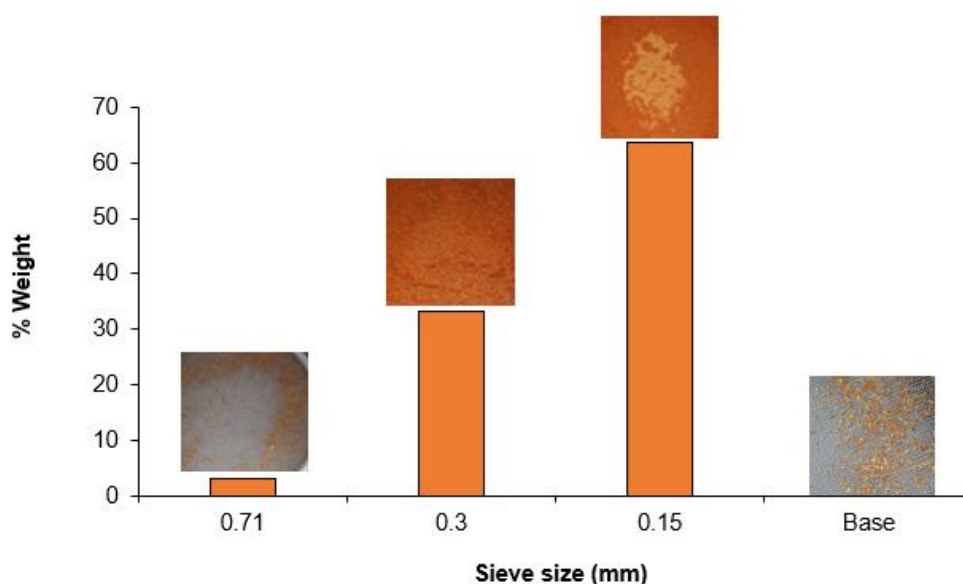
### **4.1 Tomato pomace characteristics**

Tomato pomace (TP) was mainly constituted by 66% and 23.6% of 1 mm and 2 mm size particles, respectively. The remaining 2 fractions were retained 5.3% and 5.1% in the 0.710 mm sieve or passing through to the base of the shaker, respectively (**Fig. 43**).



**Figure 43.** Distribution of unmilled tomato pomace particle size (% weight).

Authors like Kehili *et al.*<sup>92</sup> have investigated the effect of tomato peels' particle size on the extraction yield of tomato oleoresins recovered via supercritical CO<sub>2</sub> extraction. They observed that ground tomato peels of 300 µm particle size impacted not only the final yield, but also the kinetics of the extraction procedure in comparison to unground tomato peels of 1 mm particle size, that needed larger processing times to achieve similar yields than the ground peels. This revealed that grounding the starting material causes the rupture of cell walls and increases the surface area of each particle, allowing to increase the extraction yield. Thus, to optimize the extraction yield of bioactive compounds from TP, a milling step was employed via an impact-based mill, and the milled TP was again sieved to re-evaluate its granulometry (**Fig. 44**).



**Figure 44.** Distribution of milled tomato pomace particle size (% weight).

During the milling step, it was observed that the seeds fraction of the pomace deposited below the blades, and thus, remained largely un-milled, while the peels fraction was milled. This resulted in a separation between tomato peels and seeds in the subsequent sieving, thus leading to the obtention of almost exclusively peels granulometric fractions, with sparse seeds residues. The highest weight percentage of TP was observed in the 0.150 mm (63.7%) and 0.300 mm (33.2%) sieves, while the smallest particles were retained in the 0.710 mm sieve (3.1%). Therefore, the milling step successfully decreased the bulk TP particle size.

#### **4.2. Extraction yield and chemical characteristics of TP-derived extracts**

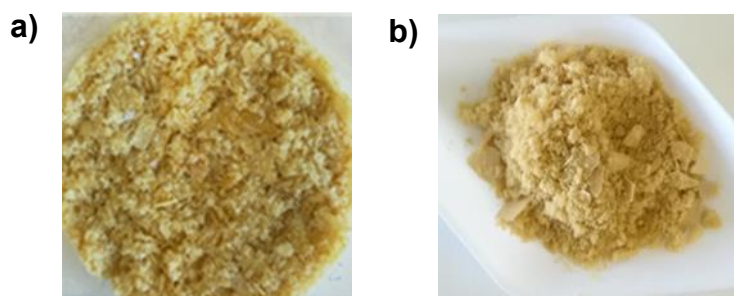
The obtention of a hot-water soluble extract (TE) with the 150  $\mu$ m fraction had a yield of 24.7% in relation to the initial TP weight. When compared to the hot-water soluble extracts of apple pomace, this value is slightly lower (29%)<sup>114</sup>, which may be due to composition differences of both pomaces. Apple pomace, for example, is rich in water soluble polysaccharides, like pectin (**Fig. 23**), which may have helped in a higher aqueous extraction yield<sup>114</sup>. Szymanska-Chargot *et al.*<sup>119</sup> analyzed four different types of pomaces, including tomato, apple, carrot, and cucumber pomace, and found that while tomato pomace contained the lowest content in cellulose between all samples, it also contained the highest amount in lignin, an insoluble polysaccharide. TP also contained the lowest content in galacturonic acid polysaccharides, thus pointing towards a low soluble polysaccharide

content. Besides, tomato peels' anatomy includes the existence of a cuticle, that forms a protecting film covering the epidermis of tomato fruits. Being composed of lipids, like cutin, that acts as a wax, polysaccharides, like cellulose, polypeptides and phenolic compounds, the plant cuticle is mainly hydrophobic, thus limiting the aqueous extraction yield of more hydrophilic bioactive compounds that are entrapped in the wax, like vitamin C<sup>65,87</sup>.

Similarly, tomato's bioactive compounds that possess hydrophobic nature, like lipid-soluble carotenoids, including lycopene and vitamin E, may not been fully extracted. In fact, when described in literature, lycopene's extraction processes normally involve the use of combination of organic solvents for the obtention of better yields, as lycopene is poorly soluble even in sole organic solvents<sup>91</sup>. However, such procedures limit lycopene's application in human-related uses, like in food or health-related products, since solvents normally possess adverse health effects and is never completely removed<sup>65</sup>. This was, in fact, also the reason that water was chosen as the extraction solvent, due to the application envisioned for this work, even if such signifies a possible decreased in the yield of bioactive compounds.

Regarding the use of 300  $\mu\text{m}$  TP fraction, a fraction with twice higher average particle size than the previous one presented, when exposed to the acidified hot-water extraction, only 13.3% of TE was obtained, which was ca. 54% less than the extraction obtained using the 150  $\mu\text{m}$  fraction. This data corroborated the particle size extraction yield dependency already mentioned by Kehili *et al.*<sup>92</sup>.

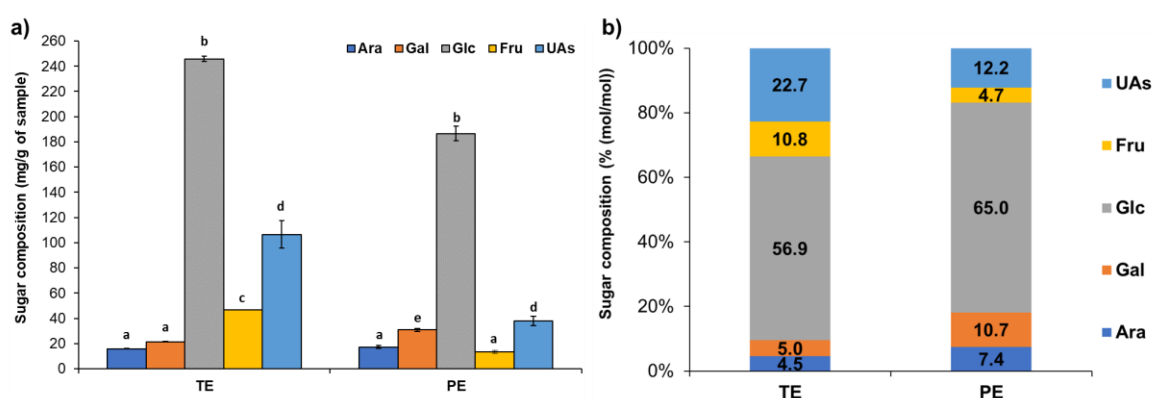
The extraction of phenolic compounds from TE via solid-phase extraction allowed to obtain a yield of 3% of PE dry weight (**Fig. 45b**), a higher extraction yield than the one reported for dry apple pomace weight.



**Figure 45.** Extracts obtained. **a)** TE and **b)** PE.

From the chemical point of view, TE and PE comprised around 14.7% and 18.5% (dry weight basis) of protein, respectively. These values are in line with those estimated by other authors in different batches of fresh tomato pomace<sup>81,82,87</sup>.

From the neutral sugar analysis (**Fig. 46**), arabinose (Ara), mannose (Man), galactose (Gal), and glucose (Glc) were the main compounds identified in TE and PE, with TE containing the higher content in sugars. Due to the epimerization reaction that occurs between glucose, mannose, and fructose during the reduction step, fructose was estimated based on the mannose content, since literature pointed towards glucose and fructose as the main sugars present in tomato pomace<sup>82</sup>. Besides neutral sugars, uronic acids (UAs) content of TE and PE were also determined (**Fig. 46**).



**Figure 46.** Sugars composition of TE and PE in **a)** concentration and **b)** mol%.

Sugars are, in fact, the major components of TE, who showed a total sugar content of 436.8 mg/g of polysaccharides (dry weight basis), with Glc (*ca.* 56 mol%), UAs (*ca.* 23 mol%), Fru (*ca.* 11 mol%) and Gal and Ara (*ca.* 5 mol% each) being the main sugars. Meanwhile, PE showed a sugar content of 286.1 mg/g, with Glc (*ca.* 65 mol%), UAs (*ca.* 12.2 mol%), Gal (*ca.* 10.7 mol%), Ara (*ca.* 7.4 mol%) and Fru (*ca.* 4.7 mol%) being the main sugars. Cabrera. *et al.*<sup>82</sup> determined a much smaller value of 38 mg/g of total sugars content in tomato pomace, but Del Valle *et al.*<sup>82</sup> determined a much closer value of 257.3 mg/g in the same byproduct. While this second one is closer to the sugar content found in PE, it differs from the value determined for TE, which presented a higher sugars content. These disparities may be due to the cultivar and ripeness differences, as Pinela *et al.*<sup>116</sup> found that sugar content varied wildly between 4 different tomato cultivars, while Agius *et al.*<sup>120</sup> noted that sugar content was higher in unripe tomato fruits in comparison to mature ones.

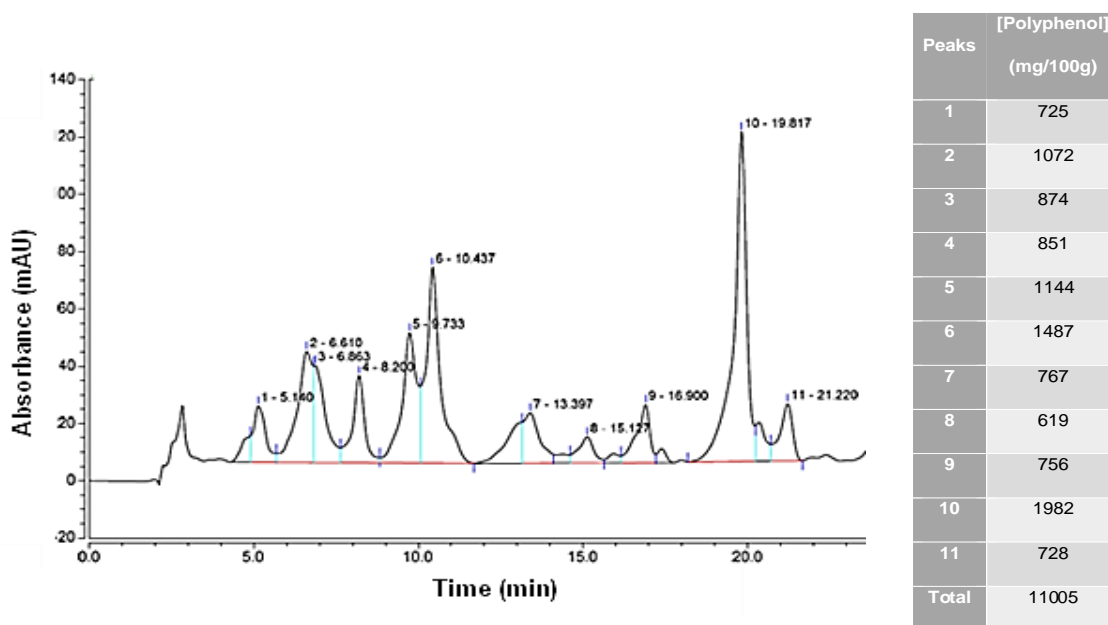
This primary composition in glucose is in agreement with tomato sugars described in the literature, that mainly pointed towards either glucose or fructose being the primary sugars in tomato, being their content variability mainly due to the tomato variety, ripeness, and growth conditions<sup>120</sup>. Glucose tends to be predominant in green and unripe fruits, for

example, while red, fully ripe fruits contain typically slightly more fructose than glucose<sup>120</sup>. On the other hand, Pinela *et al.*<sup>116</sup> found that four different varieties of tomato, *Amarelo*, *Batateiro*, *Comprido*, and *Coração* possessed different levels of sugars: all followed the order of fructose > glucose > sucrose, but the *Amarelo* variety possessed significantly more sugars than the other three varieties. In the case of tomato byproducts, processing conditions also affect sugars' total and individual content, as evidenced by De Valle *et al.*<sup>82</sup>, that observed 21 different tomato pomace samples from 10 different Spanish tomato processing industries, and found that while the majority of samples showed higher fructose content in comparison to glucose, some of the further processed samples showed variation in this order, presenting a higher glucose:fructose ratio in comparison to samples that suffered less processing.

Meanwhile, uronic acids are related to the presence of pectins (**Fig. 23**), meaning that the extracts reflect the presence of pectic polysaccharides. As tomato is botanically categorized as a fruit, these compounds are also expected to be found in tomato. Navarro-González *et al.*<sup>98</sup> investigated the composition of tomato peel fiber and found that the content of uronic acids was found to be lower than that of neutral sugars, which is not in line to the results determined in this work, that can be related to differences in the tomato source used.

According to the Folin–Ciocalteu method for the total phenolics content (TPC) determination, TE and PE evidenced a total of 2763 and 13926 mg of gallic acid equivalents (GAE)/100 g of dry weight sample, respectively, thus representing a 5-fold gain in the total phenolic content in PE when compared to TE. In both cases, the values obtained were bigger than those obtained in the literature for tomato peel, that ranged from 0.372 to 158.1 mg GAE/100 g<sup>86,98,112,116</sup>. Thus, the results obtained revealed that the tomato pomace used in this work is a rich source of phenolic compounds. Besides, since PE was constituted of 13.1% of sugars (**Fig. 46**) the existence of sugar-polyphenol structures in the samples as a result of covalent bonding should also be considered. In fact, various sugars-polyphenol complexes have been identified in tomato via HPLC or other analytical methods<sup>73,112,121</sup>.

To further characterize and quantify the phenolic compounds in PE, a HPLC analysis was done. **Figure 47** shows an example of the chromatograms obtained at 295 nm for the phenolic compounds' quantification.



**Figure 47.** HPLC chromatogram (295 nm) of PE (5 mg/mL) and quantification of the peaks found via HPLC expressed in mg of caffeic acid equivalents/100 g of dry weight sample.

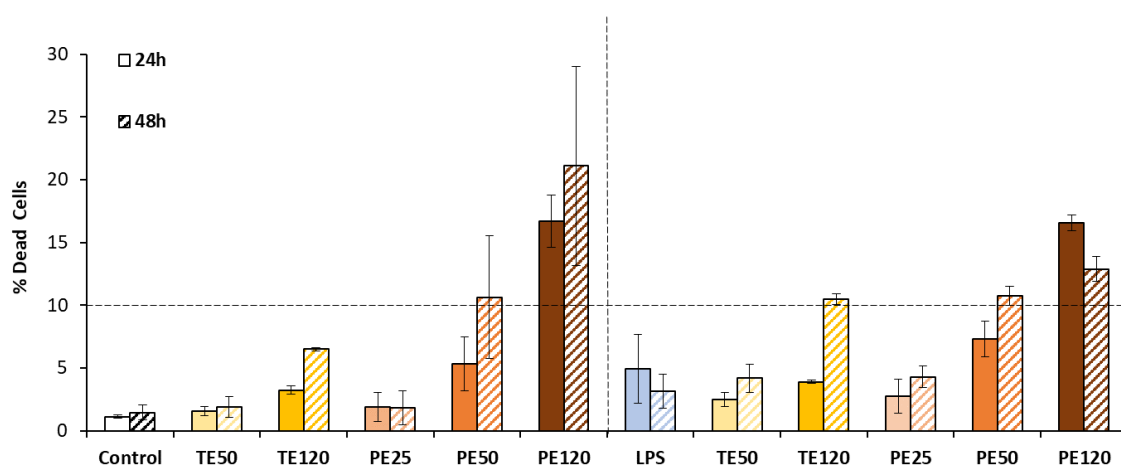
As can be observed in **Fig. 47**, peak 10 is the major peak determined, followed by peaks 6, 5, and 2. Based on literature, these biggest peaks may be related with the presence of rutin, caffeic acid (peak 4), chlorogenic acid, and gallic acid<sup>112,121,122</sup>. However, to perform an accurate identification of the phenolic constituents of PE, an Ultra Performance Liquid Chromatography (UPLC) method should be employed. Besides, the total PE phenolics amount was 11005 mg of caffeic acid equivalents/100 g of dry weight sample. Although the methods are different, this content is similar to the one determined by the TPC method (15158 mg of GAE/100 g of dry weight sample), corroborating the richness in phenolic compounds of the PE extract derived from the tomato pomace sample under study.

Regarding the TE and PE antioxidant activity, as expected, PE presented a much lower IC<sub>50</sub> value (0.804 mg/mL) in comparison with TE (2.48 mg/mL), representing a 3-fold decrease in the extract concentration necessary to scavenge 50% of DPPH molecules. The increase in the IC<sub>50</sub> value of TE is due to its lower phenolic compounds' concentration in comparison to PE. In comparison to the literature, PE antioxidant activity fits with the values found in literature. Pinela *et al.*<sup>116</sup>, for example, calculated the antioxidant activity of 4 tomato cultivars via a DPPH assay and found an IC<sub>50</sub> range of 0.55-0.75 mg/mL. Meanwhile, Silva *et al.*<sup>80</sup> calculated a range of % of inhibition of 17.1% - 31.4%, which is in line with the



results obtained, as TE had a percentage of inhibition of 19.1% while PE had a 39.0% of inhibition.

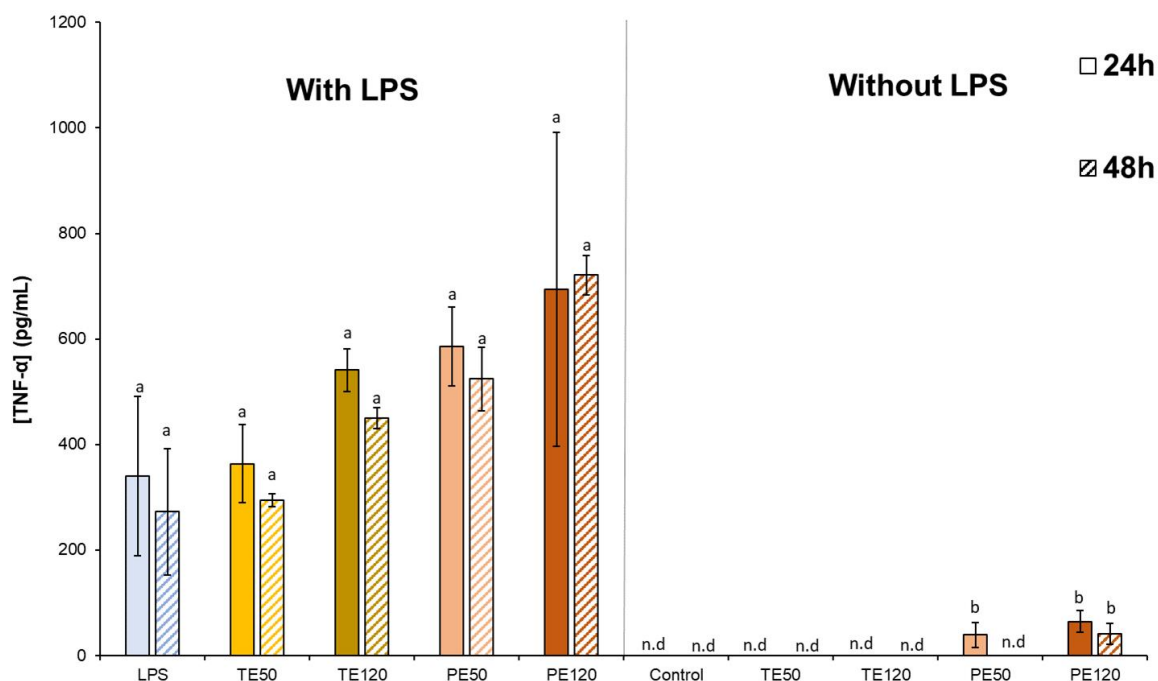
Targeting to explore TE and PE biocompatibility, their cytotoxicity was evaluated using human monocyte line cells (THP-1), in the presence and absence of pro-inflammatory LPS, for 25 µg/mL, 50 µg/mL and 120 µg/mL of samples. **Figure 48** shows that, after 48 h, PE dosages higher than 25 µg/mL exceeded the cytotoxicity limit of 10% dead cells, thus possessing cytotoxic characteristics, while TE showed no significant cytotoxicity for all the concentrations studied. The data also revealed that PE and TE cytotoxicity increased with the increase in the extract concentration.



**Figure 48.** Cytotoxicity of TE and PE after 24 h and 48h of THP-1 cell culture, in the presence and absence of pro-inflammatory LPS.

The PE cytotoxicity can be attributed to two factors: i) higher concentration in antioxidant compounds that may, in some conditions, exert pro-oxidant activity, and ii) lower sugar concentration in comparison to TE. This last point was especially curious as it was seen via manual cell counting that cells in the presence of TE grew more/faster in relation to the control. As such, a higher cell concentration resulting from the rapid cell division by the higher presence of nutrients, like glucose, resulted in a smaller percentage of dead cells in TE containing cultures, even if the number of dead cells were like the one of PE. Navarrete *et al.*<sup>123</sup> studied the cytotoxicity of aqueous tomato pulp extracts on macrophages obtained through THP-1 differentiation, in the absence and presence of LPS, via Trypan Blue manual counting, and found no significant cytotoxicity in all concentrations tested (0.1; 0.5; and 1.0 mg/mL). As tomatoes' polyphenols are found almost exclusively in the peel, discrepancies between the results obtained and that of literature were expected. Nevertheless, TE showed similar non-cytotoxic results.

TP-derived extracts had neither significant anti- nor pro-inflammatory effect when used in the culture media at concentrations of 50  $\mu\text{g/mL}$  and 120  $\mu\text{g/mL}$ , in the absence or presence of pro-inflammatory LPS (Fig. 49).

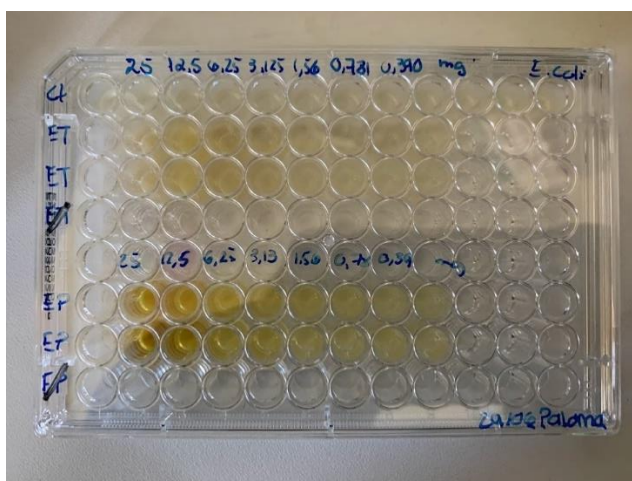


**Figure 49.** Anti-inflammatory activity of TE and PE. “n.d” denotes not detected for [TNF- $\alpha$ ] below that of the smallest standard (31.25  $\mu\text{g/mL}$ ).

This behavior may be related with the interaction of hydrophilic phenolic compounds and polysaccharides in both TE and PE with LPS, as LPS possesses hydrophilic oligosaccharides<sup>124</sup>, thus diminishing the anti-inflammatory potential that such compounds could possess. Another hypothesis is that the pro-inflammatory activity observed may be related to the dead cells present in the sample as result of the extract’s toxicity in higher concentrations, thus emitting pro-inflammatory signals upon cell death, as opposed to the idea that the results are borne from the extracts themselves. This is in accordance with cell toxicity results, as cells subjected to the mixture of LPS + TP-derived extracts showed more mortality, than those exposed to the extracts alone. The observed anti-inflammatory responses of the TP-derived extracts are not in accordance with the literature. Schwager *et al.*<sup>125</sup> observed that polyphenol-enriched aqueous tomato extract (500  $\mu\text{g/mL}$ ) reduced the concentration of TNF- $\alpha$  in a dose dependent manner in RAW267.4 macrophages stimulated with LPS for 24 h, while Abbasi-Parizad *et al.*<sup>87</sup> observed that methanolic tomato pomace extracts showed high anti-inflammatory

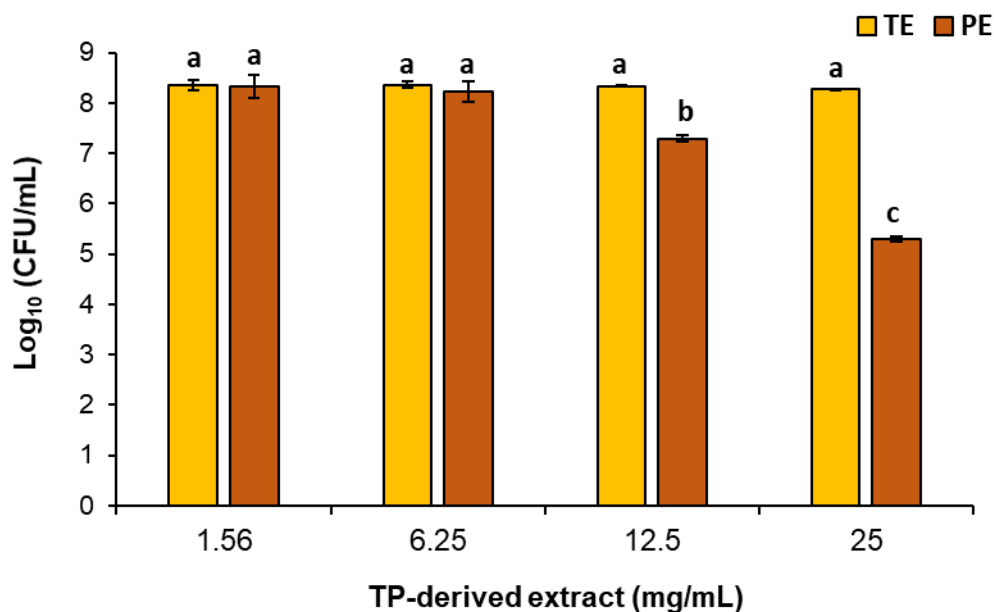
effects, being found to even reach a total inflammation elimination plateau after a dose-dependent linear phase in PCR gene analysis with IL-8. It's possible that lower concentrations of our extracts, like 10 µg/mL, would instead yield more anti-inflammatory effect than observed at higher concentrations due to a lower cytotoxicity in comparison to higher TP-derived extract concentrations.

The antimicrobial potential of TE and PE extract were also evaluated, optimizing the experimental conditions used for the determination of the minimum inhibitory concentration (MIC) for TP-derived extracts. Different conditions were tested mainly due to the extracts' color. In fact, when testing similar extract concentration used for the extracts' cytotoxicity assay, no MIC determination was possible, and thus, higher extract concentration had to be considered. However, the extracts' yellow color at higher concentrations hindered the determination of the MIC determination in higher concentrations (> 3.0 mg/mL, added color was already noticeable) (**Fig. 50**) due to the fact that natural liquid media (TSB) is already yellow, thus, in conjunction with the extracts, when the optical density was read at 600 nm (also the wavelength where yellow has its maximum absorption), the absorbance values obtained surpassed the linearity limit of 1.00 Abs, thus leading to erroneous results that led to the belief that higher extract concentrations resulted in 200% bacterial viability, in comparison to the ineffective diluted concentrations that showed no inhibitory effect (bacterial viability close to 100%).



**Figure 50.** MIC assay plate, denoting the strong yellow color due to the extracts' natural color, that hindered the bacterial O.D determination at 600 nm, where yellow absorbs the most as well.

Even then, the resulting microbial growth was re-utilized and drop-plated in hopes that solid bacterial growth would elucidate any results obtained (**Fig. 52**).



**Figure 51.** Antimicrobial activity against *Staphylococcus aureus* of TP-derived extracts.

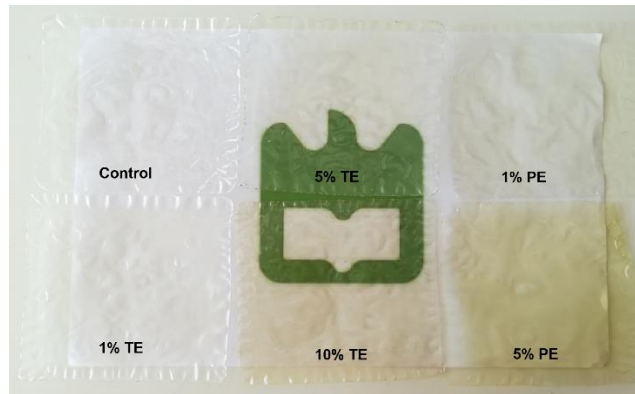
As can be seen, the two extracts presented significant different results for concentrations above 6.25 mg/mL. In fact, for TE, no concentration tested revealed antimicrobial potential, even the higher one of 25 mg/mL. Hypothesis for this kind of result can mirror those given during the cytotoxicity assay of the extracts: as TE possesses higher sugar concentration and lower polyphenol concentration than PE (five-fold difference), its antimicrobial activity diminished in favor of higher bacterial growth due to the higher presence of sugars, and, as such, its MIC can perhaps only be found using 3 to 5 times the MIC established for PE (37.5-62.5 mg/mL), for example. PE, on the other hand, caused a decrease in bacterial growth at both 12.5 and 25 mg/mL, likely for its higher concentration in phenolics and lower concentration in sugars. Therefore, until further optimization assays can be done, PE's MIC can be estimated to be 12.5 mg/mL. This is a little higher when compared to the MIC values obtained for 10 different tomato cultivar pomace methanolic extracts for *S. aureus* that ranged from 2.50 and 5.0 mg tomato peels/mL<sup>73</sup>. In comparison, PE presented a 0.3775 mg tomato peel/mL considering its yield of 3.02% in relation to the global process, representing, thus, that a better MIC was obtained in this work.

### 4.3 Characteristics of starch/TE- and starch/PE-based films

#### 4.3.1 Chromatic properties

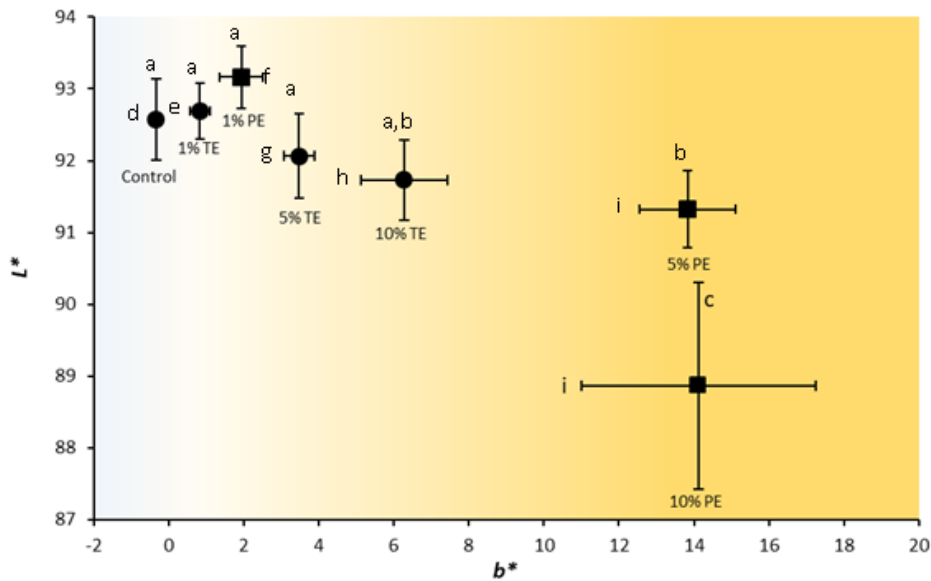
When incorporated into starch-based formulations (**Fig. 52**), TE and PE conferred a

yellowish coloration to the films, while keeping their transparency.



**Figure 52.** Visual appearance of starch-, starch/TE-, and starch/PE-based films.

The incorporation of TE and PE slightly decreased the starch-based films luminosity ( $L^*$ ), with significant variations only observed in the presence of 10% TE and 5% and 10% PE (**Fig. 53**).



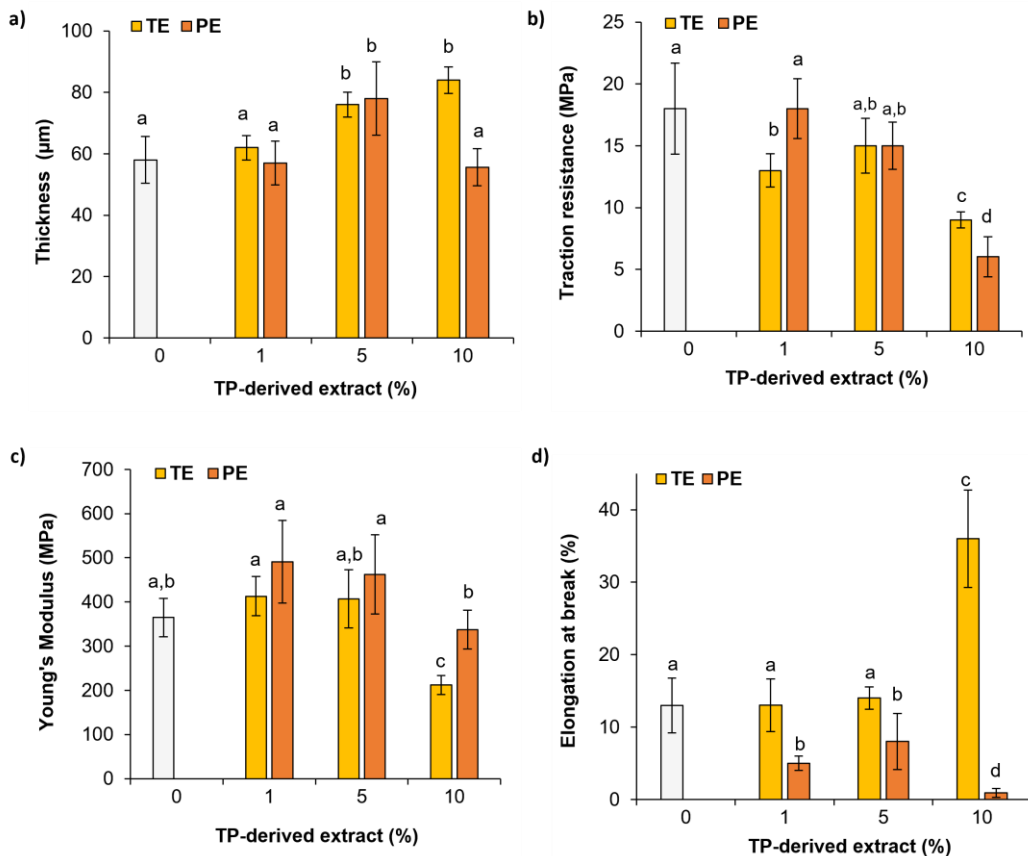
**Figure 53.** Lightness ( $L^*$ ) and blue-yellow ( $b^*$ ) coordinate of starch-, starch/TE-, and starch/PE-based films.

The decrease in the films' luminosity may be due to the light scattering provoked by the TE and PE compounds, such as the phenolic compounds<sup>126</sup>. Moreover, both TE and PE significantly increased the films' blue-yellow ( $b^*$ ) coordinate value, thus conferring a yellowish coloration, which is related with the natural yellow color of both extracts. This  $b^*$

values significantly increased with the TE and PE amounts, being more pronounced when PE were incorporated into the starch-based formulations, which can be related to its carotenoids higher content, specifically lycopene, that is known for its reddish color.  $\Delta E$  values corroborate these chromatic changes, indicating color changes that are perceptible to the human eye ( $\Delta E > 1.0$ )<sup>127</sup>, being observed variations in a dose dependent manner in the TP-derived extract films. The biggest  $\Delta E$  was observed in the 10% PE films, with a color difference of 15.5 in relation to the control film (film without TE and PE extracts), while starch/TE-based films presented a maximum  $\Delta E$  of 6.8 at a concentration of 10% TE. All these chromatic changes are in line with other works where phenolic-rich extracts were incorporated into starch-based films<sup>117,126,128,129</sup>.

### 4.3.2 Mechanical properties

When incorporated into starch-based formulations, TE increased the films thickness from 58  $\mu\text{m}$  to 76  $\mu\text{m}$  for dosages higher than 1% (**Fig. 54a**). This tendency was also observed for PE, except when 10% PE were added, in which the films thickness remained like the control sample (without any extract). The observed increase in films' thickness may be related to the hydrophilic compounds present in both TE and PE, that due to their hydroxyl compounds can establish bonds with starch, thus promoting an increase in the distance between the polymer chains and increasing the film's thickness. This, together with the fact that the 10% PE formulation showed a decrease in thickness in relation to lower PE concentrations, as opposed to 10% TE, who showed a higher thickness in relation to lower TE concentrations, may mean that other molecules (like polysaccharides) may contribute more to this phenomenon than the polyphenols. This makes sense also looking at the difference in molecular size of such compounds, as smaller molecules, like polyphenols, better fit into the intermolecular spaces that the starch matrix provides and can more easily bond with starch than the bigger polysaccharides.



**Figure 54.** Thickness **a)** and traction properties of starch-, starch/TE-, and starch/PE-based films: tensile strength **b)**, Young's modulus **c)**, and elongation at break **d)**.

Regarding the tensile strength (TS) profile (**Fig. 54b**), TE decreased the TS of starch-based films from 18 MPa to 9 MPa, except when 5% TE was added. This tendency was observed for PE dosages higher than 5%. These changes may be related to the presence of polar compounds, like phenolic compounds, that are able to interact with the hydrophilic groups of the starch molecules, causing larger spacing between the chain and providing areas of separation, thus, decreasing the cohesiveness of the matrix, and facilitating its fracture<sup>130,131</sup>. Lopes *et al*<sup>117</sup> also observed linear decreases in their starch-based films with increasing incorporation of ethanolic potato peel extract, which also possess high quantities of phenolic compounds, such as caffeic and chlorogenic acids, similar to tomato peel.

From the elastic deformation point of view, the Young's modulus (YM) data (**Fig. 54c**) showed that only dosages higher than 5% significantly decreased the starch-based films YM from 365 MPa to 212 MPa, thus promoting lower rigidity to the neat films. As was seen with the increase in thickness of the starch/TE-based films with increasing extract concentration and starch/PE-based films up to 5%, TP-derived extracts may have hydrophilic compounds that react with starch's hydroxyl groups, promoting the separation

of the chains. This may be the origin of the reduced rigidity since chain entanglement and compaction directly affect the materials' rigidity. A less cohesive matrix results in materials with decreased rigidity. The decrease in 1% TE formulation in comparison to 1% PE may be related to the presence of larger and hydrophilic compounds of TE, like polysaccharides and sugars, that may form larger spacing between starch chains. Lopes *et al*<sup>117</sup> observed similar Young's modulus decreases as obtained in this work with the increase in potato peel phenolic extract concentrations in starch-based films.

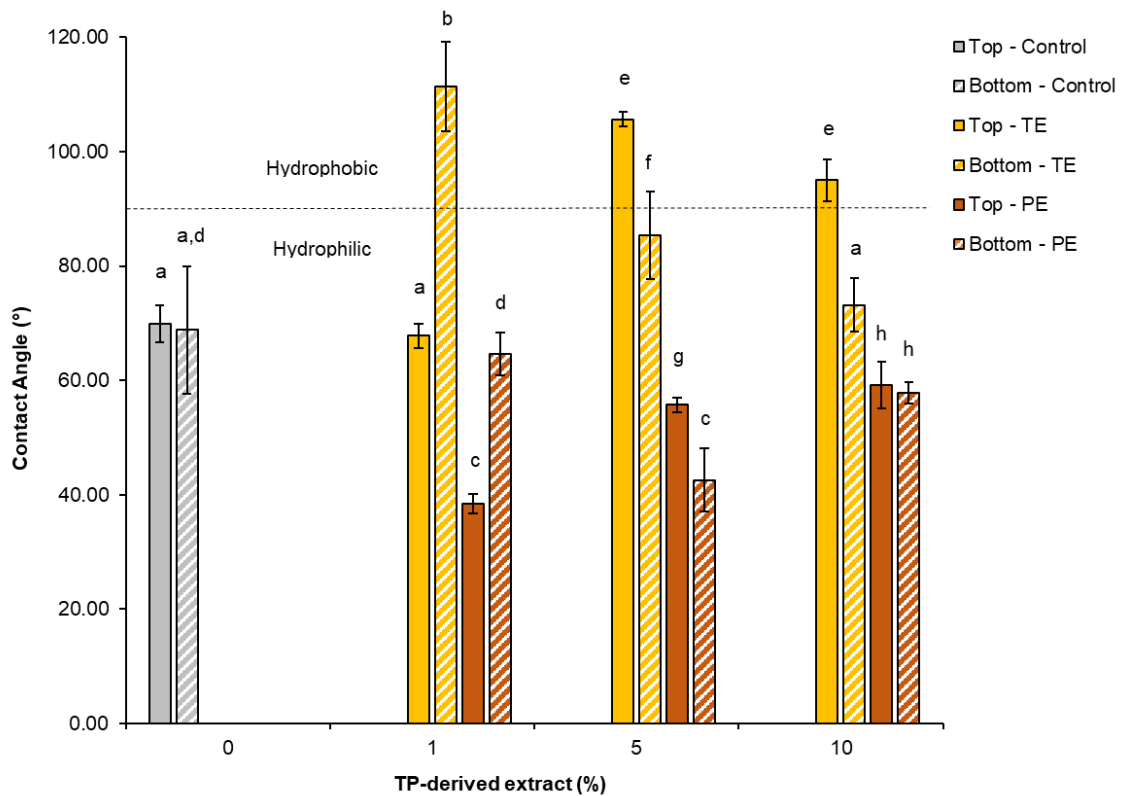
Elongation (%E) represents the film's stretchability<sup>129</sup>. TE drastically increased the %E of starch-based films from 13% to 36% for dosages higher than 5% (**Fig. 54d**), remaining similar to the control sample for lower concentrations. A similar behavior was observed for starch-based films containing potato peel-derived phenolic extract<sup>117</sup>. In turn, PE significantly decreased the films %E from 13% to 1% in all the concentrations tested. Such behavior suggests that PE acted as an antiplasticizer, even though a decrease in TS and Young's modulus would suggest otherwise. A similar trend was observed in potato starch-based films containing caffeic and chlorogenic acids rich-methanolic sunflower hull extract in a dose dependent manner<sup>132</sup>. Other works with other natural extracts have also observed such behavior, where the incorporation of *Zataria multiflora* Boiss essential oil and grape seed extract into chitosan-based films exhibited lower elongation values than the control films<sup>133</sup>, as well as for starch-based films containing coffee silverskin<sup>66</sup>. This kind of behavior is indicative that the molecules present in PE might not be large enough to stop the bonds created between starch chains, even if there is separation enough between them to lose the general matrix cohesion.

### 4.3.3 Wettability

TE significantly increased the water contact angle of the top film's surface from 69.9° to 105.6° when dosages higher than 1% was added into the formulation (**Fig. 55**). Moreover, TE only increased the water contact angle of the bottom film's surface from 68.8° to 111.3°, when 1% and 5% were used. Therefore, TE originated films with heterogeneous wettability surfaces and, depending on the concentration used, allowed to cross the threshold between hydrophilicity and hydrophobicity, established at 90°. This increase in hydrophobicity may be related to the presence of hydrophobic compounds in TE, like carotenoids or lipophilic vitamins (A, D, E, and K). Furthermore, due to a difference in size compared to the starch chains, during casting, TE compounds may be deposited at the bottom of the starch-based films at lower concentrations (1%) while higher concentrations allowed a more reliable



distribution. However, the slight decrease in water contact angle seen in 10% TE in comparison to the 5% TE suggests that while lower TE concentrations may disrupt the bonds formed between the starch chains and water, increasing the films' hydrophobicity, higher TE concentrations may promote it, perhaps due to an increase in hydrophilic compounds like polysaccharides and phenolic compounds. Similar trend were observed by Lopes, *et al.*<sup>117</sup> where starch/potato peel phenolic extract-based films showed increased hydrophobicity until a plateau was reached, from where a downward trend with further compounds concentration increase was observed.



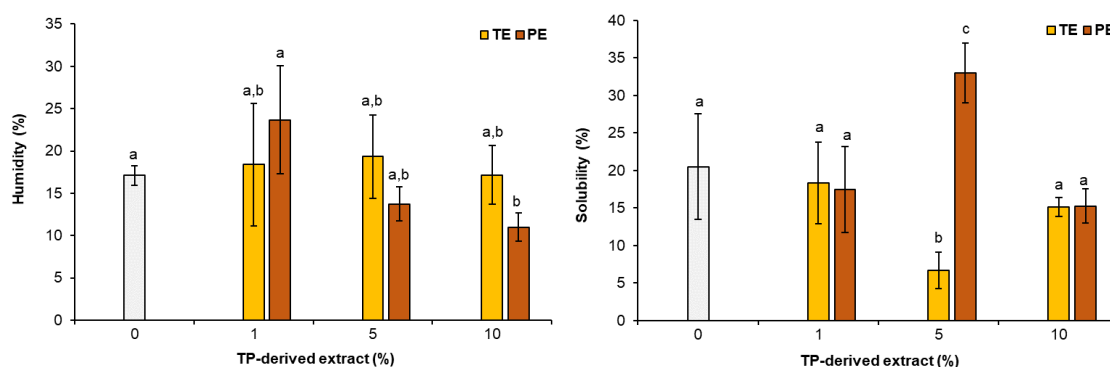
**Figure 55.** Water contact angle of starch-, starch/TE-, and starch/PE-based films. “**Top**” and “**Bottom**” are related to the film faces exposed to air and in direct contact with the plate during the solvent casting process, respectively.

On the other hand, PE decreased the water contact angle of the films top and bottom surfaces from 69.9° to 38.4° and 68.8° to 42.6°, respectively, thus improving even more the films hydrophilic character. These changes may be related to the increased concentration of hydrophilic compounds, like phenolic ones, in comparison to TE, as already shown in section 4.2. Furthermore, the smaller size of phenolic compounds when compared to the starch chains also allowed, in similarity to TE, for the deposition of PE’s compounds in the

bottom surface of the films at lower concentrations, and a more even distribution at higher PE concentrations.

#### 4.3.4 Moisture content and Water solubility

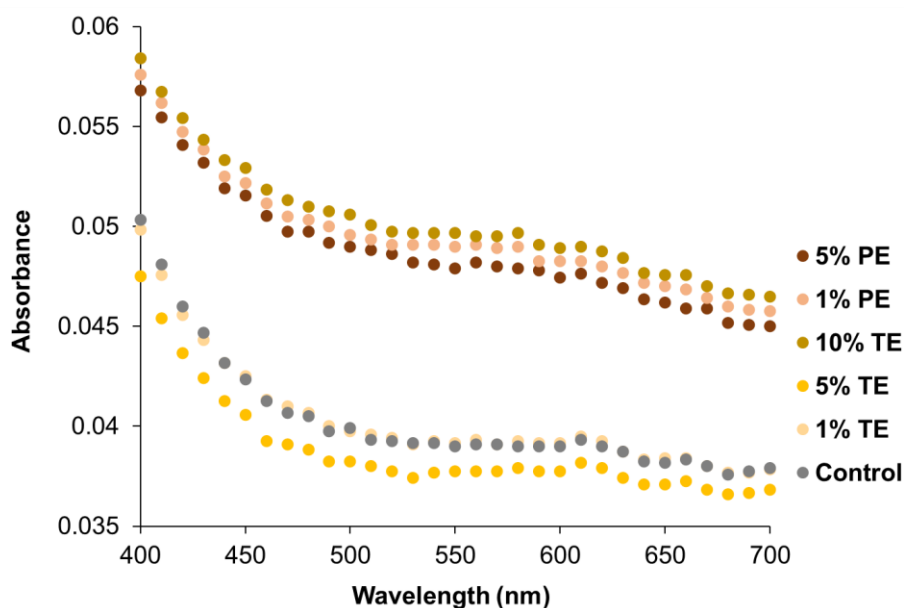
TP-derived extracts caused a decrease in the moisture content with the increase in extracts concentration in starch-based films (**Fig. 56a**). This may be related to the formation of hydrogen bonds between the extract's compounds with water molecules, thus reducing the content of free water in the films. Similarly, by increasing the concentration of TP-derived extracts, the ratio of water in relation to the total film mass changes, even if the volume used during the solvent casting process remains the same. Moreover, when immersed into aqueous solution, both TP-derived extracts did not significantly change the starch-based films water solubility, except for the films containing 5% of either TE or PE that decreased from 20.5% to 6.7%, when TE was used, and increased from 20.5% to 33.0%, when PE was added (**Fig. 56b**).



**Figure 56.** Moisture content **a)** and solubility **b)** of starch-, starch/TE-, and starch/PE-based films.

The films solubility affects their biodegradability. Films with lower solubility are more durable, which can be beneficial for prolonged application, but also means a lower biodegradability. Meanwhile, films with higher solubility may have diminished durability but represent a more environmental-friendly biodegradable alternative. Since hydrophobic compounds decrease materials' water solubility and hydrophilic compounds increase it, changes in the films' solubility depending on the extracts' composition are explainable. As PE possesses higher concentration in phenolic compounds when compared to TE, its higher solubility in comparison to the 5.0% TE formulation is explainable<sup>117</sup>. Meanwhile, the similar solubility of the 10% formulation films in comparison to the neat films' solubility may have to do with stronger leaching of compounds (**Fig. 57**), in comparison to control and

lower %TE concentrations. This behavior followed the water contact angle profiles obtained in 5% starch/TE- and 5% starch/PE-based films as well (Fig. 57).

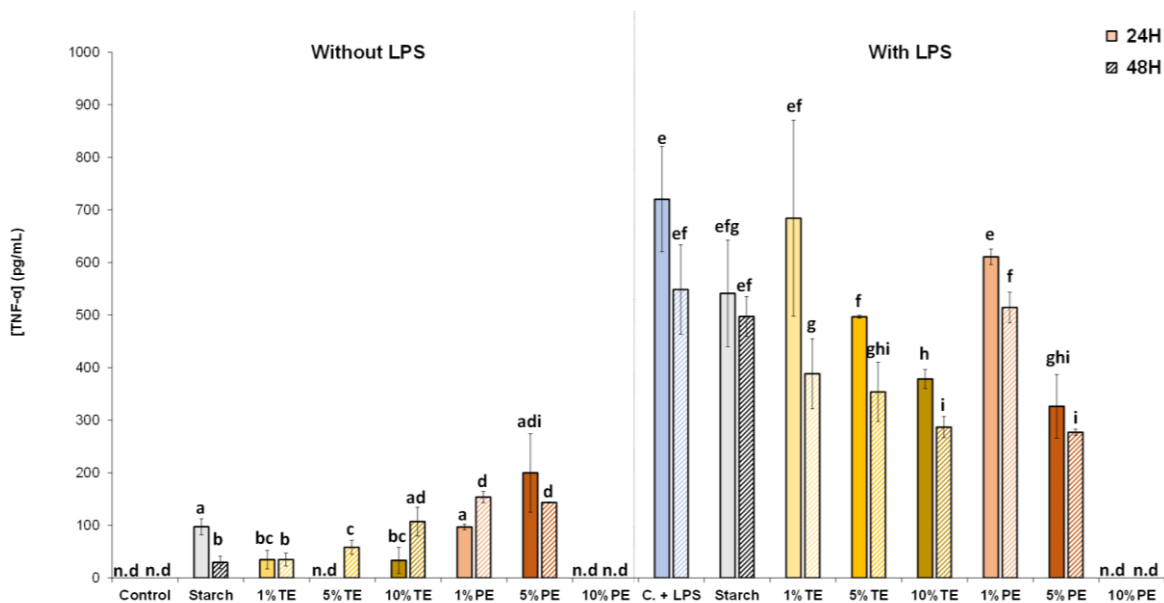


**Figure 57.** Leaching of colored compounds from the residual water resulted from the solubility assays carried out for starch-, starch/TE-, and starch/PE-based films.

#### 4.3.5 Anti-inflammatory activity

When incorporated into starch-based films and in the presence of LPS, starch/TE-based films decreased the concentration of TNF- $\alpha$  after 24 h and 48 h from 720 pg/mL to 378.4 pg/mL and from 548.6 pg/mL to 286.8 pg/mL, respectively, except for the starch/1.0% TE-based films (Fig. 58) that did not show a relevant reduction of TNF- $\alpha$  concentration in 24 h. On the other hand, starch/10% PE-based films caused a total quenching of anti-inflammatory activity after 24h, along with the lower PE concentrations that also decreased TNF- $\alpha$  concentration to 326.3 pg/mL and 277.0 pg/mL after 24 h and 48 h, respectively, except for starch/1.0% PE-based films that did not show relevant anti-inflammatory activity in 24 h. In all, after 24 h, up to a 47.5% decrease in TNF- $\alpha$  concentration was obtained with the TE concentrations increase, while increasing PE concentrations resulted in complete inflammatory activity quenching. On the other hand, in the absence of LPS (Fig. 58), only lowly-relevant TNF- $\alpha$  concentrations were obtained, as they are significantly smaller than obtained with pro-inflammatory LPS at a concentration of 2  $\mu$ g/mL in the same time frame, and thus, do not hold significance to the

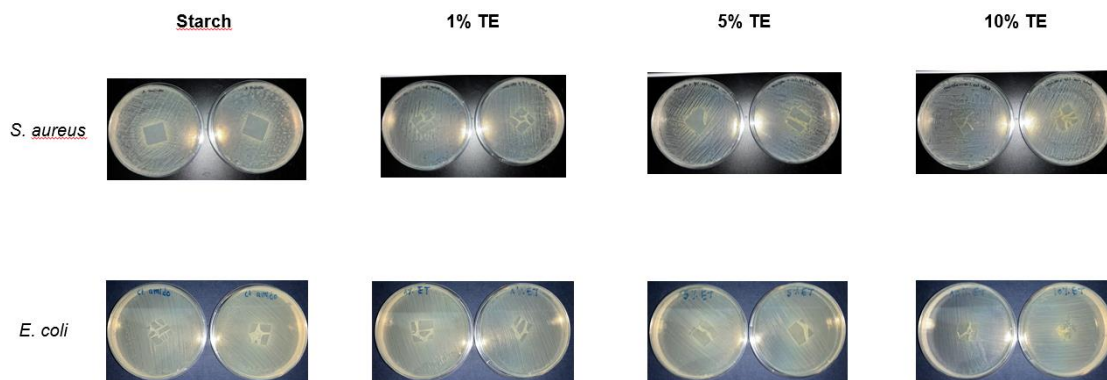
films possibly having pro-oxidant activity. To the best of our knowledge, till now, no work deals with the anti-inflammatory activity of tomato extract-biobased materials, although the promising anti-inflammatory properties already described for the tomato extracts<sup>87,125</sup>.



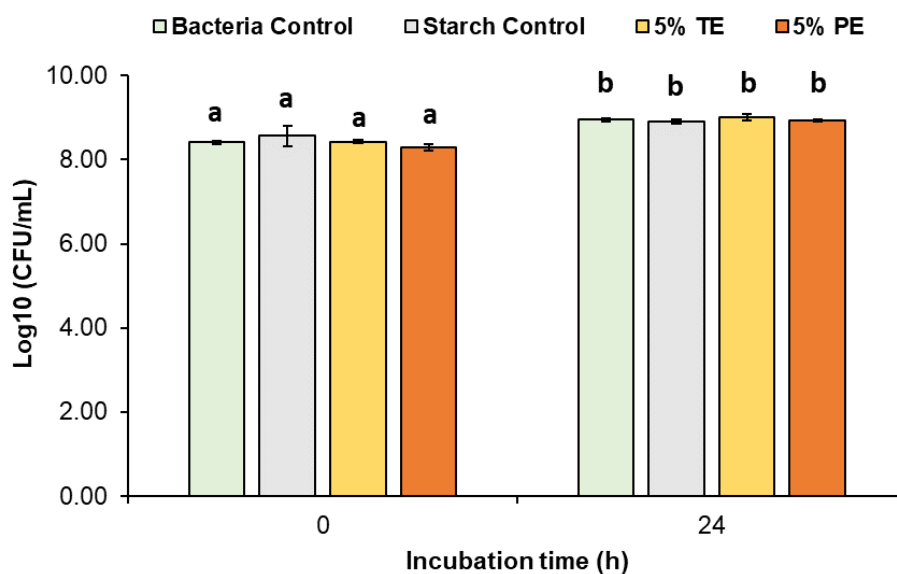
**Figure 58.** Anti-inflammatory activity of starch- and starch/TP extracts-based films. “n.d” denotes not detected for [TNF-α] below that of the smallest standard (31.25 pg/mL).

### 4.3.6 Antimicrobial activity

In the case of the films, brittleness and hydrophilicity made the determination of antimicrobial activity difficult, and thus various methodologies were employed, including the manipulation of variables like media type, media volume, and magnetic stirring. However, under the conditions performed, both the starch/TE- and starch/PE-based films did not reveal antimicrobial activity. In the antibiogram tests, no inhibition halo was observed in any of the TE films developed (**Fig. 59**) and by the bacterial culture assay none decrease of the bacterial growth was observed in 5% TE and PE films (**Fig. 60**).



**Figure 59.** Antibiogram assays carried out using starch- and starch/TE-based films.

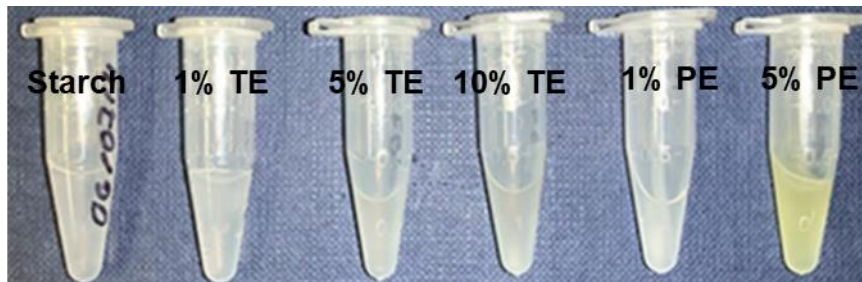


**Figure 60** Colony forming units (CFU) obtained for *Staphylococcus aureus* bacteria for starch-, starch/5% TE- and starch/5% PE-based films.

The absence of antimicrobial activity may be due to the lower concentration of the extracts incorporated into the starch-based formulation, when compared to the ones used for determining the MIC value of each extract. Some works in literature have been able to develop antimicrobial dose-dependent starch-based films when antioxidant compounds, like tea polyphenols and ethanolic propolis extract, were incorporated, but till now, none of them include the use of tomato pomace derived-molecules<sup>130,134</sup>.

### 4.3.7 Cytotoxicity

Cytotoxicity assays were done for the starch-based films similarly to those performed for the TP-derived extracts. However, a higher amount of films' debris was observed in cell culture and in subsequent cell viability measurements via flow cytometry, this debris overlapped with both live and dead cells' count, making a reliable determination of the films' cytotoxicity impossible, with results having a 10-30% reliability. Thus, they are not represented in this work. One hypothesis for this phenomenon includes the hydrolysis of the films' starch via exogenous enzymes generated by the cells, as curiously, the films did not show the same degradation when in the presence of simple RPMI culture medium for up to 48h (**Fig. 61**).


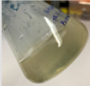




**Figure 61.** Solubility of starch-, starch/1.0-10% TE- and starch/1.0-5.0% PE-based films in RPMI cell culture medium.

### 4.4 Electrospinning of starch-based solutions

Apart from the development of starch-based films, efforts were made into the development of starch-based electrospun fibers. This was mainly addressed due to the structure that such matrix possesses, namely its porous and interlocking structure and almost similarity in structure to gauze used as wound dressing. **Table 5** show, in summary, and in a chronological order, the formulations tested during this work and its results.

**Table 5.** Formulations tested for the formation of starch-based electrospun fibers and obtained results.

Formulation			Result
Solvent	Starch (%)	Solvent:H <sub>2</sub> O	
DMSO	14	85:15	Starch precipitation 
	5	85:15	Too viscous; clogs syringe 
	14	94:6	Too viscous; clogs syringe 
	5-10	94:6	Too liquified; phase separation and electrospaying 
	14-20*	85:15	Too viscous, solvent did not evaporate in time to reach the collector
Formic Acid	40	75:25	Too viscous; clogged syringe
	20	75:25	Too liquified, needed low flow rate and high potential differential to work
	25	75:25	Too liquified still, but the use of lower differential potential and higher flow rates allowed its electrospinning

Based on the literature<sup>135</sup>, first efforts were made by using 14% of starch in various DMSO/H<sub>2</sub>O ratios, namely 75% DMSO/15% H<sub>2</sub>O, 94% DMSO/6% H<sub>2</sub>O, and 100% DMSO. The solvent to water ratio determines the extent of the starch's gelatinization (in water) vs. dissolution in the solvent. Problems arose, however, when the starch concentration used, in both 94:6 and 85:15 DMSO:H<sub>2</sub>O, ratios proved to be too viscous to allow the solution to smoothly pass the syringe's tip, and, as such, attempts of obtaining a less viscous solution were done by decreasing starch concentration. Even then, this did not prove fruitful, as a 5% starch concentration in 85:15 DMSO:H<sub>2</sub>O proved to still be too viscous, while 5-10% starch in 94:6 DMSO:H<sub>2</sub>O, proved to be too liquidly, which promoted an unstable solution that separated over time, and thus, only resulted in electrospaying of the solution, that is, the deposition of droplets onto the collector instead of a stable jet. A last attempt was made using this last DMSO:H<sub>2</sub>O ratio via gradual addition of 20% starch at room temperature over long periods of time (1 week) as opposed to the rapid addition under the influence of heat

that had been done until then. Still, while this solved the problem of syringe clogging, the solution was still too viscous and concentrated to allow DMSO's evaporation during the time the jet travels between the syringe tip and the metal collector, thus also resulting in electrospaying. These problems found during the electrospinning processing of starch-based solutions could be due to the characteristics of the recovered starch used, that drastically differs from those normally used in literature of commercial nature. Recovered starch from potato washing slurries has shown to be more amorphous than commercial starch, for example, that in comparison presents a more crystalline structure<sup>54</sup>. This is due to difference in the extent of processing, as well as in the processing conditions that both starches went through until its obtention. While commercial starch is obtained through optimized processing conditions for its recovery and eventual commercialization, recovered potato starch must go through a more extensive processing due to its byproduct nature until its use. As such, due to differences in the physical-chemical behavior, the more amorphous nature of recovered potato starch made a successful electrospinning more difficult, since such nature means shorter chains that have more difficulty in successfully aligning and entangling enough to form a cohesive jet capable of then forming cohesive fibers. Besides that, the low volatile character of DMSO, combined with low conductivity and high superficial tension of the solutions, meant that a stable jet formation and deposition instead of droplet formation was more difficult, and, in turn, fiber formation was reduced.

This led to a change in solvent from DMSO to formic acid<sup>136</sup>, in hopes that such would heighten solutions' volatility and conductivity. Better results were obtained this time, after optimizing starch concentration, because of formic acid's higher volatility and conductivity in comparison to DMSO, with results including a few loose fibers being obtained (**Fig. 62**). However, further optimization and characterization studies of the starch fibers properties need to be performed.



**Figure 62.** Electrospinning of 25% starch-based solutions prepared in 75:25 FA/H<sub>2</sub>O.



## 5. Conclusion

Hot-water extraction of tomato pomace allowed the obtention of two extracts, the water-soluble extract (TE) and the polyphenol-enriched extract (PE), obtained via subsequent solid-phase separation, with a 24.7% and 3% yield, respectively. TE showed to be chemically composed of 14.7% protein, 43.7% carbohydrates, and 2.8% phenolic compounds, while PE was composed of 18.5% protein, 28.6% carbohydrates, and 15.1% phenolic compounds. TE and PE showed substantial antioxidant activity reflected in  $IC_{50}$  values of 2.5 mg/mL and 0.8 mg/mL, respectively. Moreover, TE showed considerable amounts of sugars that prevent it from having significant antimicrobial effect against *S. aureus*, but lowered its cytotoxicity burden, contrasting with PE that showed some antimicrobial activity and higher cytotoxicity. Besides, these extracts promoted anti-inflammatory activity on the starch-based films, with starch/TE-based films being able to decrease in 48% the inflammation in only 24 h and a complete inflammation elimination in that same time by starch/PE-based films at concentrations above 5%. These extracts also decreased the luminosity and conferred a yellowish tone to the starch-based films, while maintaining their transparency. TE increased the films' extensibility and hydrophobicity, contrary to PE that had the opposite effect. Both starch/TP-derived extract-based films showed decreased stiffness and traction resistance. Starch/10% TE-based films showed increased leaching of compounds, which may be beneficial for films' application in wound healing as compounds' carrier, with increased bioactivity in relation to formulations where compounds are more immobilized, which was confirmed during anti-inflammatory assays, as these films increased anti-inflammatory activity in relation to lower TE formulations. This can also be applied to the starch/PE-based films, as it was seen that higher leaching of compounds from these films generated higher anti-inflammatory activity in the same timeframe. Based in the anti-inflammatory activity results, starch/10% PE-based films can be considered the most promising films to be used as wound dressing. Furthermore, optimization of electrospinning parameters including starch concentration, solvent type and solvent to water ratio, potential differential, distance and flow rate has allowed the obtention of sparse starch fibers, with further optimization still being needed for the obtention of higher quantity of fibers and to ensure an application as a medical device. In summary, tomato pomace-derived molecules and starch recovered from potato washing slurries revealed to be promising biomolecules for developing biobased materials with anti-inflammatory activity, thus opening an opportunity to explore their use in active skin wound healing.

## 6. Future work

To complement the developed experimental work, it is suggested to further determine the chemical composition of the extracts, like estimation of lipidic content via Soxhlet extraction or true qualitative analysis of the phenolic compounds quantified and identified through UHPLC. A methylation assay of simple sugars would also help elucidate the type of bonds that exists between the sugars quantified via GC-FID and may help in identifying the major polysaccharides present. Besides, since tomato pomace is rich in sugars, a sugar analysis without hydrolysis should be performed to complement the determination of total sugars of the extracts. These analyses would also help in further understanding of starch/TP extract-based films characteristics.

Assays that allow to determine the films' cytotoxicity via indirect methods, like Resazurin-based assays that measure cells' viability via metabolic activity could also compliment this work. In addition, the determination of total phenolic content and antioxidant activity of the films would allow a better understanding of these films' bioactivity and its physicochemical properties.

Regarding the electrospinning study, based on the most promising formulation developed in this work, the operational conditions need to be adjusted till obtain a reliable formation of electrospun starch-based fibers. Viscosity assays of electrospinning solutions could help to elucidate the optimal starch concentration for developing reliable electrospun starch-based fibers. After such is achieved, the electrospinning of starch/TE and starch/PE-based solutions should be assessed and optimized accordingly.

## References

1. FAO/STAT. Crops and Livestock Products Production Domain Data. Food and Agriculture Organization of the United Nations, Statistic Division, Accessible at: <http://www.fao.org/faostat/en/#data/QC/visualize> (2019).
2. Z. Lu, J. Wang, R. Gao, F. Ye & G. Zhao. Sustainable valorisation of tomato pomace: A comprehensive review. *Trends Food Sci. Technol.* **86**, 172–187 (2019).
3. J. Catarino, E. Mendonça, A. Picado, A. Anselmo, J. Nobre da Costa & P. Partidário. Getting value from wastewater: by-products recovery in a potato chips industry. *J. Clean. Prod.* **15**, 927–931 (2007).
4. R. Zeng, C. Lin, Z. Lin, H. Chen, W. Lu, C. Lin & H. Li. Approaches to cutaneous wound healing: basics and future directions. *Cell Tissue Res.* **374**, 217–232 (2018).
5. S.P. Zhong, Y.Z. Zhang & C.T. Lim. Tissue scaffolds for skin wound healing and dermal reconstruction. *Wiley Interdiscip. Rev. Nanomedicine Nanobiotechnology* **2**, 510–525 (2010).
6. E.M. Tottoli, R. Dorati, I. Genta, E. Chiesa, S. Pisani & B. Conti. Skin wound healing process and new emerging technologies for skin wound care and regeneration. *Pharmaceutics* **12**, 1–30 (2020).
7. D. Simões, S.P. Miguel, M.P. Ribeiro, P. Coutinho, A.G. Mendonça & I.J. Correia. Recent advances on antimicrobial wound dressing: A review. *European Journal of Pharmaceutics and Biopharmaceutics* **127**, 130–141 (2018).
8. V. Andreu, G. Mendoza, M. Arruebo & S. Irujo. Smart dressings based on nanostructured fibers containing natural origin antimicrobial, anti-inflammatory, and regenerative compounds. *Materials (Basel)*. **8**, 5154–5193 (2015).
9. R.S. Ambekar & B. Kandasubramanian. Advancements in nanofibers for wound dressing: A review. *Eur. Polym. J.* **117**, 304–336 (2019).
10. H. Sorg, D.J. Tilkorn, S. Hager, J. Hauser & U. Mirastschijski. Skin Wound Healing: An Update on the Current Knowledge and Concepts. *Eur. Surg. Res.* **58**, 81–94 (2017).
11. S. Dhivya, V.V. Padma & E. Santhini. Wound dressings - A review. *BioMedicine (Netherlands)* **5**, 24–28 (2015).
12. P. Zarrintaj, A.S. Moghaddam, S. Manouchehri, Z. Atoufi, A. Amiri, M.A. Amirkhani, M.A. Nilfroushzadeh, M.R. Saeb, M. R. Hamblin & M. Mozafari. Can regenerative medicine and nanotechnology combine to heal wounds? the search for the ideal wound dressing. *Nanomedicine* **12**, 2403–2422 (2017).

13. N.B. Menke, K.R. Ward, T.M. Witten, D.G. Bonchev & R.F. Diegelmann. Impaired wound healing. *Clin. Dermatol.* **25**, 19–25 (2007).
14. Z. Moore, P. Avsar, L. Conaty, D.H. Moore, D. Patton & T. O'Connor. The prevalence of pressure ulcers in Europe, what does the European data tell us: A systematic review. *J. Wound Care* **28**, 710–719 (2019).
15. K.A.X. Furtado, P. Infante, A. Sobral, P. Gaspar, G. Eliseu & M. Lopes. Prevalence of acute and chronic wounds – with emphasis on pressure ulcers – in integrated continuing care units in Alentejo, Portugal. *Int. Wound J.* **17**, 1002–1010 (2020).
16. H.N. Wilkinson, & M.J. Hardman. Wound healing: cellular mechanisms and pathological outcomes. *Open Biol.* **10**, 200223 (2020).
17. N.S. Greaves, K.J. Ashcroft, M. Baguneid & A. Bayat. Current understanding of molecular and cellular mechanisms in fibroplasia and angiogenesis during acute wound healing. *J. Dermatol. Sci.* **72**, 206–217 (2013).
18. G. Broughton, J.E. Janis & C.E. Attinger. Wound healing: An overview. *Plast. Reconstr. Surg.* **117**, 1–32 (2006).
19. W.K. Stadelmann, A.G. Digenis & G.R. Tobin. Impediments to wound healing. *Am. J. Surg.* **176**, 39S-47S (1998).
20. R.D. Galiano, O.M. Tepper, C.R. Pelo, K.A. Bhatt, M. Callaghan, N. Bastidas, S. Bunting, H.G. Steinmetz & G.C. Gurtner. Topical vascular endothelial growth factor accelerates diabetic wound healing through increased angiogenesis and by mobilizing and recruiting bone marrow-derived cells. *Am. J. Pathol.* **164**, 1935–1947 (2004).
21. L.I.F. Moura, A.M.A. Dias, E. Carvalho & H.C. De Sousa. Recent advances on the development of wound dressings for diabetic foot ulcer treatment - A review. *Acta Biomaterialia* **9**, 7093–7114 (2013).
22. S.L. Drinkwater, K.G. Burnand, R. Ding & A. Smith. Increased but ineffectual angiogenic drive in nonhealing venous leg ulcers. *Journal of Vascular Surgery* **38**, 1106–1112 (2003).
23. R. Edwards & K.G. Harding. Bacteria and wound healing. *Curr. Opin. Infect. Dis.* **17**, 91–96 (2004).
24. G.T. Lionelli & W.T. Lawrence. Wound dressings. *Surg. Clin. North Am.* **83**, 617–638 (2003).
25. V. Jones, J.E. Grey, & K.G. Harding. Wound dressings. *BMJ* **332**, 777–80 (2006).
26. C. Weller & G. Sussman. Wound dressings update. *Journal of Pharmacy Practice and Research* **36**, 318–324 (2006).

27. B. Gupta, R. Agarwal, & M.S. Alam. Textile-based smart wound dressings. *Indian J. Fibre Text. Res.* **35**, 174–187 (2010).
28. G.D. Winter. Effect of air exposure and occlusion on experimental human skin wounds. *Nature* **200**, 378–379 (1963).
29. G.D. Mogoşanu & A.M. Grumezescu. Natural and synthetic polymers for wounds and burns dressing. *Int. J. Pharm.* **463**, 127–136 (2014).
30. K. Vowden & P. Vowden. Wound dressings: principles and practice. *Surgery (United Kingdom)* **35**, 489–494 (2017).
31. G. Dabiri, E. Damstetter & T. Phillips. Choosing a Wound Dressing Based on Common Wound Characteristics. *Advances in Wound Care* **5**, 32–41 (2016).
32. K. Pal, A.K. Banthia & D.K. Majumdar. Preparation of transparent starch based hydrogel membrane with potential application as wound dressing. *Trends Biomater. Artif. Organs* **20**, 59–67 (2006).
33. A. Hassan, M.B.K. Niazi, A. Hussain, S. Farrukh & T. Ahmad. Development of Anti-bacterial PVA/Starch Based Hydrogel Membrane for Wound Dressing. *J. Polym. Environ.* **26**, 235–243 (2018).
34. E.A. Kamoun, E.R.S. Kenawy & X.A. Chen. Review on polymeric hydrogel membranes for wound dressing applications: PVA-based hydrogel dressings. *Journal of Advanced Research* **8**, 217–233 (2017).
35. T. Hemamalini & V.R. Giri Dev. Comprehensive review on electrospinning of starch polymer for biomedical applications. *Int. J. Biol. Macromol.* **106**, 712–718 (2018).
36. S. Chattopadhyay & R.T. Raines. Review collagen-based biomaterials for wound healing. *Biopolymers* **101**, 821–833 (2014).
37. M. Naseri-Nosar & Z.M. Zior. Wound dressings from naturally-occurring polymers: A review on homopolysaccharide-based composites. *Carbohydrate Polymers* **189**, 379–398 (2018).
38. R. Jayakumar, M. Prabakaran, P.T. Sudheesh Kumar, S.V. Nair & H. Tamura. Biomaterials based on chitin and chitosan in wound dressing applications. *Biotechnology Advances* **29**, 322–337 (2011).
39. J. Bonilla, E. Talón, L. Atarés, M. Vargas & A. Chiralt. Effect of the incorporation of antioxidants on physicochemical and antioxidant properties of wheat starch-chitosan films. *J. Food Eng.* **118**, 271–278 (2013).
40. M.F.P. Graça, S.P. Miguel, C.S.D. Cabral & I.J. Correia. Hyaluronic acid—Based wound dressings: A review. *Carbohydrate Polymers* **241**, 116364 (2020).
41. F.G. Torres, S. Commeaux & O.P. Troncoso. Starch-based biomaterials for wound-

- dressing applications. *Starch/Staerke* **65**, 543–551 (2013).
42. F. Zhu & Q. Xie. Structure and physicochemical properties of starch. *Phys. Modif. Starch* **1**, 1–14 (2018)
  43. E. Bertoft. Understanding Starch Structure: Recent Progress. *Agronomy* **7**, 56 (2017).
  44. Y. Ai & J.L. Jane. Gelatinization and rheological properties of starch. *Starch/Staerke* **67**, 213–224 (2015).
  45. H. Liu, F. Xie, L. Yu, L. Chen & L. Li. Thermal processing of starch-based polymers. *Prog. Polym. Sci.* **34**, 1348–1368 (2009).
  46. S. Wang, C. Li, L. Copeland, Q. Niu & S. Wang. Starch Retrogradation: A Comprehensive Review. *Compr. Rev. Food Sci. Food Saf.* **14**, 568–585 (2015).
  47. E. Pilling & A.M. Smith. Growth Ring Formation in the Starch Granules of Potato Tubers. *Plant Physiol.* **132**(1), 103 (2013).
  48. Q. Xie & F. Zhu. Structure and Physico-chemical Properties of Starch. *Phys. Modif. Starch* **2**, 6–12 (2014).
  49. J. Jane. Starch Properties, Modifications, and Applications. *J. Macromol. Sci. Part A Pure Appl. Chem.* **32**, 751–757 (1995).
  50. N. Laohakunjit & A. Noomhorm. Effect of plasticizers on mechanical and barrier properties of rice starch film. *Starch/Staerke* **56**, 348–356 (2004).
  51. M. Gudmundsson. Retrogradation of starch and the role of its components. *Thermochim. Acta* **246**, 329–341 (1994).
  52. J. Liang & R.D. Ludescher. Effects of glycerol on the molecular mobility and hydrogen bond network in starch matrix. *Carbohydr. Polym.* **115**, 401–407 (2015).
  53. D. Piñeros-Hernandez, C. Medina-Jaramillo, A. López-Córdoba & S. Goyanes. Edible cassava starch films carrying rosemary antioxidant extracts for potential use as active food packaging. *Food Hydrocoll.* **63**, 488–495 (2017).
  54. I. Gonçalves, J. Lopes, A. Barra, D. Hernández, C. Nunes, K. Kapusniak, J. Kapusniak, D.V. Evtugin, J.A. Lopes da Silva, P. Ferreira & M.A Coimbra. Tailoring the surface properties and flexibility of starch-based films using oil and waxes recovered from potato chips byproducts. *Int. J. Biol. Macromol.* **163**, 251–259 (2020).
  55. O. Moreno, L. Atarés & A. Chiralt. Effect of the incorporation of antimicrobial/antioxidant proteins on the properties of potato starch films. *Carbohydr. Polym.* **133**, 353–364 (2015).
  56. V. Goudarzi, I. Shahabi-Ghahfarrokhi & A. Babaei-Ghazvini. Preparation of ecofriendly UV-protective food packaging material by starch/TiO<sub>2</sub> bio-

- nanocomposite: Characterization. *Int. J. Biol. Macromol.* **95**, 306–313 (2017).
57. R. Pyla, T.J. Kim, J.L. Silva & Y.S. Jung. Enhanced antimicrobial activity of starch-based film impregnated with thermally processed tannic acid, a strong antioxidant. *Int. J. Food Microbiol.* **137**, 154–160 (2010).
  58. V. Ramnath, S. Sekar, S. Sankar, T.P. Sastry & A.B. Mandal. In vivo evaluation of composite wound dressing material containing soya protein and sago starch. *Int. J. Pharm. Pharm. Sci.* **4**, 414–419 (2012).
  59. M. Ansarizadeh, S.A. Haddadi, M. Amini, M. Hasany & A. Ramazani Saadat Abadi. Sustained release of CIP from TiO-PVDF/starch nanocomposite mats with potential application in wound dressing. *J. Appl. Polym. Sci.* **137**, 48916 (2020).
  60. S. Baghaie, M.T. Khorasani, A. Zarrabi & J. Moshtaghian. Wound healing properties of PVA/starch/chitosan hydrogel membranes with nano Zinc oxide as antibacterial wound dressing material. *J. Biomater. Sci. Polym. Ed.* **28**, 2220–2241 (2017).
  61. A. Das, R. Uppaluri & C. Das. Feasibility of poly-vinyl alcohol/starch/glycerol/citric acid composite films for wound dressing applications. *Int. J. Biol. Macromol.* **131**, 998–1007 (2019).
  62. S. Batool, Z. Hussain, M.B.K. Niazi, U. Liaqat & M. Afzal. Biogenic synthesis of silver nanoparticles and evaluation of physical and antimicrobial properties of Ag/PVA/starch nanocomposites hydrogel membranes for wound dressing application. *J. Drug Deliv. Sci. Technol.* **52**, 403–414 (2019).
  63. Å. Stenmarck, C. Jensen, T. Quested, G. Moates, B. Cseh, S. Juul, A. Parry, A. Politano, B. Redlingshofer, S. Scherhauser, K. Silvennoinen, H. Soethoudt, C. Zübert & K. Östergren. *Estimates of European food waste levels. Fusions* (2016).
  64. J. Gustavsson, C. Cederberg, U. Sonesson, R. van Otterdijk & A. Meybeck. *Food loss and food waste: Causes and solutions. Food Loss and Food Waste: Causes and Solutions* (2019).
  65. C. Fritsch, A. Staebler, A. Happel, M.A. Cubero Márquez, I. Aguiló-Aguayo, M. Abadias, M. Gallur, I.M. Cigognini, A. Montanari, M.J. López, F. Suárez-Estrella, N. Brunton, E. Luengo, L. Sisti, M. Ferri & G. Belotti. Processing, Valorization and Application of Bio-Waste Derived Compounds from Potato, Tomato, Olive and Cereals: A Review. *Sustain.* **9**, 1492 (2017).
  66. G. Oliveira, I. Gonçalves, A. Barra, C. Nunes, P. Ferreira & M.A. Coimbra. Coffee silverskin and starch-rich potato washing slurries as raw materials for elastic, antioxidant, and UV-protective biobased films. *Food Res. Int.* **138**, 109733 (2020).
  67. M. Añibarro-Ortega, J. Pinela, A. Ćirić, V. Martins, F. Rocha, M.D. Soković, A.M.

- Barata, A.M. Carvalho, L. Barros & I.C.F.R. Ferreira. Valorisation of table tomato crop by-products: Phenolic profiles and in vitro antioxidant and antimicrobial activities. *Food Bioprod. Process.* **124**, 307–319 (2020).
68. J. Pinela, M.B.P.P. Oliveira & I.C.F.R. Ferreira. Bioactive Compounds of Tomatoes as Health Promoters. *Nat. Bioact. Compd. from Fruits Veg. as Heal. Promot. Part II* 48-91 (2016)
69. EUROSTAT. Crop production in national humidity. <https://appsso.eurostat.ec.europa.eu/nui/submitViewTableAction.do> (2020).
70. INE. Previsões Agrícolas 31 de outubro 2019 - Produção de maçã com registo historicamente elevado. 1–6 (2019).
71. INE. Previsões Agrícolas 31 de outubro 2020 - Fruteiras e olival com campanhas pouco favoráveis. 1–6 (2020).
72. K. Szabo, F.V. Dulf, B. Teleky, P. Eleni, C. Boukouvalas, M. Krokida, N. Kapsalis, A.V. Rusu, C.T. Socol & D.C. Vodnar. Evaluation of the Bioactive Compounds Found in Tomato Seed Oil and Tomato Peels Influenced by Industrial Heat Treatments. *Foods* **10**, 110 (2021).
73. K. Szabo, Z. Diaconeasa, A.F. Cătoi & D.C. Vodnar. Screening of Ten Tomato Varieties Processing Waste for Bioactive Components and Their Related Antioxidant and Antimicrobial Activities. *Antioxidants* **8**, 292 (2019).
74. F. Tilesi, A. Lombardi & A. Mazzucato. Scientometric and Methodological Analysis of the Recent Literature on the Health-Related Effects of Tomato and Tomato Products. *Foods* **10**, 1905 (2021).
75. D.S. Kim, Y. Kwack, J.H. Lee & C. Chun. Antimicrobial Activity of Various Parts of Tomato Plants Varied with Different Solvent Extracts. *Plant Pathol. J.* **35**, 149 (2019).
76. USDA Database. Tomatoes, year round average, raw, ripe, red nutrition facts and analysis. Accessible at: [https://www.nutritionvalue.org/Tomatoes%2C\\_year\\_round\\_average%2C\\_raw%2C\\_ripe%2C\\_red\\_nutritional\\_value.html?size=100](https://www.nutritionvalue.org/Tomatoes%2C_year_round_average%2C_raw%2C_ripe%2C_red_nutritional_value.html?size=100) g.
77. J. Costa-Rodrigues, O. Pinho & P.R.R. Monteiro. Can lycopene be considered an effective protection against cardiovascular disease? *Food Chemistry* **245**, 1148–1153 (2018).
78. A. Mordente, B. Guantario, E. Meucci, A. Silverstrini, E. Lombardi, G. E. Martorana, B. Giardina & V. Bohm. Lycopene and Cardiovascular Diseases: An Update. *Curr. Med. Chem.* **18**, 1146–1163 (2011).
79. A. V. Rao & S. Agarwal. Role of Antioxidant Lycopene in Cancer and Heart Disease.



- J. Am. Coll. Nutr.* **19**, 563–569 (2000).
80. Y.P.A. Silva, B.C. Borba, V.A. Pereira, M.G. Reis, M. Caliari, M. Su-Ling Brooks & T.A.P.C. Ferreira. Characterization of tomato processing by-product for use as a potential functional food ingredient: nutritional composition, antioxidant activity and bioactive compounds. *Int. J. Food Sci. Nutr.* **70**, 150–160 (2019).
81. D. Shao, G.G. Atungulu, Z. Pan, T. Yue, A. Zhang & X. Chen. Separation Methods and Chemical and Nutritional Characteristics of Tomato Pomace. *Trans. ASABE* **56**, 261–268 (2013).
82. M. Del Valle, M. Cámara & M. Torija. Chemical characterization of tomato pomace. *J. Sci. Food Agric.* **86**, 1232–1236 (2006).
83. M. Knoblich, B. Anderson & D. Latshaw. Analyses of tomato peel and seed byproducts and their use as a source of carotenoids. *J. Sci. Food Agric.* **85**, 1166–1170 (2005).
84. E. Elbadrawy & A. Sello. Evaluation of nutritional value and antioxidant activity of tomato peel extracts. *Arab. J. Chem.* **9**, S1010–S1018 (2016).
85. P. García Herrera, M.C. Sánchez-Mata & M. Cámara. Nutritional characterization of tomato fiber as a useful ingredient for food industry. *Innovative Food Science and Emerging Technologies* **11** 707–711 (2010).
86. E. Fuentes, R. Carle, L. Astudillo, L. Guzmán, M. Gutiérrez, G. Carrasco & I. Palomo. Antioxidant and antiplatelet activities in extracts from green and fully ripe tomato fruits (*Solanum lycopersicum*) and pomace from industrial tomato processing. *Evidence-based Complement. Altern. Med.* **2013**, 1–9 (2013).
87. P. Abbasi-Parizad, P. De Nisi, F. Adani, T.P. Sciarria, P. Squillace, A. Scarafoni, S. Iametti & B. Scaglia. Antioxidant and Anti-Inflammatory Activities of the Crude Extracts of Raw and Fermented Tomato Pomace and Their Correlations with Aglycate-Polyphenols. *Antioxidants* **9**, 179 (2020).
88. Q. Wang, Z. Xiong, G. Li, X. Zhao, H. Wu & Y. Ren. Tomato peel powder as fat replacement in low-fat sausages: Formulations with mechanically crushed powder exhibit higher stability than those with airflow ultra-micro crushed powder. *Eur. J. Lipid Sci. Technol.* **118**, 175–184 (2016).
89. A.N. Grassino, J. Halambek, S. Djaković, S. Rimac Brnčić, M. Dent & Z. Grabarić. Utilization of tomato peel waste from canning factory as a potential source for pectin production and application as tin corrosion inhibitor. *Food Hydrocoll.* **52**, 265–274 (2016).
90. G.A. Piyakina & T.S. Yunusov. General characteristics of the proteins of tomato seed

- flour and tomato skin flour. *Chem. Nat. Compd.* **31**, 495–499 (1995).
91. K.K.H.Y. Ho, M.G. Ferruzzi, A.M. Liceaga & M.F. San Martín-González. Microwave-assisted extraction of lycopene in tomato peels: Effect of extraction conditions on all-trans and cis-isomer yields. *LWT - Food Sci. Technol.* **62**, 160–168 (2015).
  92. M. Kehili, M. Kammlott, S. Choura, A. Zammel, C. Zetzi, I. Smirnova, N. Allouche & S. Sayadi. Supercritical CO<sub>2</sub> extraction and antioxidant activity of lycopene and  $\beta$ -carotene-enriched oleoresin from tomato (*Lycopersicon esculentum* L.) peels by-product of a Tunisian industry. *Food Bioprod. Process.* **102**, 340–349 (2017).
  93. E. Yilmaz, B Aydeniz, O. Güneşer & E.S. Arsunar. Sensory and physico-chemical properties of cold press-produced tomato (*Lycopersicon esculentum* L.) seed oils. *JAOCS, J. Am. Oil Chem. Soc.* **92**, 833–842 (2015).
  94. M. Mechmeche, F. Kachouri, M. Chouabi, H. Ksontini, K. Setti & M. Hamdi. Optimization of Extraction Parameters of Protein Isolate from Tomato Seed Using Response Surface Methodology. *Food Anal. Methods* **10**, 809–819 (2017).
  95. A.M.Giuffrè & M. Capocasale. Physicochemical composition of tomato seed oil for an edible use: The effect of cultivar. *Int. Food Res. J.* **23**, 583–591 (2016).
  96. S. Savadkoobi & A. Farahnaky. Dynamic rheological and thermal study of the heat-induced gelation of tomato-seed proteins. *J. Food Eng.* **113**, 479–485 (2012).
  97. H. Al-wandawi, M. Abdul-rahman & K. Al-shaikhly. Tomato Processing Wastes as Essential Raw Materials Source. *J. Agric. Food Chem.* **33**, 804–807 (1985).
  98. I. Navarro-González, V. García-Valverde, J. García-Alonso & M.J. Periago. Chemical profile, functional and antioxidant properties of tomato peel fiber. *Food Res. Int.* **44**, 1528–1535 (2011).
  99. M. Cámara Hurtado, L.C. Greve & J.M. Labavitch. Changes in Cell Wall Pectins Accompanying Tomato (*Lycopersicon esculentum* Mill.) Paste Manufacture. *J. Agric. Food Chem.* **50**, 273–278 (2001).
  100. S. Goetz, M. Rejzek, S.A. Nepogodiev & R.A. Field. The impact of aminopyrene trisulfonate (APTS) label in acceptor glycan substrates for profiling plant pectin  $\beta$ -galactosyltransferase activities. *Carbohydr. Res.* **433**, 97–105 (2016).
  101. S.K. Clinton. Lycopene: Chemistry, biology, and implications for human health and disease. *Nutr. Rev.* **56**, 35–51 (1998).
  102. J. Costa-Rodrigues, O. Pinho & P.R.R. Monteiro, Can lycopene be considered an effective protection against cardiovascular disease? *Food Chem.* **245**, 1148–1153 (2018).
  103. S. Agarwal & A.V. Rao. Tomato lycopene and its role in human health and chronic

- diseases. *Cmaj* **163**, 739–744 (2000).
104. W. Stahl & H. Sies. Lycopene: A Biologically Important Carotenoid for Humans? *Arch. Biochem. Biophys.* **336**, 1–9 (1996).
  105. J. Shi & M. Le Maguer. Lycopene in tomatoes: Chemical and physical properties affected by food processing. *Critical Reviews in Food Science and Nutrition* **40**(1), 1–42 (2000).
  106. B. George, C. Kaur, D.S. Khurdiya & H.C. Kapoor. Antioxidants in tomato (*Lycopersium esculentum*) as a function of genotype. *Food Chem.* **84**, 45–51 (2004).
  107. J. L. Guil-Guerrero & M. M. Reboloso-Fuentes. Nutrient composition and antioxidant activity of eight tomato (*Lycopersicon esculentum*) varieties. *J. Food Compos. Anal.* **22**, 123–129 (2009).
  108. M.W. Davey, M.V. Montagu, D. Inze, M. Sanmartin, A. Kanellis, N. Smirno, I.J.J. Benzie, J. J. Strain, D. Favell & J. Fletcher. Plant L -ascorbic acid : chemistry , function , metabolism , bioavailability and effects of processing. **860**, 825–860 (2000).
  109. A. Baiano & M.A. Del Nobile. Antioxidant Compounds from Vegetable Matrices: Biosynthesis, Occurrence, and Extraction Systems. *Crit. Rev. Food Sci. Nutr.* **56**, 2053–2068 (2016).
  110. F. Tilesi, A. Lombardi & Mazzucato, A. Scientometric and Methodological Analysis of the Recent Literature on the Health-Related Effects of Tomato and Tomato Products. *Foods* **10**, 1905 (2021).
  111. L. Barros, M. Dueñas, J. Pinela, A.M. Carvalho, C.S. Buelga & I.C.F.R. Ferreira. Characterization and Quantification of Phenolic Compounds in Four Tomato (*Lycopersicon esculentum* L.) Farmers' Varieties in Northeastern Portugal Homegardens. *Plant Foods Hum. Nutr.* **67**, 229–234 (2012).
  112. M. Minoggio, L. Bramati, P. Simonetti, C. Gardana, L. Iemoli, E. Santangelo, P.L. Mauri, P. Spigno, G.P. Soressi & P.G. Pietta. Polyphenol pattern and antioxidant activity of different tomato lines and cultivars. *Ann. Nutr. Metab.* **47**, 64–69 (2003).
  113. M. Biesaga, U. Ochnik & K. Pyrzyńska. Fast analysis of prominent flavonoids in tomato using a monolithic column and isocratic HPLC. *J. Sep. Sci.* **32**, 2835–2840 (2009).
  114. P.A.R. Fernandes, S.S. Ferreira, R. Bastos, I. Ferreira, M.T. Cruz, A. Pinto, E. Coelho, C.P. Passos, M. A. Coimbra, S.M. Cardoso & D. F. Wessel. Apple pomace extract as a sustainable food ingredient. *Antioxidants* **8**, 189 (2019).
  115. S. Fujihara, A. Kasuga & Y. Aoyagi. Calculation of Nitrogen-To-Protein Conversion Factors for Food Products . *J. Food Sci.* **66**, 412–415 (1982).

116. J. Pinela, L. Barros, A. M. Carvalho & I.C.F.R. Ferreira. Nutritional composition and antioxidant activity of four tomato (*Lycopersicon esculentum* L.) farmer' varieties in Northeastern Portugal homegardens. *Food Chem. Toxicol.* **50**, 829–834 (2012).
117. J. Lopes, I. Gonçalves, C. Nunes, B. Teixeira, R. Mendes, P. Ferreira & M.A. Coimbra. Potato peel phenolics as additives for developing active starch-based films with potential to pack smoked fish fillets. *Food Packag. Shelf Life* **28**, 100644 (2021).
118. PeproTech, ELISA: Sandwich TMB. Accessible at: <https://www.peprotech.com/gb/ELISA-Sandwich-TMB>.
119. M. Szymanska-Chargot, M. Chylinska, K. Gdula, A. Koziol & A. Zdunek. Isolation and characterization of cellulose from different fruit and vegetable pomaces. *Polymers (Basel)*. **9**, (2017).
120. C. Agius, S. von Tucher, B. Poppenberger & W. Rozhon. Quantification of sugars and organic acids in tomato fruits. *MethodsX* **5**, 537–550 (2018).
121. A. Vallverdú-Queralt, A. Medina-Remón, M. Martínez-Huélamo, O. Jáuregui, C. Andres-Lacueva & R. M. Lamuela-Raventos. Phenolic profile and hydrophilic antioxidant capacity as chemotaxonomic markers of tomato varieties. *J. Agric. Food Chem.* **59**, 3994–4001 (2011).
122. L. Helyes, A. Lugasi, H. G. Daood & Z. Pék. The simultaneous effect of water supply and genotype on yield quantity, antioxidants content and composition of processing tomatoes. *Not. Bot. Horti Agrobot. Cluj-Napoca* **42**, 143–149 (2014).
123. S. Navarrete, M. Alarcón & I. Palomo. Aqueous Extract of Tomato (*Solanum lycopersicum* L.) and Ferulic Acid Reduce the Expression of TNF- $\alpha$  and IL-1 $\beta$  in LPS-Activated Macrophages. *Mol.* **20**, 15319–15329 (2015).
124. P.R. Mayeux. Pathobiology of lipopolysaccharide. *J. Toxicol. Environ. Health* **51**, 415–435 (1997).
125. J. Schwager, N. Richard, B. Mussler & D. Raederstorff. Tomato Aqueous Extract Modulates the Inflammatory Profile of Immune Cells and Endothelial Cells. *Mol.* **21**, 168 (2016).
126. B. Saberi, Q. V. Vuong, S. Chockchaisawasdee, J. B. Golding, C. J. Scarlett & E. Costas Stathopoulos. Physical, Barrier, and Antioxidant Properties of Pea Starch-Guar Gum Biocomposite Edible Films by Incorporation of Natural Plant Extracts. *Food Bioprocess Technol.* **10**, 2240–2250 (2017).
127. Z. Schuessler. Delta E 101. Accessible at: <http://zschuessler.github.io/DeltaE/learn/> (2016).
128. M. Leon-Bejarano, Y. Durmus, M. Ovando-Martínez, & S. Simsek. Physical, Barrier,

- Mechanical, and Biodegradability Properties of Modified Starch Films with Nut By-Products Extracts. *Foods* **9**, 226 (2020).
129. U. Siripatrawan & B. R. Harte. Physical properties and antioxidant activity of an active film from chitosan incorporated with green tea extract. *Food Hydrocoll.* **24**, 770–775 (2010).
  130. A. Eskandarinia, M. Rafienia, S. Navid & M. Agheb. Physicochemical, Antimicrobial and Cytotoxic Characteristics of Corn Starch Film Containing Propolis for Wound Dressing. *J. Polym. Environ.* **26**, 3345–3351 (2018).
  131. A.M. Cruz-Gálvez, J. Castro-Rosas, M.L. Rodríguez-Marín, A. Cadena-Ramírez, A. Tellez-Jurado, X. Tovar-Jiménez, E.A. Chavez-Urbiola, A. Abreu-Corona, & C.A. Gómez-Aldapa. Antimicrobial activity and physicochemical characterization of a potato starch-based film containing acetic and methanolic extracts of *Hibiscus sabdariffa* for use in sausage. *Lwt* **93**, 300–305 (2018).
  132. C. Menzel, C. González-Martínez, A. Chiralt & F. Vilaplana. Antioxidant starch films containing sunflower hull extracts. *Carbohydr. Polym.* **214**, 142–151 (2019).
  133. M. Moradi, H. Tajik, S.M. Razavi Rohani, A.R. Oromiehie, H. Malekinejad, J. Aliakbarlu & M. Hadian. Characterization of antioxidant chitosan film incorporated with *Zataria multiflora* Boiss essential oil and grape seed extract. *LWT - Food Sci. Technol.* **46**, 477–484 (2012).
  134. M. Feng, L. Yu, P. Zhu, X. Zhou, H. Liu, Y. Yang, J. Zhou, C. Gao, X. Bao. & P. Chen. Development and preparation of active starch films carrying tea polyphenol. *Carbohydr. Polym.* **196**, 162–167 (2018).
  135. W. Wang, H. Wang, X. Jin, H. Wang, T. Lin & Z. Zhu. Effects of hydrogen bonding on starch granule dissolution, spinnability of starch solution, and properties of electrospun starch fibers. *Polymer (Guildf)*. **153**, 643–652 (2018).
  136. L.M. Fonseca, F.T. da Silva, M.D. Antunes, S.L. Mello El Halal, L.T. Lim & A.R.G. Dias. Aging Time of Soluble Potato Starch Solutions for Ultrafine Fibers Formation by Electrospinning. *Starch/Staerke* **71**, 1–7 (2019).

## Annex

### Table Index:

**Table A1.** Granulometric analysis of unmilled tomato pomace.

**Table A2.** Granulometric analysis of milled tomato pomace.

**Table A3.** Cell viability assays results for TP-derived extracts cytotoxicity determination. 25; 50 and 120 denotes de extract concentration in vitro ( $\mu\text{g/mL}$ ).

**Table A4.** Optical parameters  $L^*$ ,  $a^*$ ,  $b^*$  and  $\Delta E$  of starch- and TP-derived extracts/starch-based films.

**Table A5.** Thickness, traction resistance, Young's modulus and elongation of starch- and TP-derived extracts/starch based films.

**Table A6.** Water contact angle, moisture content and solubility values of starch and TP-derived extracts/starch-based films

**Table A1.** Granulometric analysis of unmilled tomato pomace.

Granulometry	Pack 1		Pack 2		Pack 3		Pack 4	
	(g)	%	(g)	%	(g)	%	(g)	%
2 mm	15.73	29.5	10.97	21.4	12.61	21.4	10.87	22.0
1 mm	32.25	60.5	34.56	67.4	40.24	68.2	33.51	67.8
0.710 mm	2.67	5.0	2.91	5.7	3.19	5.4	2.56	5.2
-	2.61	4.9	2.80	5.5	2.97	5.0	2.50	5.1

**Table A2.** Granulometric analysis of milled tomato pomace.

Granulometry	(g)	%
0.710 mm	1.44	3.1
0.300 mm	15.44	33.2
0.150 mm	29.68	63.7
-	0.0	0.0

**Table A3.** Cell viability assays results for TP-derived extracts cytotoxicity determination. 25; 50 and 120 denotes de extract concentration in vitro ( $\mu\text{g/mL}$ ).

Cell Mortality (%)			
	Condition	24h	48h
	LPS Present	LPS	4.9 $\pm$ 2.7
TE50		2.5 $\pm$ 0.6	4.2 $\pm$ 1.1
TE120		3.9 $\pm$ 0.1	10.5 $\pm$ 0.4
PE25		2.8 $\pm$ 1.3	4.3 $\pm$ 0.9
PE50		7.3 $\pm$ 1.4	10.8 $\pm$ 0.8
PE120		16.6 $\pm$ 0.6	12.9 $\pm$ 1.0
LPS Absent	Control	1.1 $\pm$ 0.2	1.5 $\pm$ 0.6
	TE50	1.6 $\pm$ 0.4	1.9 $\pm$ 0.9
	TE120	3.3 $\pm$ 0.4	6.5 $\pm$ 0.1
	PE25	1.9 $\pm$ 1.1	1.9 $\pm$ 1.3
	PE50	5.3 $\pm$ 2.2	10.7 $\pm$ 4.9
	PE120	16.7 $\pm$ 2.1	21.1 $\pm$ 7.9

**Table A4.** Optical parameters  $L^*$ ,  $a^*$ ,  $b^*$ , and  $\Delta E$  values of starch- and TP-derived extracts/starch-based films.

Sample	$L^*$	$a^*$	$b^*$	$\Delta E$
Control	92.08 $\pm$ 0.57 <sup>a</sup>	1.34 $\pm$ 0.04 <sup>c</sup>	-0.033 $\pm$ 0.08 <sup>h</sup>	-
1% TE	92.19 $\pm$ 0.39 <sup>a</sup>	1.00 $\pm$ 0.08 <sup>d</sup>	0.083 $\pm$ 0.28 <sup>i</sup>	1.22
5% TE	91.57 $\pm$ 0.59 <sup>a</sup>	0.44 $\pm$ 0.10 <sup>e</sup>	3.48 $\pm$ 0.41 <sup>j</sup>	3.95
10% TE	91.23 $\pm$ 0.56 <sup>a,b</sup>	-0.14 $\pm$ 0.28 <sup>f</sup>	6.27 $\pm$ 1.15 <sup>k</sup>	6.82
1% PE	92.67 $\pm$ 0.43 <sup>a</sup>	0.62 $\pm$ 0.17 <sup>e</sup>	1.94 $\pm$ 0.58 <sup>i</sup>	2.46
5% PE	90.82 $\pm$ 0.53 <sup>b</sup>	-2.95 $\pm$ 0.55 <sup>g</sup>	13.73 $\pm$ 2.22 <sup>l</sup>	14.76
10% PE	88.37 $\pm$ 1.44 <sup>c</sup>	-2.77 $\pm$ 0.53 <sup>g</sup>	14.12 $\pm$ 3.12 <sup>l</sup>	15.48

**Table A5.** Thickness, traction resistance, Young's modulus and elongation of starch- and TP-derived extracts/starch based films.

Sample	Thickness ( $\mu\text{m}$ )	Traction Resistance (MPa)	Young's Modulus (MPa)	Elongation at Break (%)
Control	58 $\pm$ 8 <sup>a</sup>	18 $\pm$ 4 <sup>a</sup>	365 $\pm$ 43 <sup>a,b</sup>	14 $\pm$ 3 <sup>a</sup>
1% TE	62 $\pm$ 4 <sup>a</sup>	13 $\pm$ 1 <sup>b</sup>	413 $\pm$ 44 <sup>a</sup>	12 $\pm$ 5 <sup>a</sup>
5% TE	76 $\pm$ 4 <sup>b</sup>	15 $\pm$ 2 <sup>a,b</sup>	407 $\pm$ 66 <sup>a,b</sup>	14 $\pm$ 2 <sup>a</sup>
10% TE	84 $\pm$ 4 <sup>b</sup>	9 $\pm$ 1 <sup>c</sup>	212 $\pm$ 21 <sup>c</sup>	36 $\pm$ 7 <sup>c</sup>
1% PE	57 $\pm$ 7 <sup>a</sup>	18 $\pm$ 2 <sup>a</sup>	491 $\pm$ 94 <sup>a</sup>	6 $\pm$ 3 <sup>b</sup>
5% PE	78 $\pm$ 12 <sup>b</sup>	15 $\pm$ 2 <sup>a,b</sup>	462 $\pm$ 90 <sup>a</sup>	11 $\pm$ 5 <sup>b</sup>
10% PE	56 $\pm$ 6 <sup>a</sup>	6 $\pm$ 2 <sup>d</sup>	338 $\pm$ 44 <sup>b</sup>	1 $\pm$ 0.6 <sup>d</sup>

**Table A6.** Water contact angle, moisture content and solubility values of starch and TP-derived extracts/starch-based films

Sample	Water contact angle (°)		Moisture content (%)	Solubility (%)
	Top surface	Bottom surface		
Control	70 ± 3 <sup>a</sup>	69 ± 11 <sup>a,d</sup>	17.1 ± 1.1 <sup>a</sup>	20 ± 7.0 <sup>a</sup>
1% TE	68 ± 2 <sup>a</sup>	111 ± 8 <sup>b</sup>	18.4 ± 7.2 <sup>a,b</sup>	18.4 ± 5.4 <sup>a</sup>
5% TE	106 ± 1 <sup>e</sup>	85 ± 5 <sup>f</sup>	19.3 ± 4.9 <sup>a,b</sup>	6.7 ± 2.4 <sup>b</sup>
10% TE	95 ± 4 <sup>e</sup>	73 ± 4 <sup>a</sup>	17.2 ± 3.4 <sup>a,b</sup>	15.2 ± 1.2 <sup>a</sup>
1% PE	38 ± 2 <sup>c</sup>	65 ± 4 <sup>d</sup>	23.7 ± 6.4 <sup>a</sup>	17.5 ± 5.7 <sup>a</sup>
5% PE	56 ± 1 <sup>g</sup>	43 ± 7 <sup>c</sup>	13.7 ± 2.0 <sup>a,b</sup>	33 ± 4.0 <sup>c</sup>
10% PE	59 ± 4 <sup>h</sup>	58 ± 2 <sup>h</sup>	11.0 ± 1.7 <sup>b</sup>	15.3 ± 2.3 <sup>a</sup>



## Figure Index:

**Figure A1.** Gas chromatography chromatograms obtained from **a)** TE and **b)** PE for neutral sugars analysis.

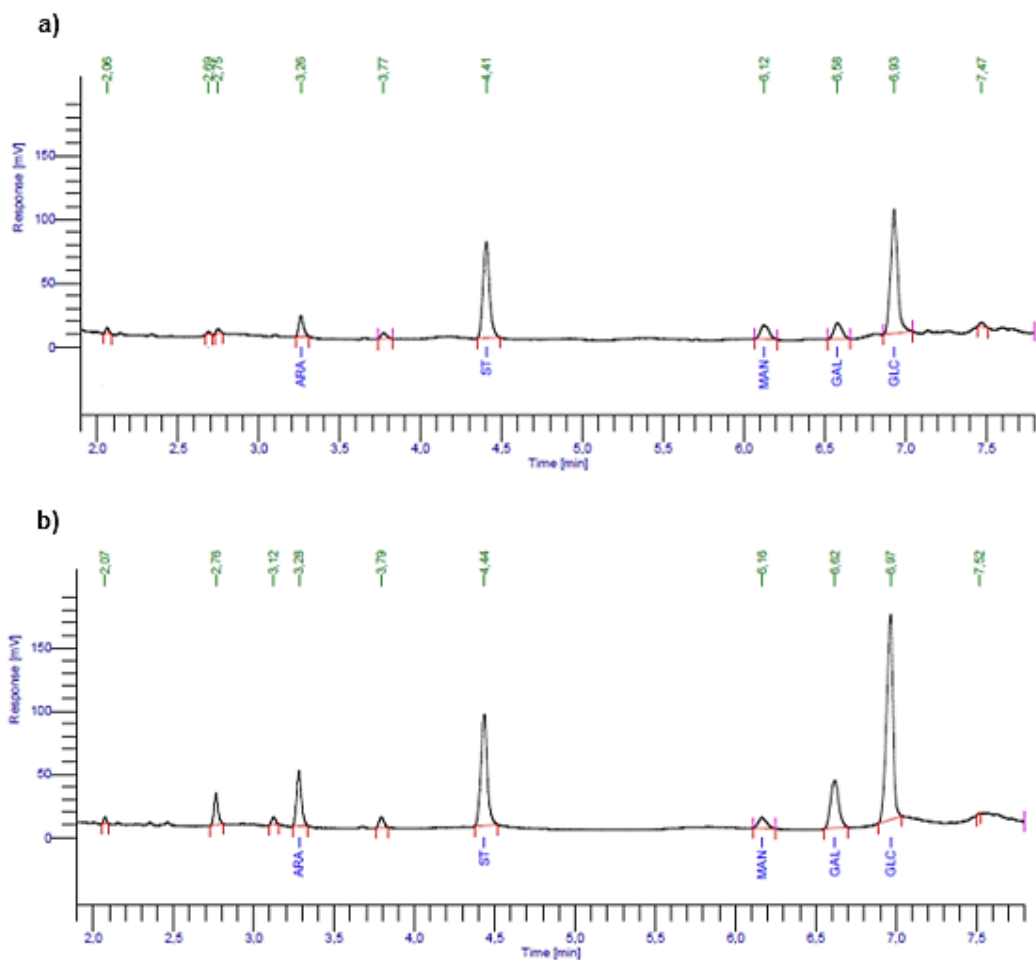
**Figure A2.** Galacturonic acid (GalA) calibration curve for uronic acids estimation.

**Figure A3.** Gallic acid calibration curve for total phenolic content estimation.

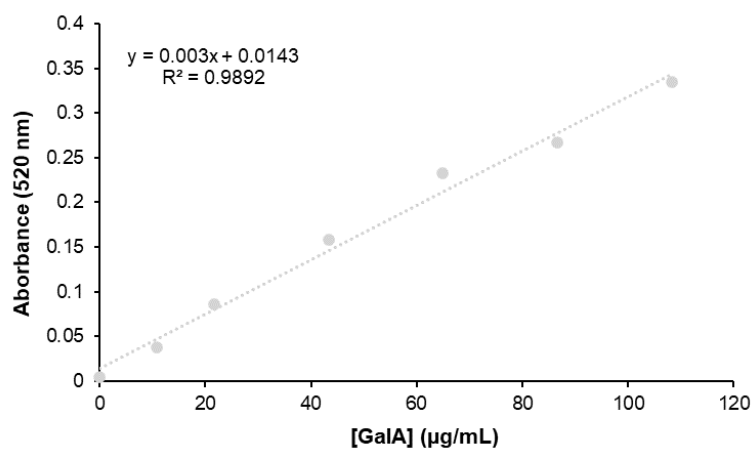
**Figure A4.** Caffeic acid calibration curve for phenolics quantification via HPLC.

**Figure A5.** DPPH scavenging activity vs. **a)** TE and **b)** PE concentration calibration curve for antioxidant activity determination.

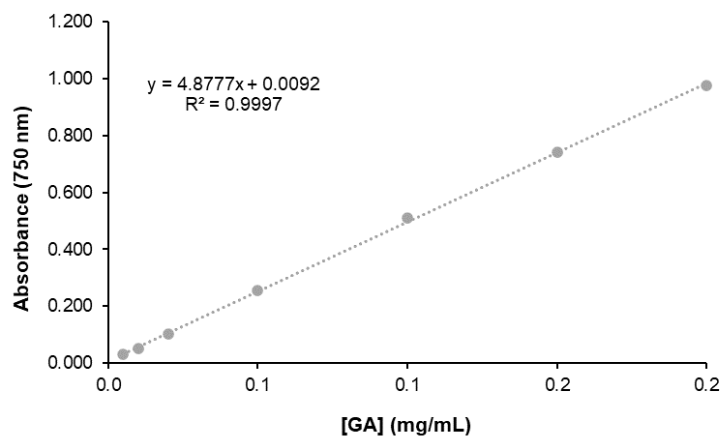
**Figure A6.** TNF- $\alpha$  calibration curve for **a)** TP-derived extracts and **b)** starch/ and TP-derived extracts/starch-based films' anti-inflammatory activity determination.



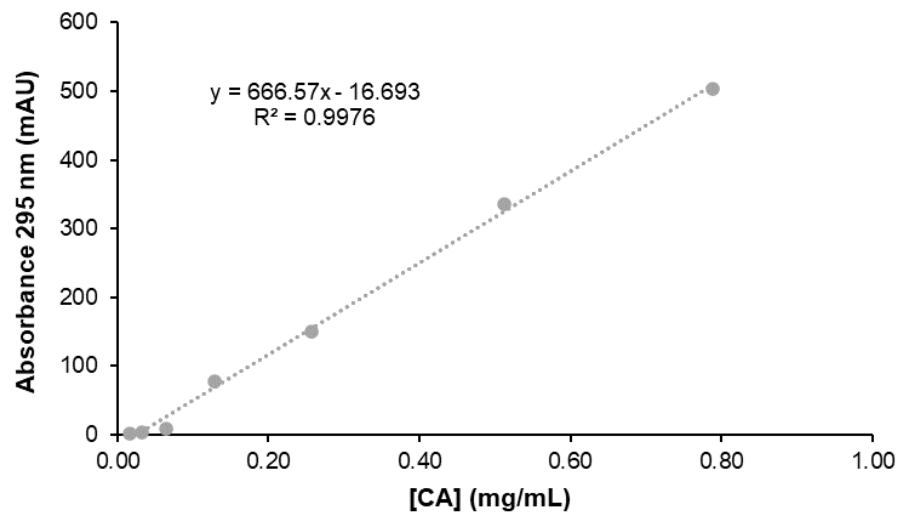
**Figure A1.** Gas chromatography chromatograms obtained from **a)** TE and **b)** PE for neutral sugars analysis.



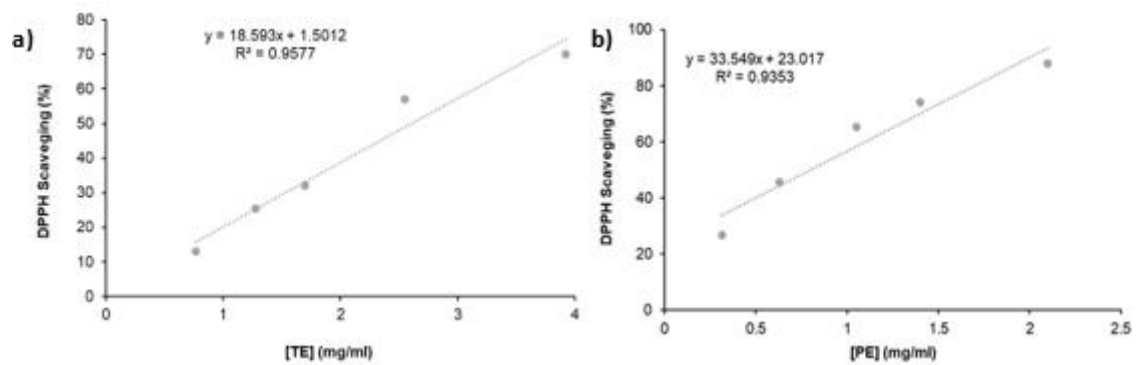
**Figure A2.** Galacturonic acid (GalA) calibration curve for uronic acids estimation.



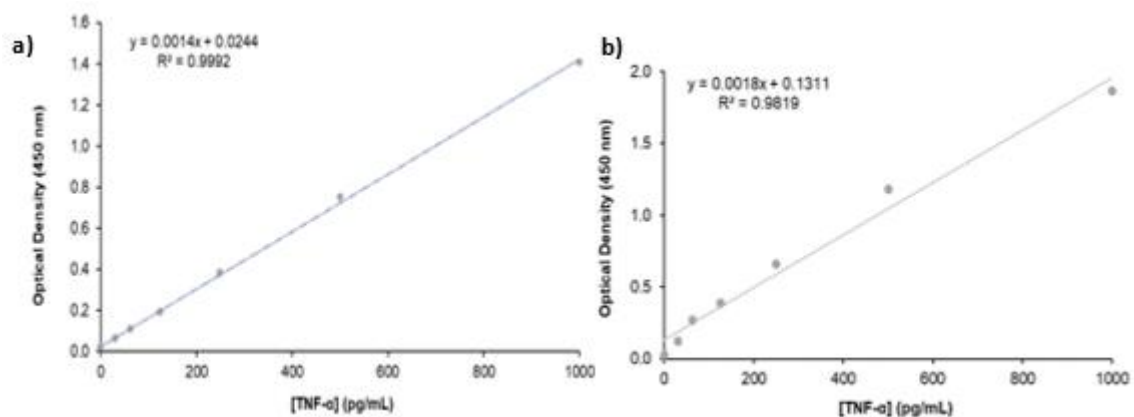
**Figure A3.** Gallic acid calibration curve for total phenolic content estimation.



**Figure A4.** Caffeic acid calibration curve for phenolics quantification via HPLC.



**Figure A5.** DPPH scavenging activity vs. a) TE and b) PE concentration calibration curve for antioxidant activity determination.



**Figure A6.** TNF- $\alpha$  calibration curve for **a)** TP-derived extracts and **b)** starch/ and TP-derived extracts/starch-based films' anti-inflammatory activity determination.